First Order Statistical Analysis

Headwaters to Westhope, North Dakota

Trends and Nonstationarities in Observed Hydrometeorological Records

Souris River, Saskatchewan & North Dakota

September 2020

Table of Contents

Table of Figures

Table of Tables

1 Background

Recent scientific evidence shows that in some places, climate change is shifting the climatological baseline about which natural climate variability occurs and may be changing the range of that variability as well. This is relevant to hydrologic analysis because the assumptions of stationary climatic baselines and a fixed range of natural variability, as captured in the historic hydrologic record, may no longer be appropriate for long-term projections of basin conditions.

In order to better understand the potential impact of climate change on the hydrology of the Souris River Basin, observed, hydrometeorological datasets are analyzed for trends and nonstationarities in accordance to U.S Army Corps of Engineers (USACE) Engineering Construction Bulletin (ECB) 2018-14, *Guidance for Incorporating Climate Change Impacts to Inland Hydrology in Civil Works Studies, Designs and Projects* (Reference 14), as well as USACE Engineering Technical Letter (ETL) 1100-2-3 *Guidance for Detection of Nonstationarities in Annual Maximum Discharges* (Reference 4).

The USACE Nonstationarity Detection Tool (Reference 19) and the USACE Climate Change Assessment Tool (Reference 18) are used to evaluate trends and nonstationarities in observed, annual peak streamflow records. The USACE Time Series Toolbox (Reference 20) is used to analyze nonstationarities and monotonic trends in temperature, precipitation, unregulated flow records, as well as observed, streamflow records.

Observed streamflow data are obtained from the U.S Geological Survey (USGS; Reference 15). Observed precipitation and temperature data in North Dakota are obtained from the National Centers for Environmental Information (NCEI; Reference 8, 10, 11, 12) and Iowa Environmental Mesonet (IEM) North Dakota Automated Surface Observing System (ASOS) network (Reference 6). Unregulated flows at Minot, ND are analyzed as part of this assessment. The temperature and precipitation data in Saskatchewan are obtained from the National Climate Data Archive of Environment and Climate Change Canada (Reference 5). The unregulated flow record at Minot was derived using observed USGS streamflow datasets collected throughout the Souris River Basin above Minot, ND and a HEC-ResSim model for the Souris River Plan of Study (Reference 17). The inputs (reservoir inflows, local flows, tributary flows) used to generate the unregulated flow record for 1946-2011 were developed in support of a 2013 USACE Hydrology Study (Reference 13). This flow record was expanded upon to include water years 1930-1945 and 2012-2017 as part of the *Regional & Reconstructed Hydrology Extension* (HH1) for the Souris River Plan of Study (PoS; Reference 15).

When analyzing changes in climate, the record length of datasets is important. Climate is typical weather patterns of a specific region described over a long period of time. Typically, 30 year periods are considered the minimum length of time for assessing climate. Weather is a short term description of atmospheric conditions and is commonly observed on a day to day basis,

but is also within the range of a few years or a decade. The period of record length is important when analyzing hydrometeorological datasets for human-driven climate change.

Another challenge associated with using historic hydrometeorological records to try to identify locations impacted by human-driven climate change is that gaged hydrometeorological records include both the effects of natural, climate variability and the response of the hydrometeorological system to human-driven climate change. Natural variability in hydroclimate is present as both a signal within the historic record and as noise. This makes it difficult to isolate the impact of human-driven climate change in both meteorological and streamflow records. The effects of regulation, land use changes and land cover changes compound the issue when trying to isolate the effects of human-driven climate change within streamflow records.

2 Nonstationarity Detection

Both the USACE Time Series Toolbox (Reference 20) and the USACE Nonstationarity Detection Tool (Reference 19) apply twelve statistical tests to evaluate the nonstationarity of timeseries data being analyzed. The statistical methods applied by the Nonstationarity Detection Tool are used to assess observed, peak streamflow datasets collected up to water year 2014. The Time Series Toolbox is used to analyze streamflow datasets up to water year 2017 and meteorological records through 2018. For all hydrologic analysis, the period of analysis for the Plan of Study (PoS) is 1930-2017. The statistical tests identify nonstationarities based on both abrupt and smooth changes in mean, variance, and overall statistical distribution. Abrupt, distribution-based tests include Cramer-Von-Mises (CVM), Kolmogorov-Smirnov (KS), LePage (LP), and Energy Divisive (END). Abrupt, mean-based tests include Lombard-Wilcoxon (LW), Pettitt (PT), Mann-Whitney (MW), and Bayesian CPD (BAY). Abrupt, variance-based tests are Lombard Mood (LM) and Mood (MD). Smooth, or gradual, statistical changes within a dataset are detected using the mean-based Smooth Lombard-Wilcoxon and variance-based Smooth Lombard-Mood tests. If a smooth test detects a flux in statistical properties over less than a five-year span, it can be used as evidence similar to an abrupt change statistical test. With the exception of the BAY test, all statistical tests applied are non-parametric. Parameters for each of the statistical tests are kept at the default setting in Timeseries Toolbox, consistent with default parameters in the Nonstationarity Detection Tool. See Figure 1 for Timeseries Toolbox test parameters.

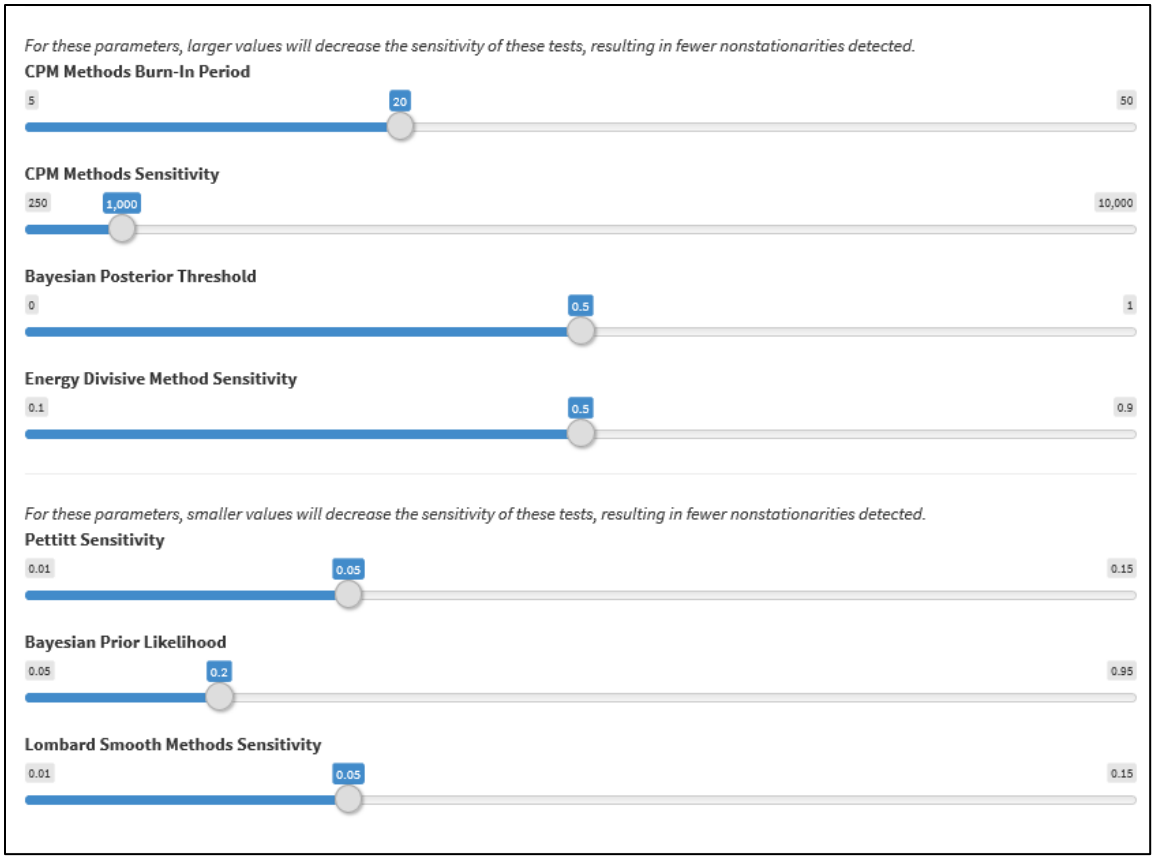

Figure 1. Configuration testing parameters for Timeseries Toolbox analysis.

A strong, operationally significant nonstationarity is one that demonstrates consensus and robustness in terms of the number of tests identifying a nonstationarity at a given point in time. Additionally, to be considered strong, the nonstationarity detected must be tied to a significant change in either or both the mean and standard deviation/variance of the dataset. If multiple tests detect nonstationarities in different years within a five-year span, it can be considered representative of a single year. To establish consensus, a nonstationarity must be detected by multiple statistical tests targeted at detecting changes in the same statistical property (i.e. mean, variance, and distribution). To be considered robust, two or more tests targeted at identifying changes in different statistical properties must be identifying the same nonstationarity.

3 Trend Analysis

Datasets are analyzed for trends using both the full period of record of data available, as well as the portion of the period of record after any identified nonstationarities. Simple linear regression analysis is performed on all datasets analyzed. Simple linear regression analysis is performed using both Microsoft Excel and the USACE Climate Change Hydrology Assessment Tool (CHAT; Reference 18). The CHAT tool only facilitates an assessment of observed, USGS annual peak streamflow. Microsoft Excel is used to analyze all other data types assessed as part

of this study. P-values are used to conclude if a statistically significant trend can be detected within datasets being analyzed. The generally accepted p-value<0.05 is used as the threshold for statistical significance. In order to identify the presence of monotonic trends, the Mann-Kendall and Spearman Rank-Order statistical tests (α =.05 level of significance) are also applied to period of record datasets analyzed. These statistical tests are available within the USACE Time Series Toolbox (Reference 20) and the USACE Nonstationarity Detection Tool (Reference 19).

4 First Order Statistical Analysis of Basin Hydrology

This portion of the climate change analysis focuses on carrying out first order statistical analysis using streamflow records observed at USGS gages within the Souris River Basin. Streamflow records are analyzed for nonstationarities and trends. Analysis is carried out using observed flow recorded at relatively "pristine," long-term tributary gage sites, as well as by analyzing an unregulated streamflow record at Minot, ND. Streamflow records are described as "pristine" when there are minimal man-made flood control structures impacting peak flows. By assessing "pristine" gage sites and unregulated flow records, the chance of detecting a nonstationarity in flows caused by the construction of a water resources project is reduced. In unregulated flow records or in a "pristine" basin, detected nonstationarities can be attributed to either a distributed land use/land cover change (example: widespread ditching or a change from forest to agricultural land) or climate change (natural climate cycles, natural long-term persistent climate change or human driven climate change).

4.1 Trends & Nonstationarities in Peak Streamflow

This portion of the climate change analysis focuses on carrying out first order statistical analysis using annual peak streamflow. Analysis is carried out using observed, annual instantaneous flows recorded at three, relatively "pristine," long-term tributary gage sites: USGS gage 05120500, Wintering River near Karlsruhe, ND; USGS gage 05113600, Long Creek near Noonan, ND; and USGS gage 04116500, Des Lacs River at Foxholm, ND.

USGS gage 05120500 is located along the Wintering River near Karlsruhe, ND. The Karlsruhe gage has a continuous period of record of 1937 to the present year (2019) and captures a drainage area of 705 square miles (of which 420 square miles probably is noncontributing). As part of the Souris River Plan of Study (PoS), this streamflow record was back extended to 1930 (Reference 15). Both the observed record and the augmented daily streamflow record (1930-2017) are used to analyze trends and nonstationarities in flows along the Wintering River. Within the Wintering River watershed, there is some minimal regulation by Fish and Wildlife Service (USFWS) dams on Cottonwood and Wintering Lakes, which includes about 850 acre-feet of storage capacity. However, it is unlikely that these structures offer enough regulatory impacts to affect the stationarity of the streamflow record at Karlsruhe.

USGS gage 05113600 is located along the Long Creek near Noonan, ND; upstream of Boundary Reservoir. The Noonan gage has a continuous period of record of 1960 to the present year

(2019) and captures a drainage area of 1,790 square miles（of which 1,160 square miles probably is noncontributing).

USGS gage 04116500 is located on the Des Lacs River at Foxholm, ND. The Des Lacs gage has a continuous period of record of 1946 to the present year (2019) and captures a drainage area of 936 square miles (400 square miles of which is probably non-contributing.) The Des Lacs River above Foxholm, ND is impacted by the Des Lacs National Wildlife Refuge (NWR) structures. The structures were originally constructed in the 1930s to create eight impoundments. Each dike is equipped with water control structures to permit water level manipulations. The maximum storage capacity of the impoundments is 53, 879 acre-feet. However, control is limited and the impoundments are not currently operated for flood control.

Statistical tests are also applied to unregulated flow records developed as part of the Souris River Plan of Study, using observed streamflow data recorded at the USGS streamflow gage sites Souris River at Minot, ND (USGS 05117500) and Wintering River near Karlsruhe, ND (USGS gage 05120500). Annual peak streamflow timeseries are determined from a mean, daily streamflow record (Reference 15 & 17). Annual timeseries are calculated in water years, which begin October 1.

The same statistical tests are applied to Water Survey of Canada (WSC) gage 05NF002 located on Antler River near Melita, MB. The Antler River is one of the tributaries that flow into the mainstem of the Souris River in Manitoba. The Melita gage has been operated as a seasonal gage for the period 1943 to 1977, then it was operated as a continuous gage for the period 1978 to 1997, and then for the period 1998 to present year (2019) it has been operated as a seasonal gage. Seasonal operation of WSC gages begins March 1 and ends October 31. The Melita gage captures a drainage area of 3,220 square km. The R software package “tidyhydat” is used to download and process the streamflow data for the Melita gage.

4.1.1 Detection of Nonstationarities in Observed Annual Peak Streamflow Records

The USACE Nonstationarity Detection Tool (Reference 19) and USACE Timeseries Toolbox (Reference 20) are applied to determine whether or not the flows recorded in the Souris River Basin between 1930 and 2017 are representative of homogenous (stationary) hydro-climatic conditions.

4.1.1.1 Nonstationarity Detection Tool -“Pristine” Tributary Locations

Using the USACE Nonstationarity Detection Tool (Reference 19), a series of twelve statistical tests are applied to assess the stationarity of the observed, annual peak, flow record for USGS gage 05120500, located along the Wintering River near Karlsruhe, North Dakota (water years: 1937-2014). As can be seen in Figure 2, only the Energy Divisive (END) method detects a statistically significant change point in the flow record at Karlsruhe in 1969. Because only the END method is detecting a change point, the results of this assessment does not singularly, provide enough evidence to warrant rendering the flow record recorded at the Karlsruhe nonstationary. When the record back-extended to 1930 is analyzed through 2017 (Reference

15) using the Timeseries Toolbox a strong nonstationarity is detected in 1941 by the statistical tests Cramer von Mises (CVM), LePage (LP), and Mann Whitney (MW). Figure 3 provides the results from the Timeseries Toolbox (Reference 20) for the unregulated, annual peak streamflow for USGS gage 05120500. Since multiple distribution-based tests detect 1941 as nonstationary, 1941 meets the criteria of consensus. The detected nonstationarity in the Timeseries Toolbox is considered robust because mean and distribution-based tests are detecting the year 1941 in the record. The third criteria, a significant shift in magnitude, is met because a shift appears in the mean, variance, and standard deviation between the sub datasets 1930-1940 (mean= 30 cfs; variance= 910; standard deviation (std. dev.)= 30) and 1942-2017 (mean= 310 cfs; variance= 190,000; std. dev. = 440).

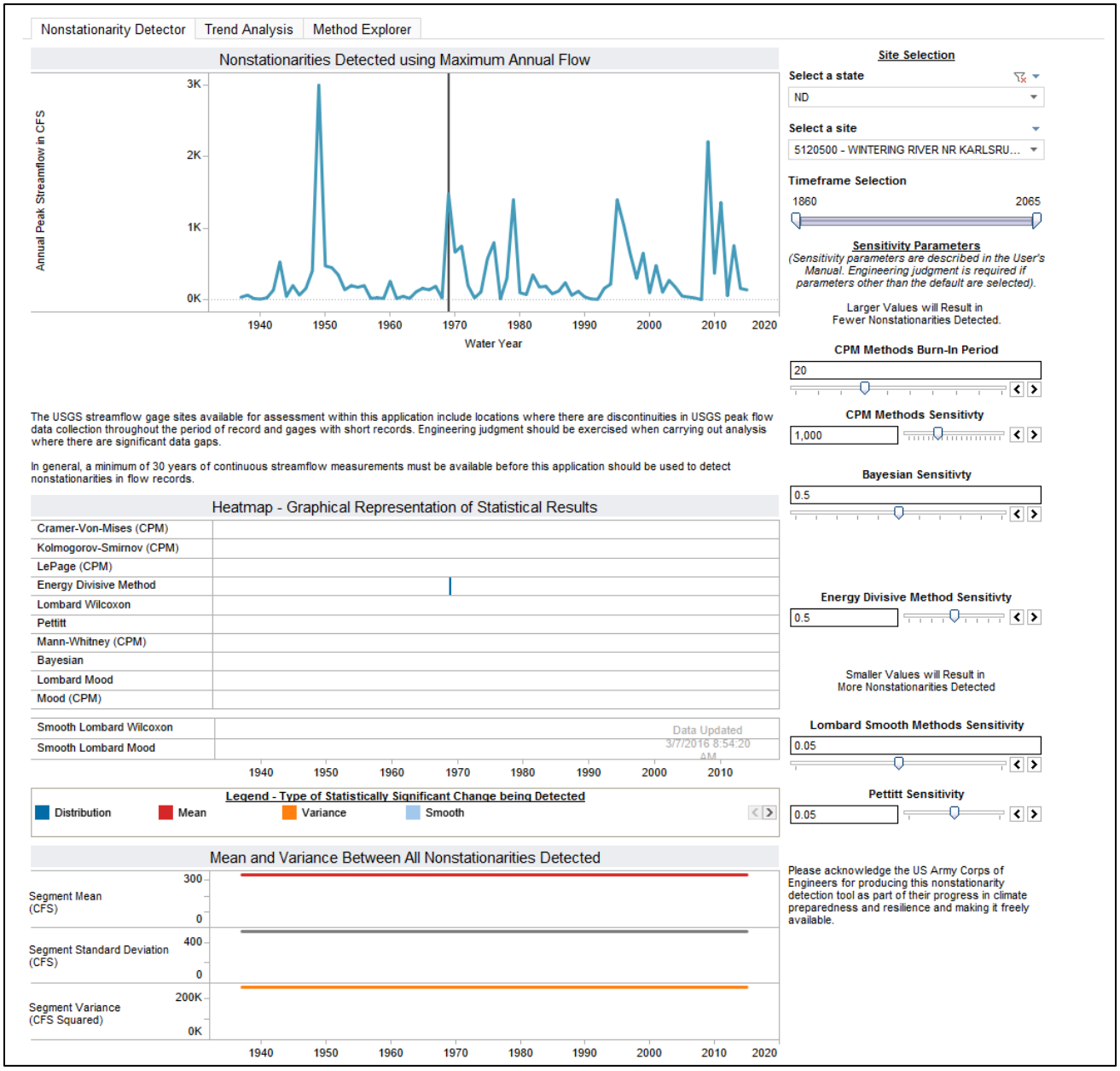

Figure 2. Nonstationarity analysis with Nonstationarity Detection Tool- annual peak flow- Wintering River near Karlsruhe, ND

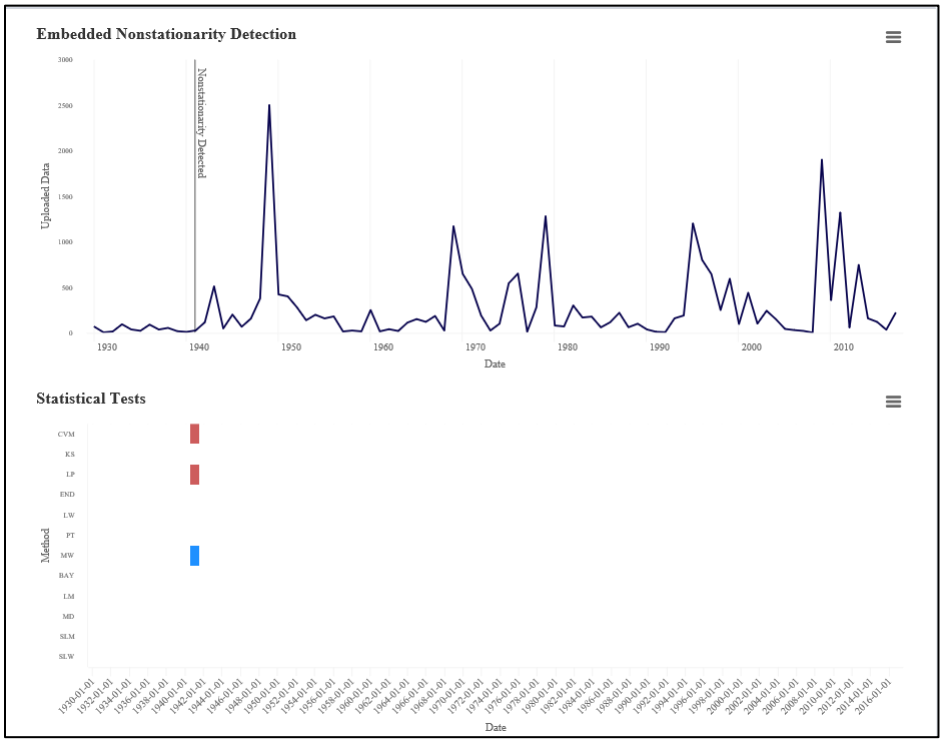

Type: Mean Distribution Variance Smooth

Note: y-axis is annual peak flow in cfs

Abbreviation	Statistical Method	Abbreviation	Statistical Method
CVM	Cramer-von-Mises	BAY	Bayesian
KS	Kolmogorov-Smirnov	LM	Lombard Mood
LP	LePage	MD	Mood
END	Energy Divisive	SLM	Smooth Lombard Mood
LW	Lombard Wilcoxon	SLW	Smooth Lombard Wilcoxon
PT	Pettitt	MW	Mann-Whitney

Figure 3. Nonstationarity Analysis with Timeseries Toolbox- Annual Peak Unregulated- Wintering River near Karlsruhe, ND

An assessment of stationarity is also carried out for the observed annual instantaneous peak flow record (water years: 1960-2014) collected at USGS gage 05113600, located along Long Creek near Noonan, ND. As can be seen in Figure 4, no statistically significant nonstationarities are detected within the flow record at Noonan.

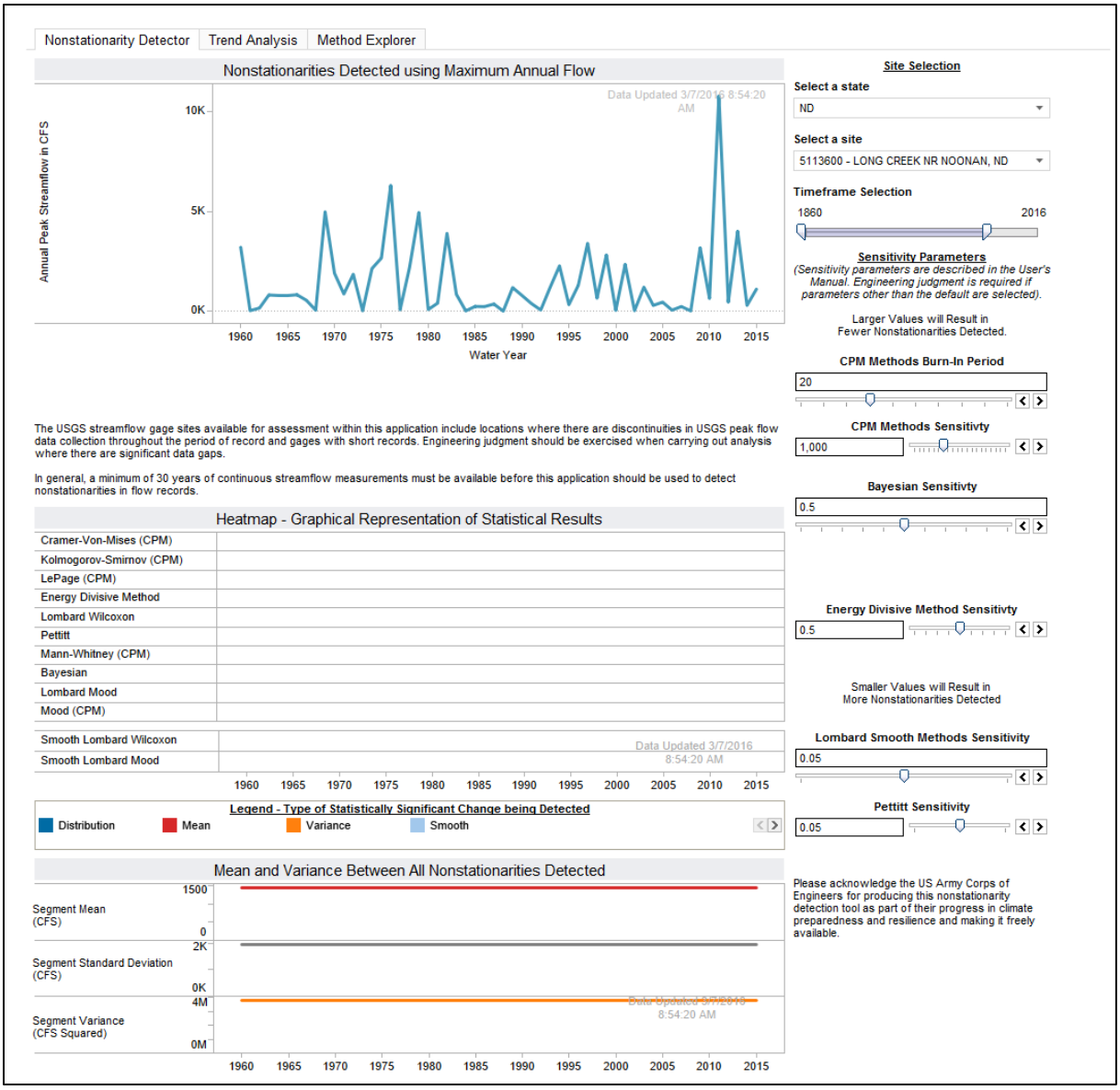

Figure 4. Nonstationarity analysis- annual peak flow- Long Creek near Noonan, ND

Using the USACE Nonstationarity Detection tool a series of twelve statistical tests are applied to assess the stationarity of the observed, annual instantaneous peak, flow record for the Des Lacs gage for water years 1946 to 2014. As can be seen in Figure 5 in 1980 a statistically significant changepoint in the dataset's overall statistical distribution is being detected by the END method. In 2003, the Lombard Mood (LM) abrupt and smooth tests are detecting a statistically significant change in the variance.

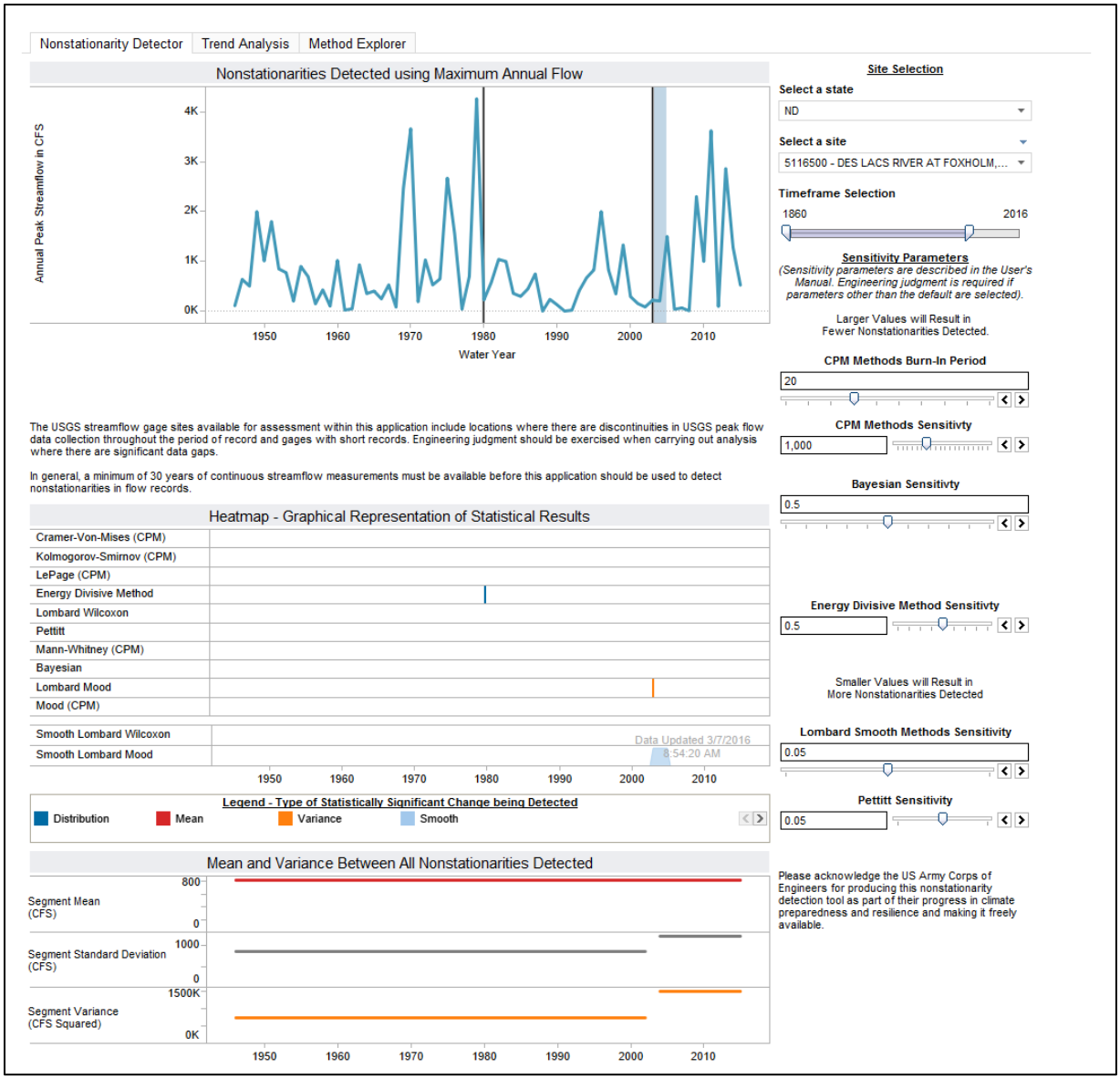

Figure 5. Nonstationarity analysis- annual peak flow -Des Lacs River at Foxholm, ND

Because only the END method is detecting a change point in 1980 and only the Lombard tests are detecting a change point in 2003, the results of this assessment do not singularly, provide enough evidence to warrant rendering the observed flow record on the Des Lacs River nonstationary.

4.1.1.2 Timeseries Toolbox- Unregulated Peak Records – Souris River Mainstem

To assess the stationarity of streamflow recorded on the mainstem of the Souris River, an unregulated record was developed as part of the Plan of Study to be representative of flows recorded at USGS gage 05117500, Souris River above Minot, ND. The USACE Timeseries Toolbox (Reference 20) is applied to generate this analysis because it facilitates user-inputted timeseries. Annual maximum flow timeseries is generated using HEC-DSSVue (Reference 2)

math functions that determine annual maximum streamflow from a mean daily flow timeseries. At the time of analysis, the Souris River Plan of Study Phase 2 HEC-ResSim (Reference 17) unregulated, model results were used as the source of this flow record.

Nonstationarity detection results for the period of analysis, water years 1930-2017, are displayed in Figure 6. A strong, nonstationarity is identified circa water year 1941. The Cramer-Von-Mises test (CVM; 1941), LePage test (LP; 1937), and Mann Whitney test (MW; 1941) all detect abrupt nonstationarities within a five-year span that encompasses 1941. Additionally, the Smooth Lombard Wilcoxon (SLW) test indicates that the mean of the dataset is in flux between 1935 and 1942.

The 1941 nonstationarity is considered strong because it demonstrates a degree of consensus, robustness and a significant shift in the magnitude of the dataset's statistical properties. The criteria of consensus are fulfilled because multiple tests targeted at detecting shifts in the distribution (CVM and LP) of the dataset are indicating a nonstationarity. The detected nonstationarity is considered robust because tests targeted at detecting abrupt shifts in multiple statistical properties, overall distribution and mean, are indicating 1941 as a nonstationarity. Additionally, the results presented by the Timeseries Toolbox indicate a significant shift in both the magnitude of the mean and standard deviation (variance) around 1941. The Timeseries Toolbox indicates a significant shift in the mean and variance of the data subsets: 1930-1934 (mean=490 cfs; variance= 160,000) and 1943-2017 (mean=3,300 cfs; variance=18,000,000). Note that the small number of years in the first subset of data could have an influence on the magnitude shift.

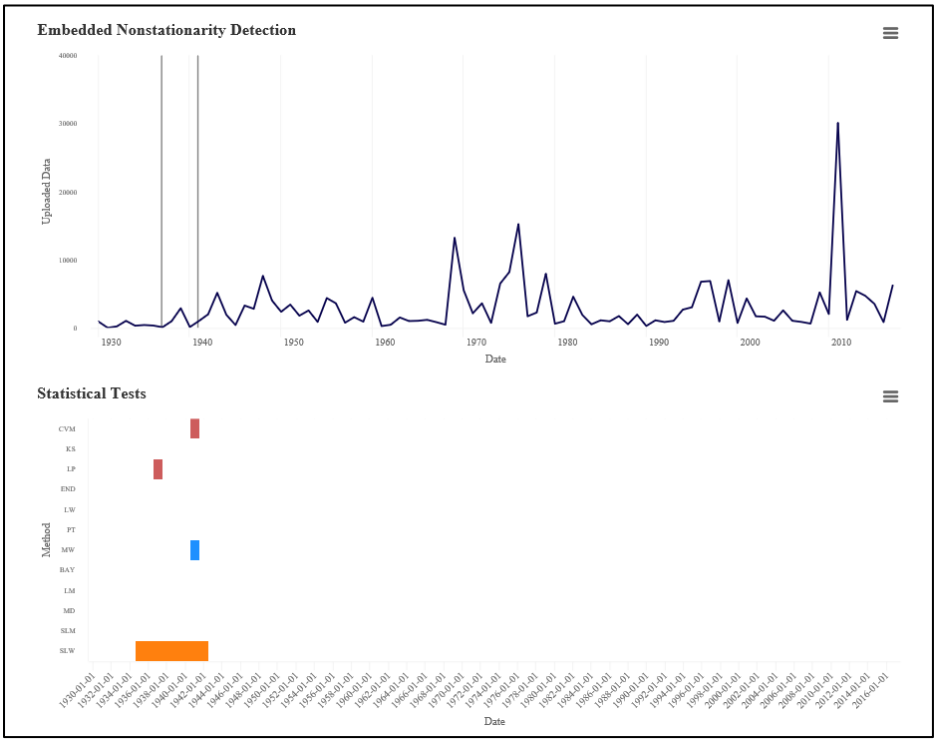

Type: Mean Distribution Variance Smooth

Note: y-axis is annual peak flow in cfs

Abbreviation	Statistical Method	Abbreviation	Statistical Method
CVM	Cramer-von-Mises	BAY	Bayesian
KS	Kolmogorov-Smirnov	LM	Lombard Mood
LP	LePage	MD	Mood
END	Energy Divisive	SLM	Smooth Lombard Mood
LW	Lombard Wilcoxon	SLW	Smooth Lombard Wilcoxon
PT	Pettitt	MW	Mann-Whitney

Figure 6. Nonstationarity analysis- annual peak unregulated- Souris River at Minot, ND

4.1.1.3 Nonstationarity Detection Tool – Antler River

The USACE Timeseries Toolbox (Reference 20) is used to detect nonstationarity for Antler River near Melita gage (WSC: 05NF002) for the water years 1943 to 2018. As seen in the Figure 7, no statistically significant nonstationarities are detected within the annual peak flow record at Melita.

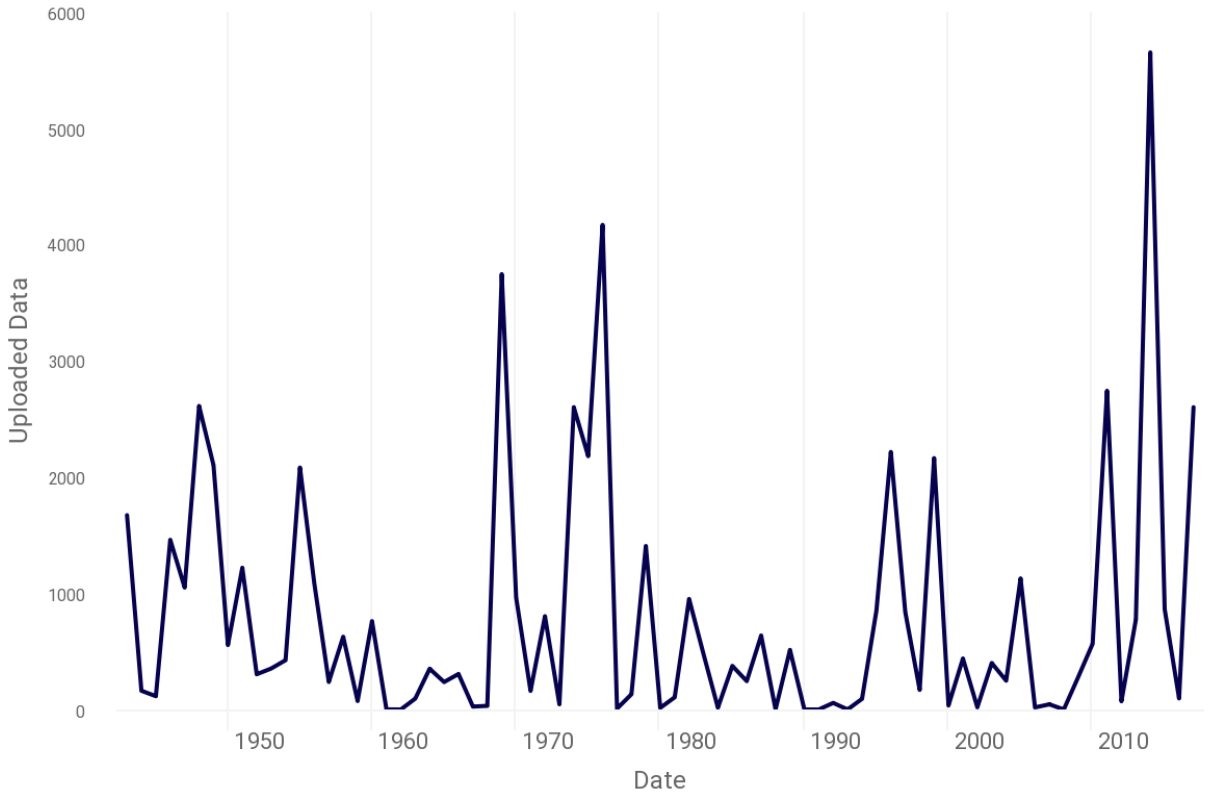

Figure 7. Nonstationarity analysis – annual peak streamflow – Antler River near Melita, MB

4.1.2 Detection of Nonstationarities in Seasonal Peak Streamflow Records

The USACE Timeseries Toolbox (Reference 20) is applied to determine whether nonstationarities are present within the seasonal streamflow peaks recorded along the Wintering River and the unregulated record approximated for the Souris River at Minot, ND. Seasonal, annual peak streamflow records are extracted from mean daily streamflow records based on month using Microsoft Excel. These annual timeseries are quantified in water years (beginning October 1). Seasons analyzed are spring (March- May), summer (June- August), and fall (September- November). Since the water year ends September 30, fall annual timeseries are analyzed in calendar years to incorporate September data within the timeseries of the sequential October and November. Winter flows are not assessed because flows over the winter months are not large enough to be operationally significant due to frozen basin conditions.

The majority of the period of record for the WSC gage for Antler River near Melita is operated as a seasonal gage from March- October. It is assumed that the majority of the fall flow will occur in September and October, and that the flows occurring in November are not large enough to be operationally significant. Therefore, the fall season will be assessed as

September- October for the Melita gage. Seasonal, annual peak streamflow records for the Melita gage are extracted from mean daily streamflow records based on month using R.

4.1.2.1 Timeseries Toolbox – Seasonal Unregulated Peak Records- Souris River Mainstem

The seasonal peak streamflow records are analyzed for nonstationarities using the unregulated Souris River at Minot, ND record for water years 1930-2017. No strong nonstationarities are detected in the spring annual peak streamflow dataset. For the summer, a nonstationarity is detected in 1942 by the Cramer-von-Mises (CVM), LePage (LP), and Mann-Whitney (MW) tests. The Mood test (MD; 1945 detection) detects a nonstationarity in 1945. Additionally, the Smooth Lombard Mood (SLM) indicates that the variance of the dataset is in flux between 1938 and 1947, see Figure 8 for results. 1942 is considered a strong nonstationarity because it meets the criteria of consensus, robustness, and magnitude. It meets consensus because multiple distribution-based statistical tests (CVM and LP) detected 1942 as a nonstationarity. The criteria of robustness is met because tests based on mean (MW), distribution (CVM & LP), and variance (MD, SLM) all detect 1942 as a nonstationary year. The USACE Timeseries Toolbox (Reference 20) indicates significant shifts in the magnitude of statistical properties between the 1930-1937 (mean=150 cfs; variance=75,000), 1948-1967 (mean=630 cfs; variance= 350,000) and 1969-2017 (mean=1600 cfs; variance= 18,000,000) subsets of data. The shift in magnitude occurs around the time of the 1942 nonstationarity, meeting the criteria of magnitude.

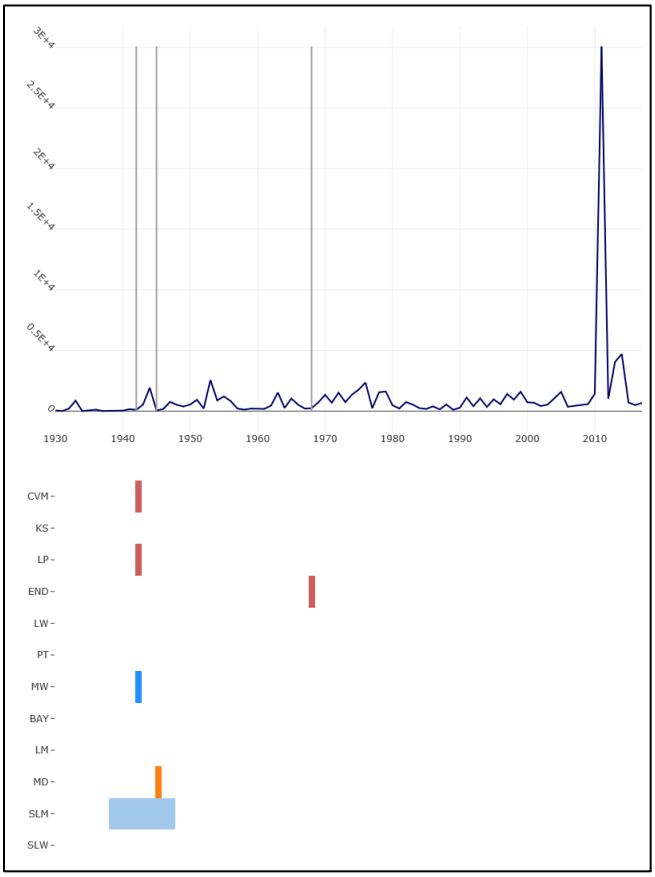

Type: Mean Distribution Variance Smooth

Note: y-axis is summer annual peak flow in cfs

Abbreviation	Statistical Method	Abbreviation	Statistical Method
CVM	Cramer-von-Mises	BAY	Bayesian
KS	Kolmogorov-Smirnov	LM	Lombard Mood
LP	LePage	MD	Mood
END	Energy Divisive	SLM	Smooth Lombard Mood
LW	Lombard Wilcoxon	SLW	Smooth Lombard Wilcoxon
PT	Pettitt	MW	Mann-Whitney

Figure 8. Nonstationarity analysis – unregulated peak summer flows -Souris River at Minot, ND

In the fall annual maximum streamflow record, nonstationarities are identified in 1941, 1945 and 1990 (Figure 9). The 1941 nonstationarity is detected by the CVM and MD statistical tests. The 1945 nonstationarity is detected by the LP and MW statistical tests. The 1990 nonstationarity is detected by the CVM, LP, and Energy Divisive (END) tests; with additional detections in 1989 by MW and Lombard Wilcoxon (LW) statistical tests. The SLM test indicates

a flux in the variance of the dataset between 1930 and 1945, while the Smooth Lombard Wilcoxon (SLW) test indicates a flux in mean between 1930 and 2010. The nonstationarities detected in 1990 exhibit consensus because multiple tests targeted at detecting changes in mean and variance are concurrently detecting it as a nonstationarity. 1941 and 1945 are within five years of each other and meet consensus of multiple distribution-based tests when observed together (CVM in 1941; LP in 1945). Multiple tests targeted at detecting changes in different statistical properties (distribution, mean, and variance) detect 1941, 1945 and 1990 as nonstationarities, meeting the criteria of robustness. With a SLM test indicating a gradual change of statistical properties over most of the fall maximum streamflow record (in years 1930-2010), the magnitude of abrupt shifts is not determined by the Timeseries Toolbox.

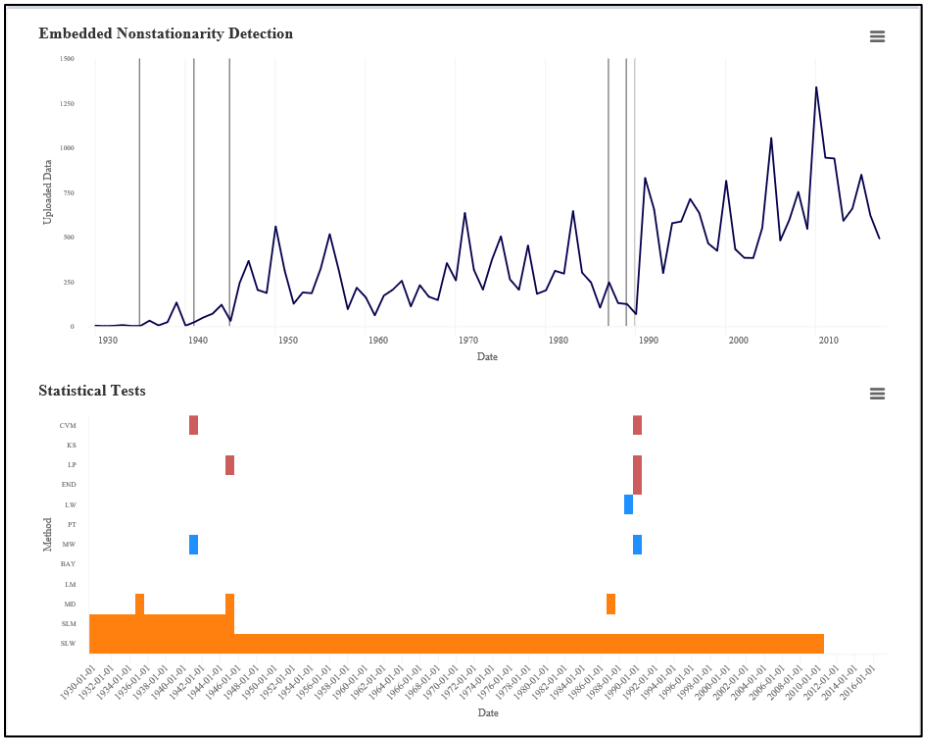

Type: Mean Distribution Variance Smooth

Note: y-axis is fall annual peak flow in cfs

Abbreviation	Statistical Method	Abbreviation	Statistical Method
CVM	Cramer-von-Mises	BAY	Bayesian
KS	Kolmogorov-Smirnov	LM	Lombard Mood
LP	LePage	MD	Mood
END	Energy Divisive	SLM	Smooth Lombard Mood
LW	Lombard Wilcoxon	SLW	Smooth Lombard Wilcoxon
PT	Pettitt	MW	Mann-Whitney

Figure 9. Nonstationarity analysis – unregulated peak fall flows -Souris River at Minot, ND.

4.1.2.2 Timeseries Toolbox – Seasonal Pristine Peak Records –Wintering River

Seasonal peak streamflow collected between water years 1930 and 2017 for the Wintering River at Karlsruhe, ND is tested for nonstationarities using the USACE Timeseries Toolbox (Reference 20). Similarly to the Souris River at Minot, ND, no nonstationarities are detected in the spring.

For summer peak streamflow, a nonstationarity is detected in 1992 by the Cramer-von-Mises (CVM), Energy Divisive (END), and Mann-Whitney (MW) statistical tests (Figure 10). This is considered a strong nonstationarity because it meets criteria of consensus (multiple distribution-based test detections), robustness (detection in distribution and mean-based tests), and the Timeseries Toolbox indicates a shift in the magnitude of mean circa 1992. The sub dataset 1930-1990 has a mean of 35 cfs then jumps to 100 cfs in the 1993-2017 sub dataset.

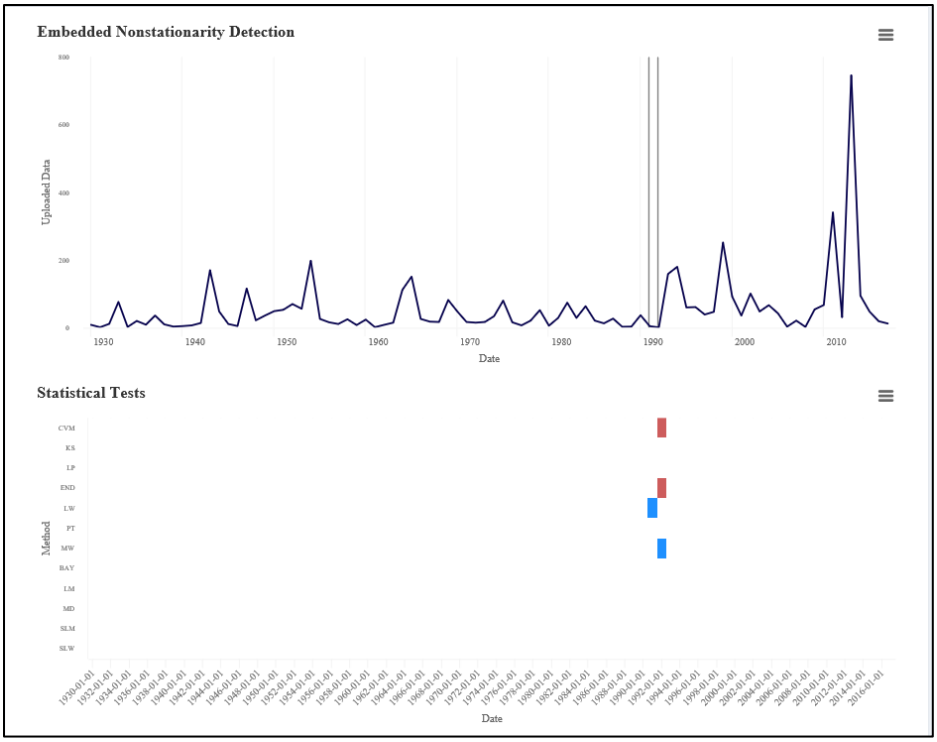

Type: Mean Distribution Variance Smooth

Note: y-axis is summer annual peak flow in cfs

Abbreviation	Statistical Method	Abbreviation	Statistical Method
CVM	Cramer-von-Mises	BAY	Bayesian
KS	Kolmogorov-Smirnov	LM	Lombard Mood
LP	LePage	MD	Mood
END	Energy Divisive	SLM	Smooth Lombard Mood
LW	Lombard Wilcoxon	SLW	Smooth Lombard Wilcoxon
PT	Pettitt	MW	Mann-Whitney

Figure 10. Nonstationarity analysis – peak summer flows -Wintering River near Karlsruhe, ND.

A nonstationarity is identified in 1940 within the fall annual peak streamflow data (Figure 11). Statistical tests identifying the 1940 nonstationarity include: LePage (LP; 1940), END (1940), Mood (MD; 1940), CVM (1939), and MW (1939). Additionally, the Smooth Lombard Mood (SLM) test indicates a flux in variance between 1935 and 1940. In accordance with USACE Engineering Technical Letter (ETL) 1100-2-3 (Reference 4), a smooth Lombard detection over a five-year (or less) span can be used to support an abrupt change, nonstationarity detection. Multiple distribution based tests (CVM, LP, and END) reach consensus in detecting 1940 as a nonstationarity. 1940 is considered a robust nonstationarity because it is detected by tests targeting changes in mean (MW), distribution (LP, END, CVM), and variance (MD, SLM). The Timeseries Toolbox also indicates a shift in the magnitude of mean and variance between the

sub datasets 1930-1934 (mean=0.57 cfs; variance=0.31) and 1941-1958 (mean=11 cfs; variance=100).

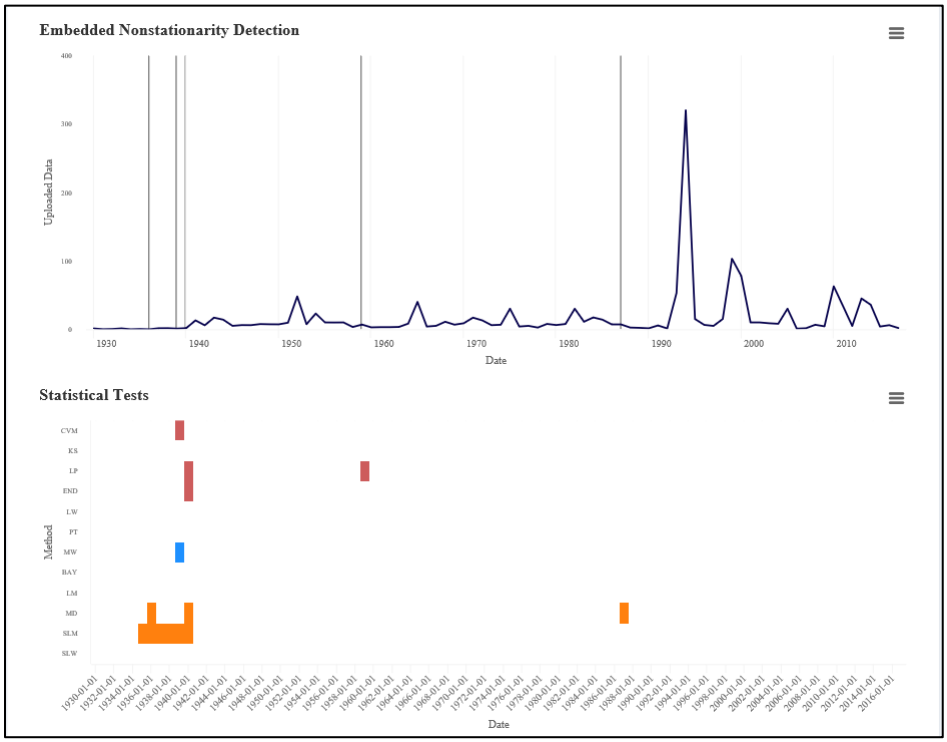

Type: Mean Distribution Variance Smooth

Note: y-axis is fall annual peak flow in cfs

Abbreviation	Statistical Method	Abbreviation	Statistical Method
CVM	Cramer-von-Mises	BAY	Bayesian
KS	Kolmogorov-Smirnov	LM	Lombard Mood
LP	LePage	MD	Mood
END	Energy Divisive	SLM	Smooth Lombard Mood
LW	Lombard Wilcoxon	SLW	Smooth Lombard Wilcoxon
PT	Pettitt	MW	Mann-Whitney

Figure 11. Nonstationarity analysis – peak fall flows -Wintering River near Karlsruhe, ND.

4.1.2.3 Timeseries Toolbox Seasonal Pristine Peak Records – Antler River

The USACE Timeseries Toolbox (Reference 20) is used to detect nonstationarities in the seasonal peak streamflow between 1943 and 2018 for Antler River near Melita, MB. For the spring peak streamflow, no statistically significant nonstationarities are detected.

For the summer peak streamflow, no strong nonstationarities were detected. Several tests indicate change points in: 1956 (MW), 1957 (LP), 1968 (MW), 1976 (CVM and MW), 1994 (CVM and MW), and 2009 (LP). However, none of these meet the criteria of consensus, and robustness; see Figure 12.

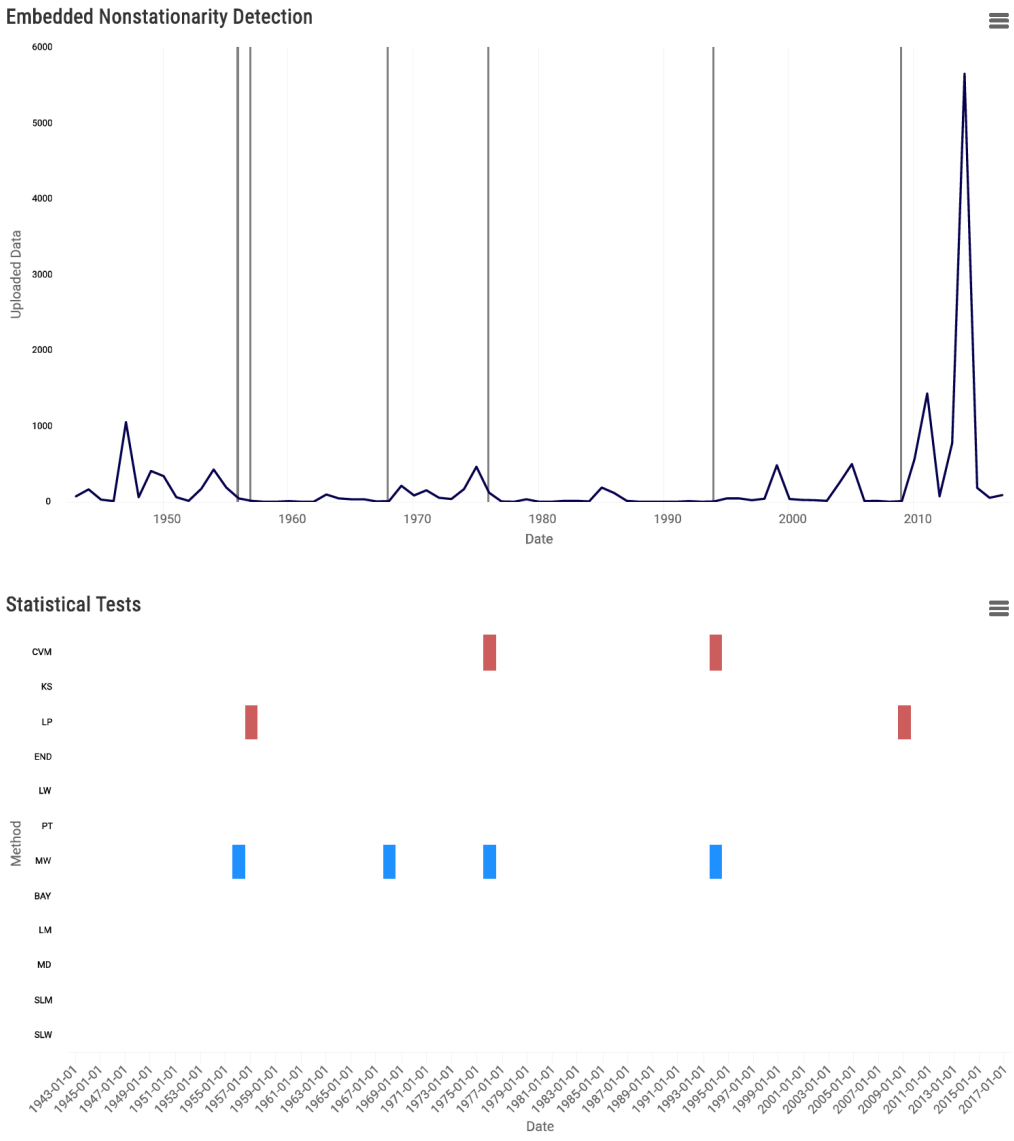

Note: y-axis is summer peak flow in cfs

Abbreviation	Statistical Method	Abbreviation	Statistical Method
CVM	Cramer-von-Mises	BAY	Bayesian
KS	Kolmogorov-Smirnov	LM	Lombard Mood
LP	LePage	MD	Mood
END	Energy Divisive	SLM	Smooth Lombard Mood
LW	Lombard Wilcoxon	SLW	Smooth Lombard Wilcoxon
PT	Pettitt	MW	Mann-Whitney

Figure 12. Nonstationarity analysis – peak summer flows – Antler River near Melita, MB

For fallfall peak streamflow, a strong nonstationarity is detected in 2009 by the Cramer-von-Mises (CVM; 2009 detection), LePage (LP; 2006 detection), Lombard Wilcoxon (LW; 2008 detection), Mann-Whitney (MW; 2009 detection), and Lombard Mood (LM; 2011 detection), see Figure 13. This nonstationarity exhibits consensus because multiple tests targeted at detecting changes in distribution and mean are detecting nonstationarity within a 5 year span. It shows robustness because multiple test targeted at different statistical properties are detecting nonstationarity within a 5 year span.

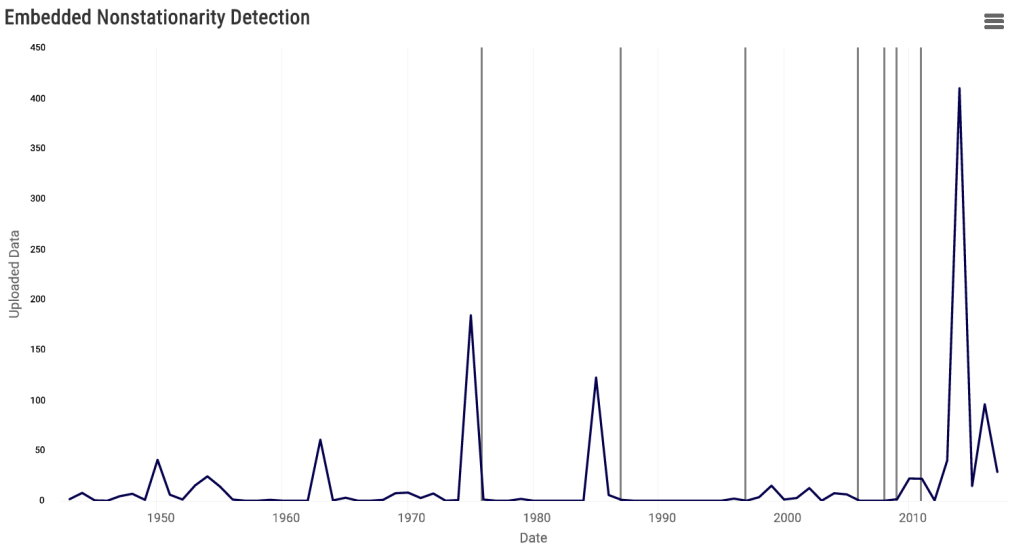

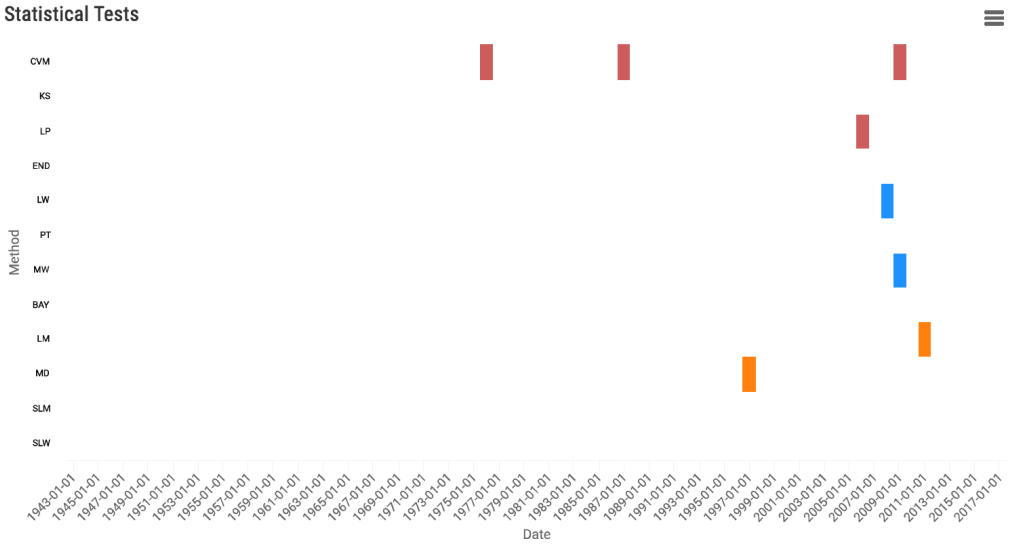

Type: Mean Distribution Variance Smooth

Note: y-axis is fall peak flow in cfs

Abbreviation	Statistical Method	Abbreviation	Statistical Method
CVM	Cramer-von-Mises	BAY	Bayesian
KS	Kolmogorov-Smirnov	LM	Lombard Mood
LP	LePage	MD	Mood
END	Energy Divisive	SLM	Smooth Lombard Mood
LW	Lombard Wilcoxon	SLW	Smooth Lombard Wilcoxon
PT	Pettitt	MW	Mann-Whitney

Figure 13. Nonstationarity analysis – peak fall flows – Antler River near Melita

4.1.3 Detection of Trends in Observed Annual Peak Streamflow Records

In addition to testing for nonstationarity, a monotonic trend analysis is carried out using linear regression, the t-Test, Mann-Kendall, and the Spearman Rank Order test at all streamflow gage sites analyzed. At the pristine, gaged locations on tributaries to the Souris River, the USACE Climate Hydrology Assessment Tool (Reference 18) is used to apply a linear regression to the peak annual discharges and the USACE Nonstationarity Detection Tool (Reference 19) is used to apply the Mann-Kendall and Spearman Tests. At Minot, where unregulated flows are analyzed and for the Antler River near Melita, Microsoft Excel is used to apply a linear regression analysis to the peak annual streamflow and the USACE Time Series Toolbox (Reference 20) is used to apply the t-Test, Mann-Kendall, and Spearman Tests.

4.1.3.1 Analysis at "Pristine" Tributary Gage Sites – Trend Analysis

For the three tributary gage locations analyzed: Wintering River, Long Creek and Des Lacs River, the results of the linear regression analysis are displayed in Figure 14, Figure 15, and Figure 16. The p-values associated with the trend lines determined for all three tributary locations are greater than 0.05. This indicates that the trend lines do not have a statistically significant slope at the 95% level of confidence. The results derived using the USACE Nonstationarity Detection Tool (Reference 19) to perform Mann Kendall Tests and Spearman Tests for the tributary gage locations are consistent with the results derived using simple linear regression. There are no trends in the annual peak streamflow datasets observed along the Wintering River, Long Creek and the Des Lacs River.

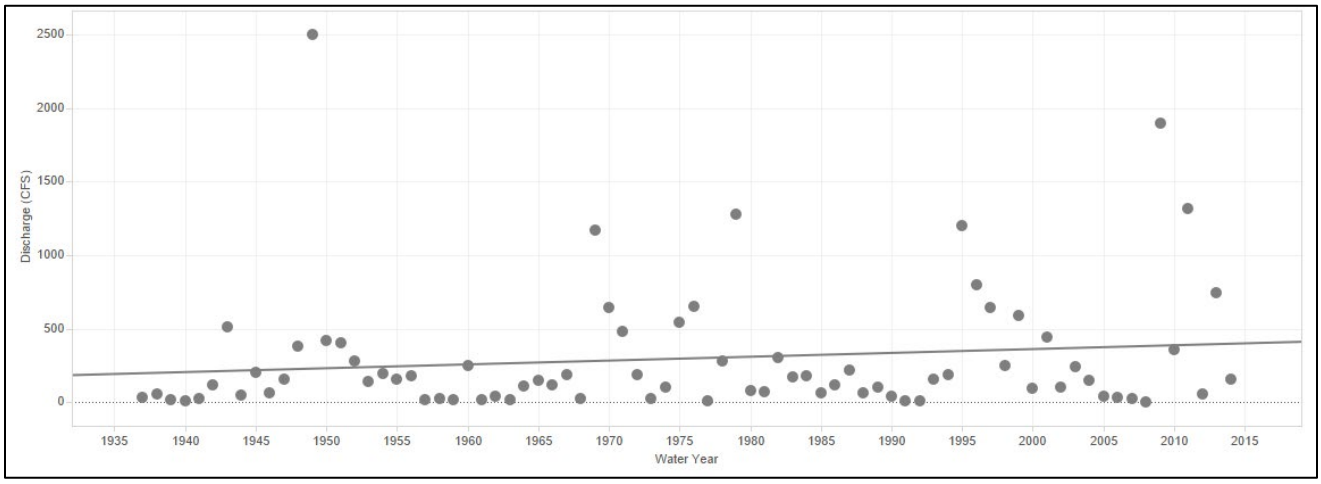

Figure 14. Trend analysis- annual peak streamflow - Wintering River near Karlsruhe, ND 1937-2014; p-value = 0.237

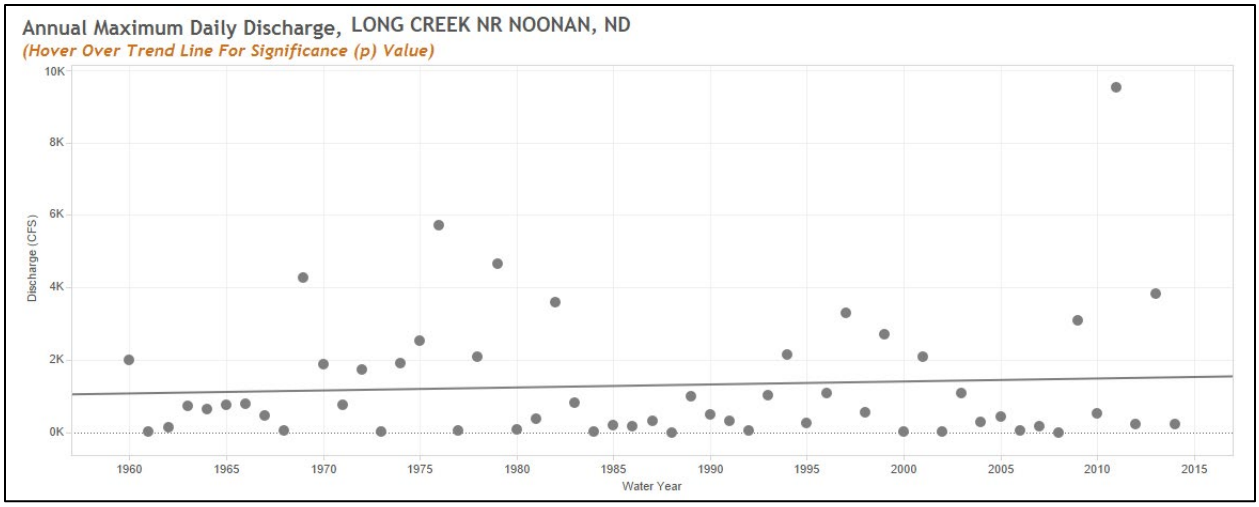

Figure 15. Trend analysis- annual peak streamflow - Long Creek near Noonan, ND; p-value = 0.588

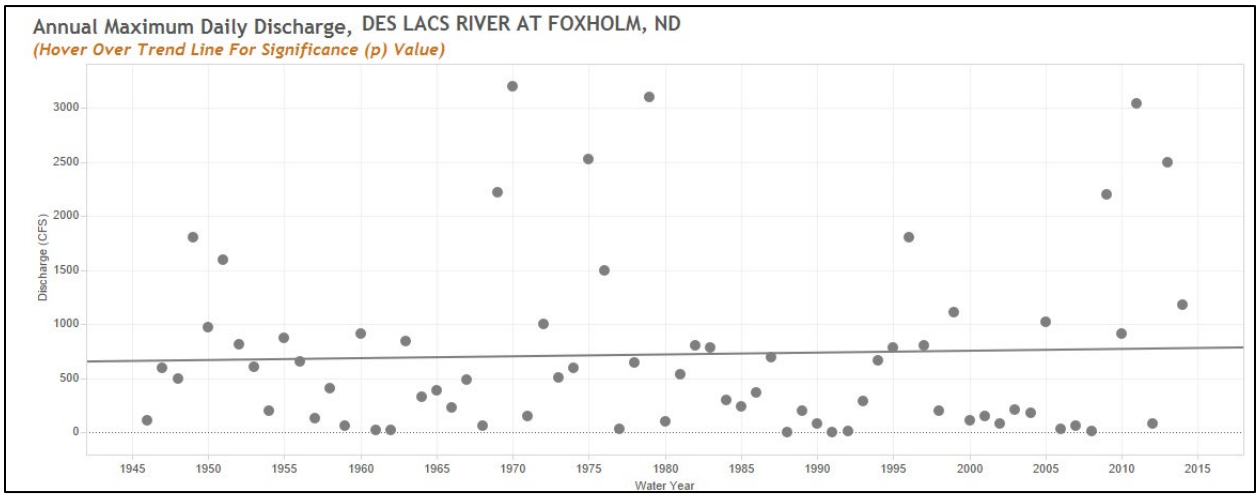

Figure 16. Trend analysis- annual peak streamflow - Des Lacs River at Foxholm, ND; p-value = 0.727

When the extended record (1930-2017) for annual peak flows at the Wintering River near Karlsruhe, ND (Reference 15) are analyzed with the USACE Timeseries Toolbox (Reference 20), the Mann-Kendall (p-value= 0.034) and Spearman Rank-Order (p-value= 0.027) statistical tests detect a statistically significant trend. The t-Test (p-value= 0.126) and linear regression in Excel (p-value= 0.147) do not indicate a trend (Figure 17).

Linear regression analysis at the detect nonstationarity in 1941 does not indicate a significant trend in either the datasets prior to the nonstationarity (1930-1940; p-value= 0.614) or after 1941 (1942-2017; p-value= 0.773).

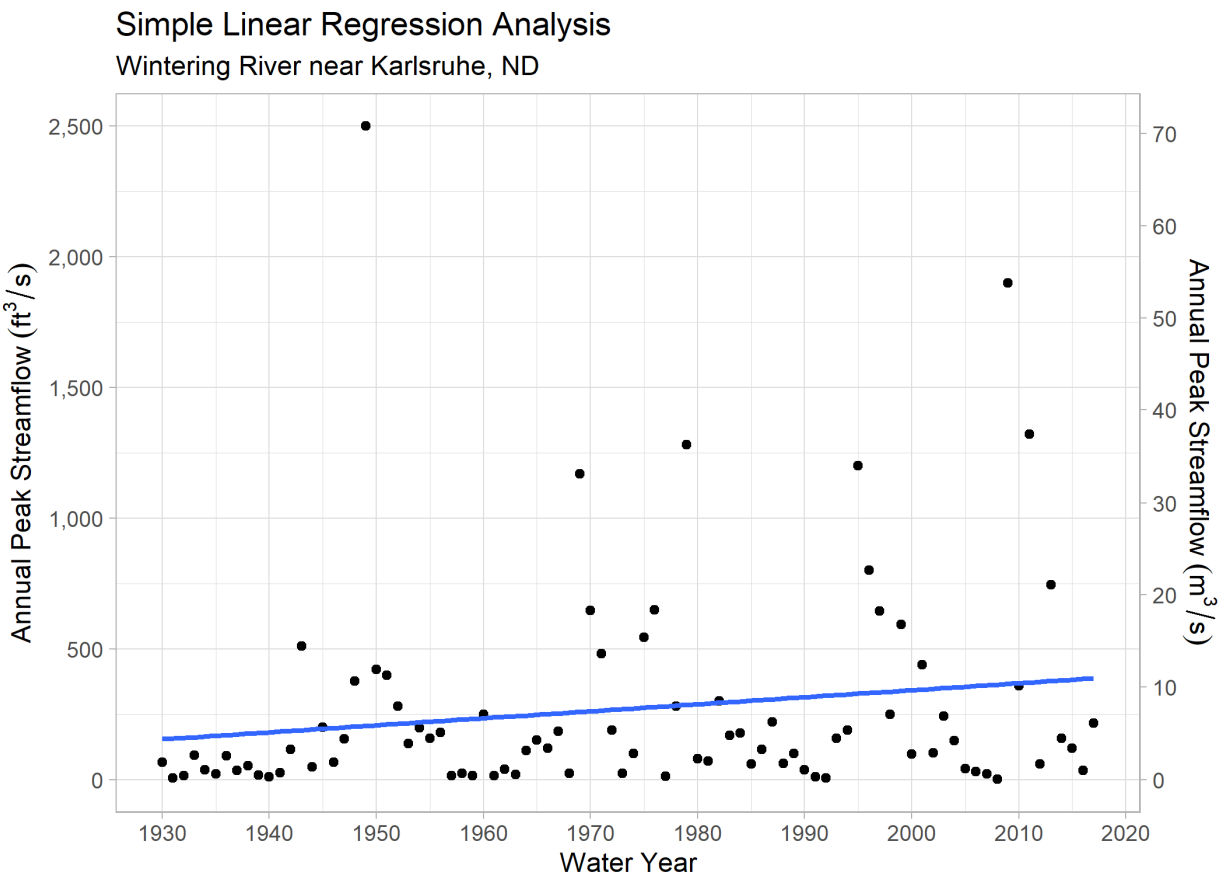

Figure 17. Trend analysis - annual unregulated peak streamflow - Wintering River near Karlsruhe 1930-2017, ND; p-value 0.1466.

4.1.3.2 Unregulated Souris River Mainstem – Trend Analysis

For the annual maximum unregulated streamflow record (1930-2017) at Minot, ND, trend analysis indicates a significant increasing trend using the t-Test (p-value=0.036), Mann-Kendall (p-value=0.013), Spearman Rank-Order (p-value=0.012), and linear regression (p-value=0.045) tests. Figure 18 shows the plot of annual maximum streamflow for the full period of record analyzed using linear regression in Microsoft Excel. When the streamflow record is subdivided into pre- and post-nonstationarity datasets, no statistically significant trends are detected in either dataset (1930-1940 p-value=0.382; 1942-2017 p-value=0.348).

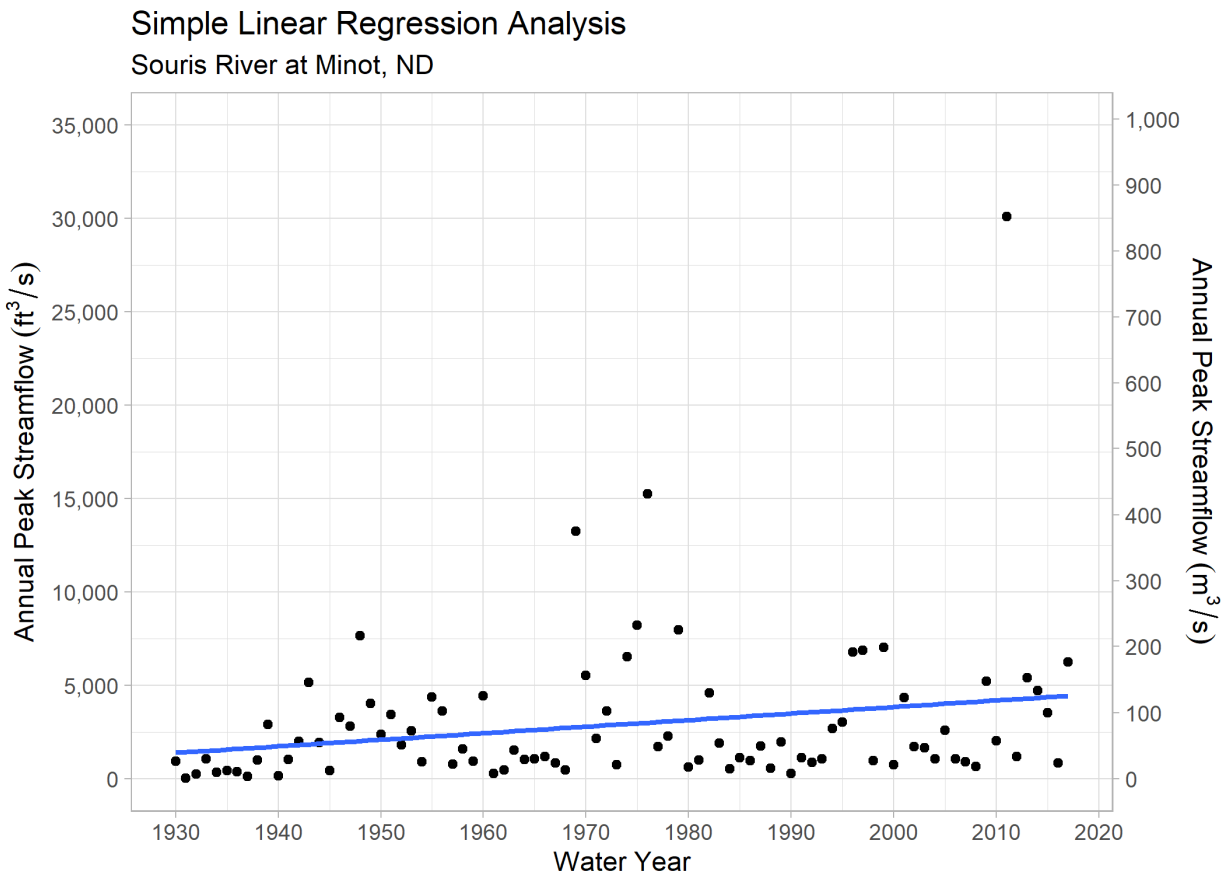

Figure 18. Trend analysis - annual unregulated peak streamflow - Souris River at Minot, ND; p-value 0.0446

4.1.3.3 Analysis at Antler River – Trend Analysis

For the tributary gage analyzed at Antler River near Melita, the results of the linear regression analysis are displayed in the Figure 19. The p-value determined for the trend line is 0.975. This indicates that the trend line does not have a statistically significant slope at a 95% level of confidence, since the p-value is greater than 0.05. The USACE Time Series Toolbox (Reference 20) was also used to perform a t-Test (p-value =0.921) Mann Kendall Test (p-value = 0.330), and Spearman Rank-Order Test (p-value = 0.362) on the Melita gage. These results are consistent with the results of the simple linear regression. There is no trend in the annual peak streamflow data set observed along Antler River near Melita, MB.

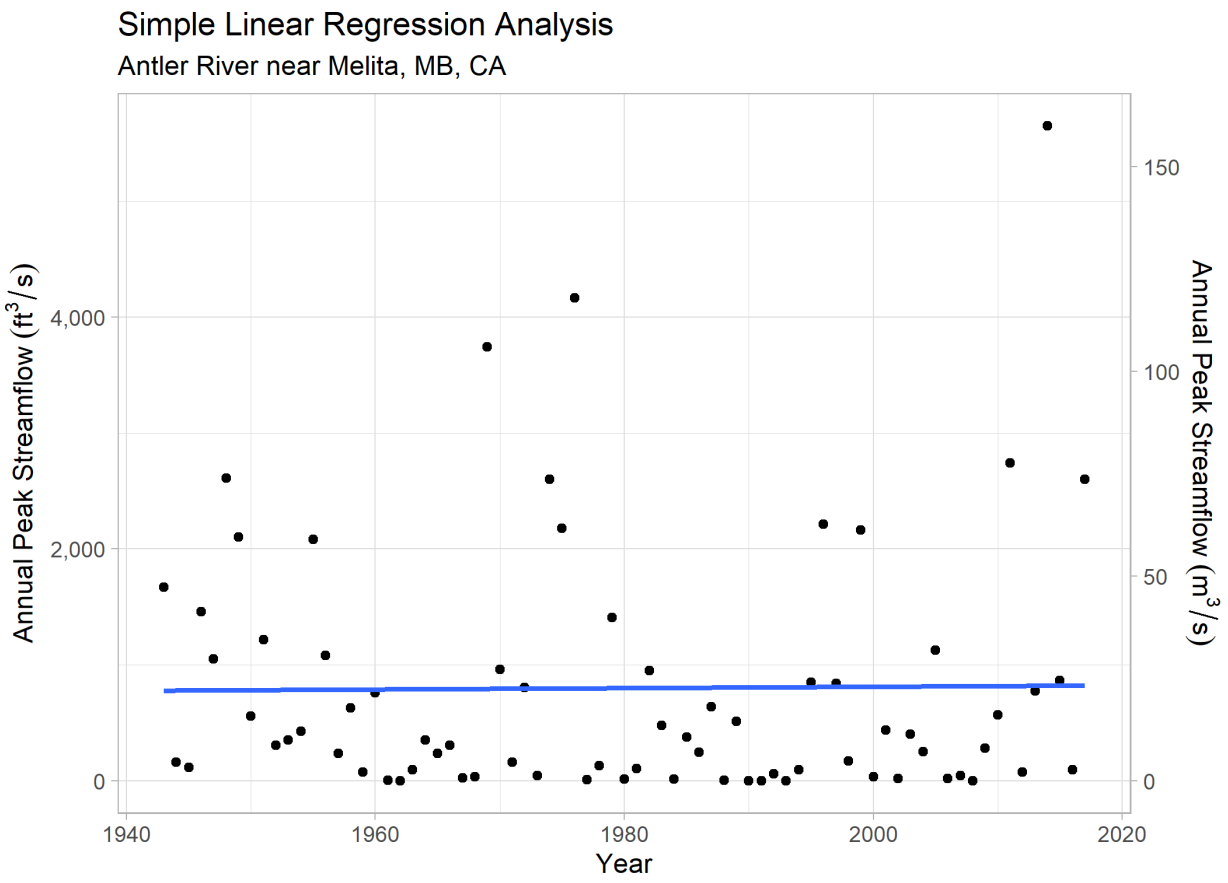

Figure 19. Trend analysis – annual peak streamflow – Antler River near Melita, MB; p-value 0.975

4.1.4 Detection of Trends in Seasonal Annual Peak Streamflow Records

The USACE Timeseries Toolbox (Reference 20) and Microsoft Excel are applied to determine whether trends are present within the seasonal streamflow peaks recorded along the Wintering River and the unregulated, seasonal peak, streamflow records approximated for the Souris River at Minot, ND. Seasonal, annual peak streamflow records are extracted from daily streamflow based on month using Microsoft Excel. Seasons analyzed are spring (March- May), summer (June- August), and fall (September- November). Winter flows are not assessed because flows over the winter months are not large enough to be operationally significant due to frozen basin conditions.

The majority of the period of record for the WSC gage for Antler River near Melita is operated as a seasonal gage from March- October. It is assumed that the majority of the fall flow will occur in September and October, and that the flows occurring in November are not large enough to be operationally significant. Therefore, the fall season will be assessed as September- October for the Melita gage. Seasonal, annual peak streamflow records for the Melita gage are extracted from mean daily streamflow records based on month using R.

4.1.4.1 Seasonal Trend Analysis- Unregulated Souris River Mainstem

Seasonal trend analysis on the annual peak, unregulated streamflow timeseries for Minot, ND is performed using the period of analysis: 1930 through 2017. In the spring peak streamflow record, the Mann-Kendall (p-value= 0.037) and Spearman Rank-Order (p-value=0.040) detect a statistically significant increasing trend, however, the t-Test (p-value=0.080) and simple linear regression test does not detect a statistically significant trend (p-value= 0.099), see Figure 20.

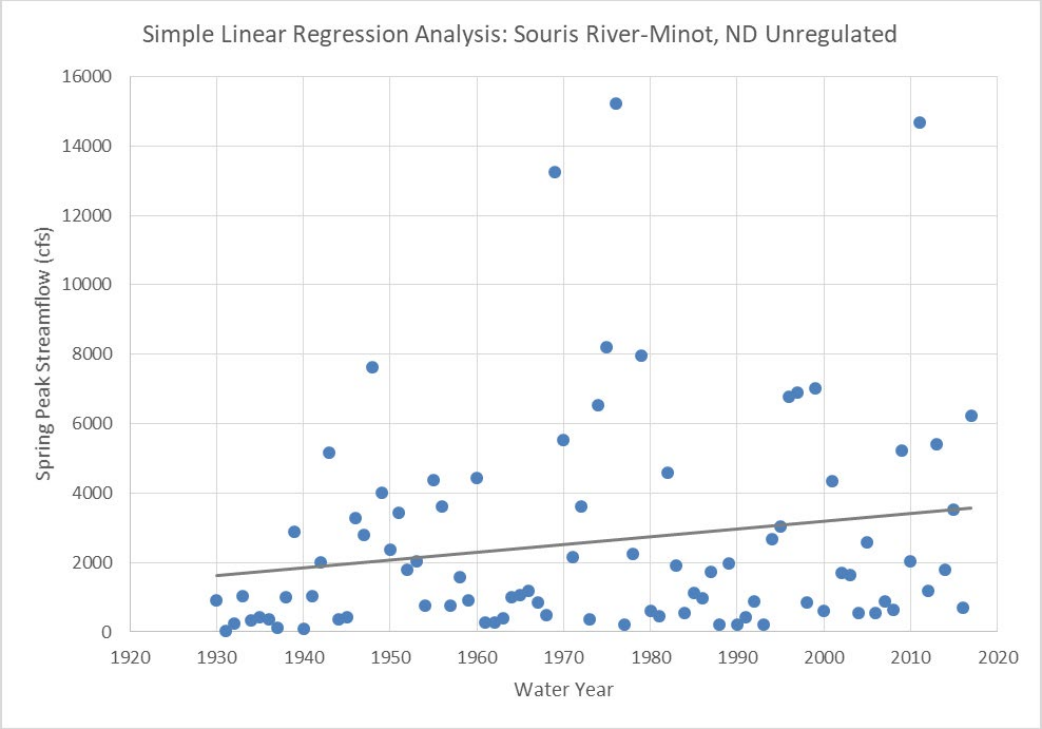

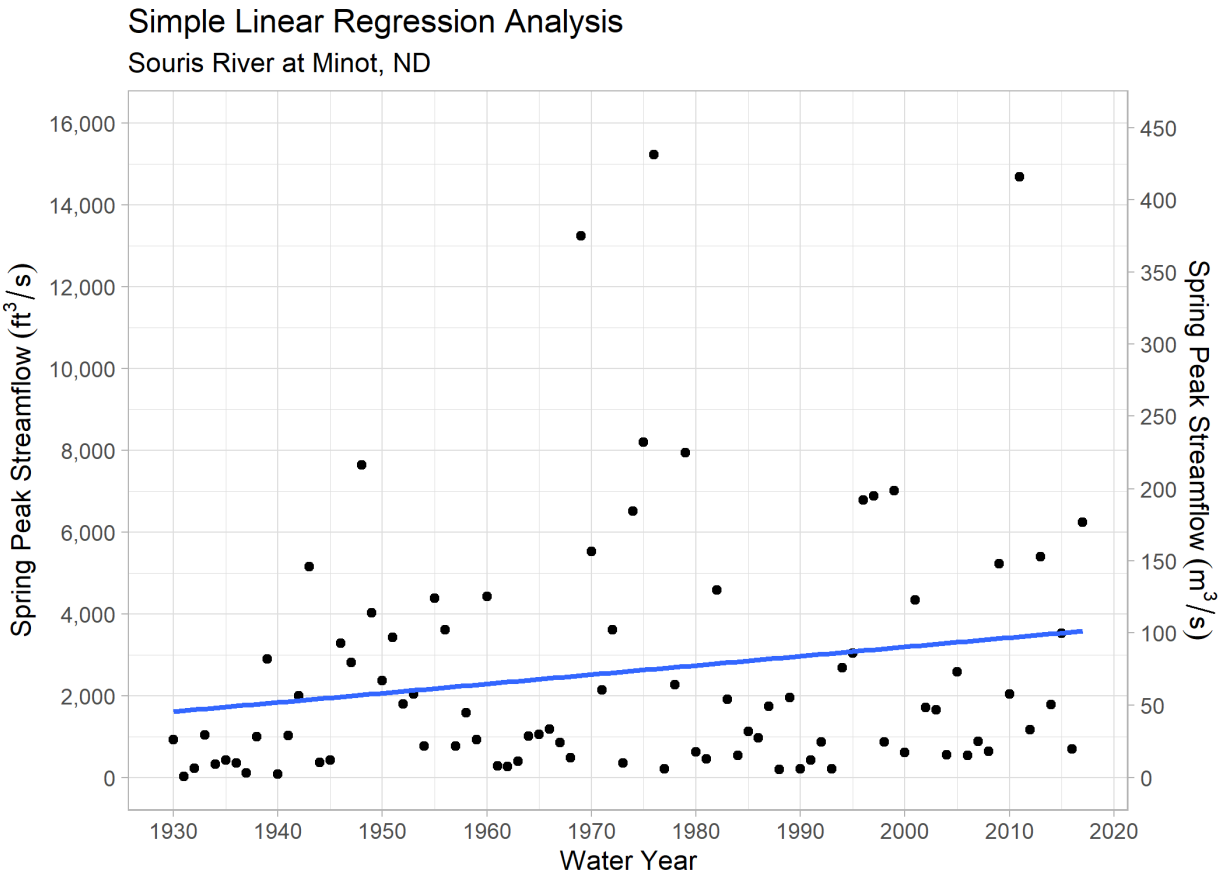

Figure 20. Trend analysis - spring, unregulated peak streamflow - Souris River at Minot, ND; p-value 0.099.

Trend analysis applied to summer, unregulated peak streamflow record approximated for the Souris River at Minot, ND indicates a statistically significant, increasing trend. The t-Test (p-value=0.025), Mann-Kendall (p-value= 2.27×10^{-6}), Spearman Rank-Order (p-value= 3.77×10^{-6}), and simple linear regression (p-value=0.027) methods all identify a statistically significant trend. Figure 21 displays a plot of the summer peak flow data analyzed using simple linear regression. In addition to assessing the full period of record, analysis was applied to the portion of the period of record prior to and after the nonstationarity detected in summer peaks. There are not statistically significant trends in summer peak flows in the pre-nonstationarity dataset (1930-1941; p-value=0.532) or the post-nonstationarity dataset (1943-2017; p-value=0.075).

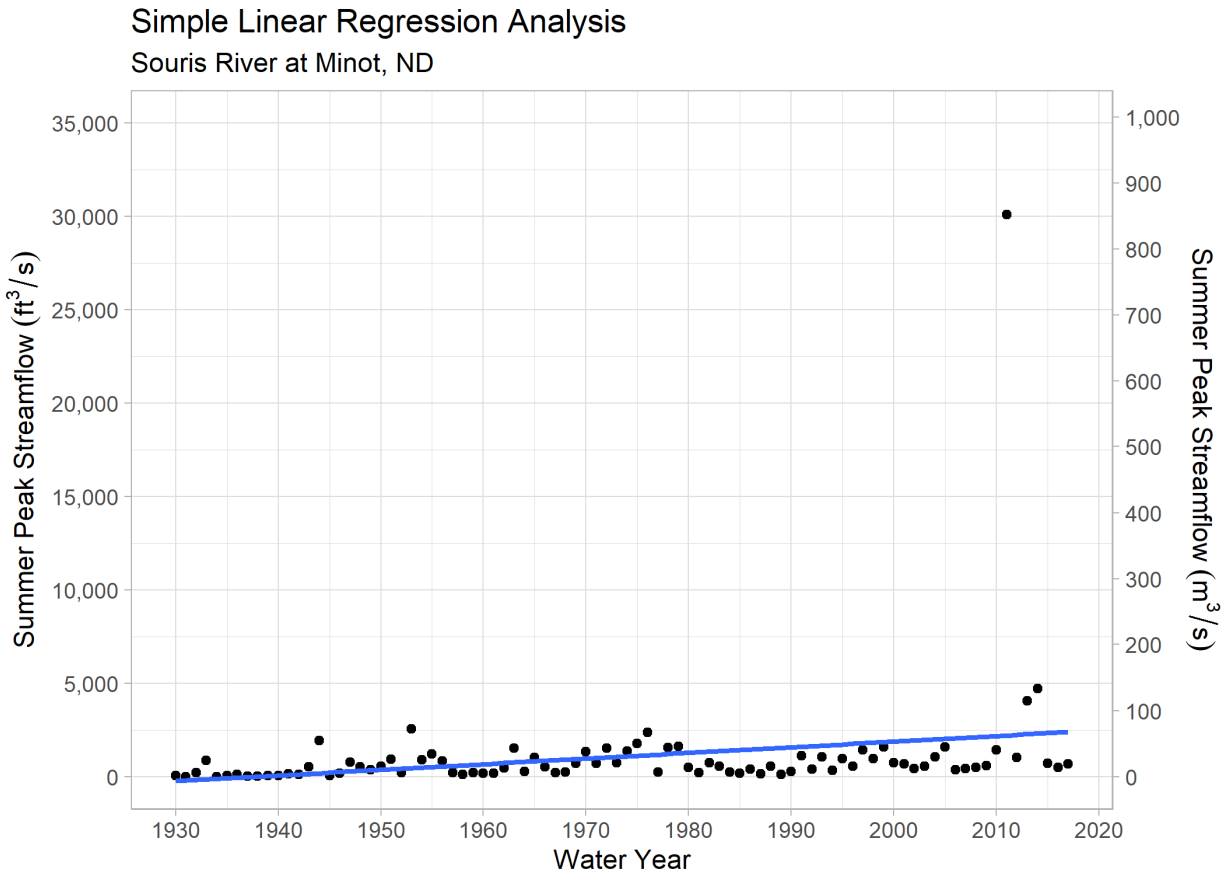

Figure 21. Trend analysis – summer, unregulated peak streamflow - Souris River at Minot, ND; p-value= 0.027.

For trend analysis on the fall peak streamflow record, a statistically significant, increasing trend is detected by the t-Test (p-value=2.25×10^{-17}), Mann-Kendall (p-value= 2.2×10^{-16}), Spearman Rank-Order (9.26×10^{-20}), and simple linear regression (p-value= 6.36×10^{-17}) tests (see Figure 22). Linear regression analysis is also conducted for the detected, strong nonstationarities in 1941 and 1990. In 1941 the pre-nonstationarity dataset does not indicate a statistically significant trend (1930-1940; p-value=0.140), but a statistically significant increasing trend is identified in the post-1941 dataset (1942-2017; p-value=5.51×10^{-9}). The 1990 nonstationarity exhibits a

statistically significant increasing trend prior to 1990 (1930-1989; p-value=2.45×10^{-5}), but not in the data collected post-1990 (1991-2017; p-value= 0.189).

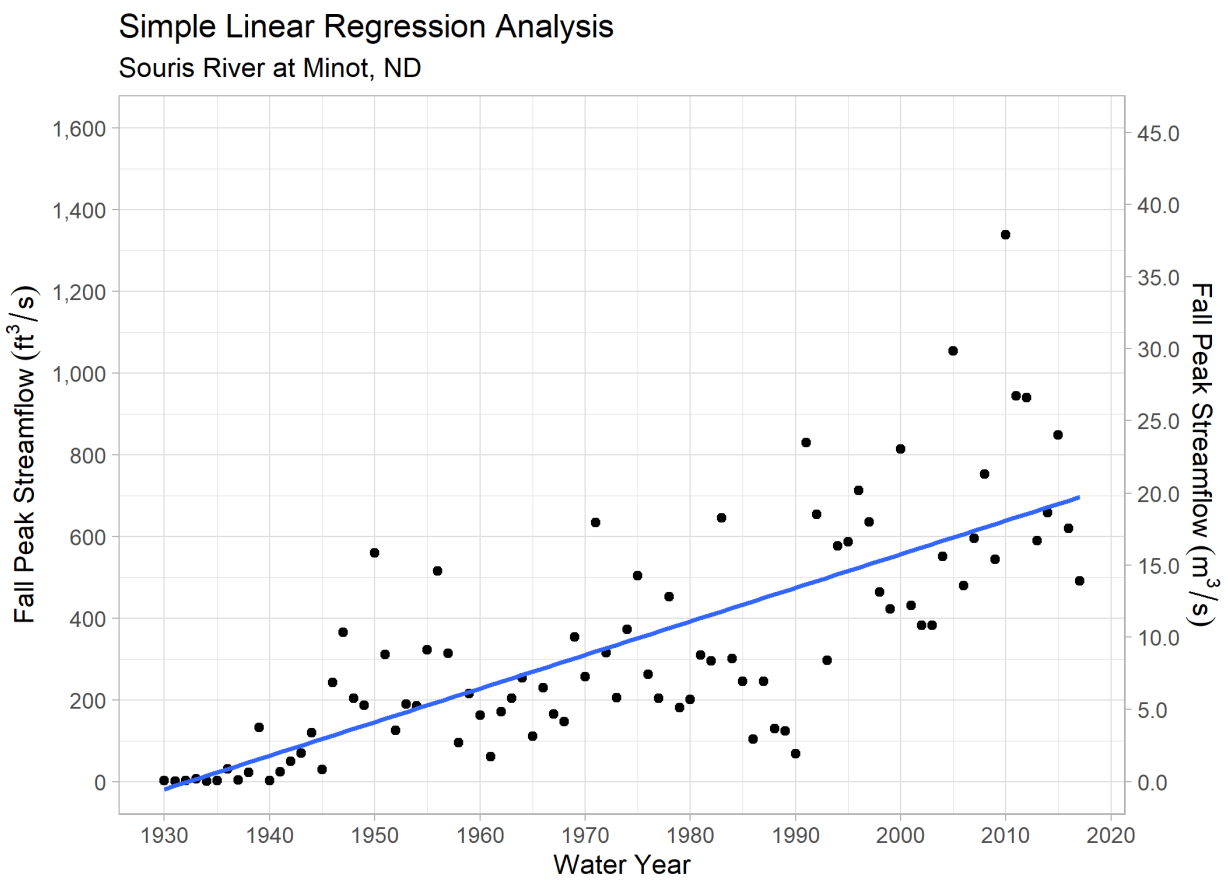

Figure 22. Trend analysis – fall, annual unregulated peak streamflow - Souris River at Minot, ND; p-value= 6.36×10^{-17}

4.1.4.2 Seasonal Trend Analysis – Wintering River

Seasonal trend analysis is performed on the annual peak streamflow timeseries for the Wintering River in Karlsruhe, ND based on the extended mean daily streamflow period of record from 1930 to 2017 (Reference 15). No statistically, significant trends in spring annual peaks are indicated by the t-Test (p-value=0.251), Mann-Kendall (p-value= 0.106), Spearman Rank-Order (p-value= 0.093), or simple linear regression (p-value= 0.195) statistical tests. Refer to Figure 23 for plotted data of the spring record.

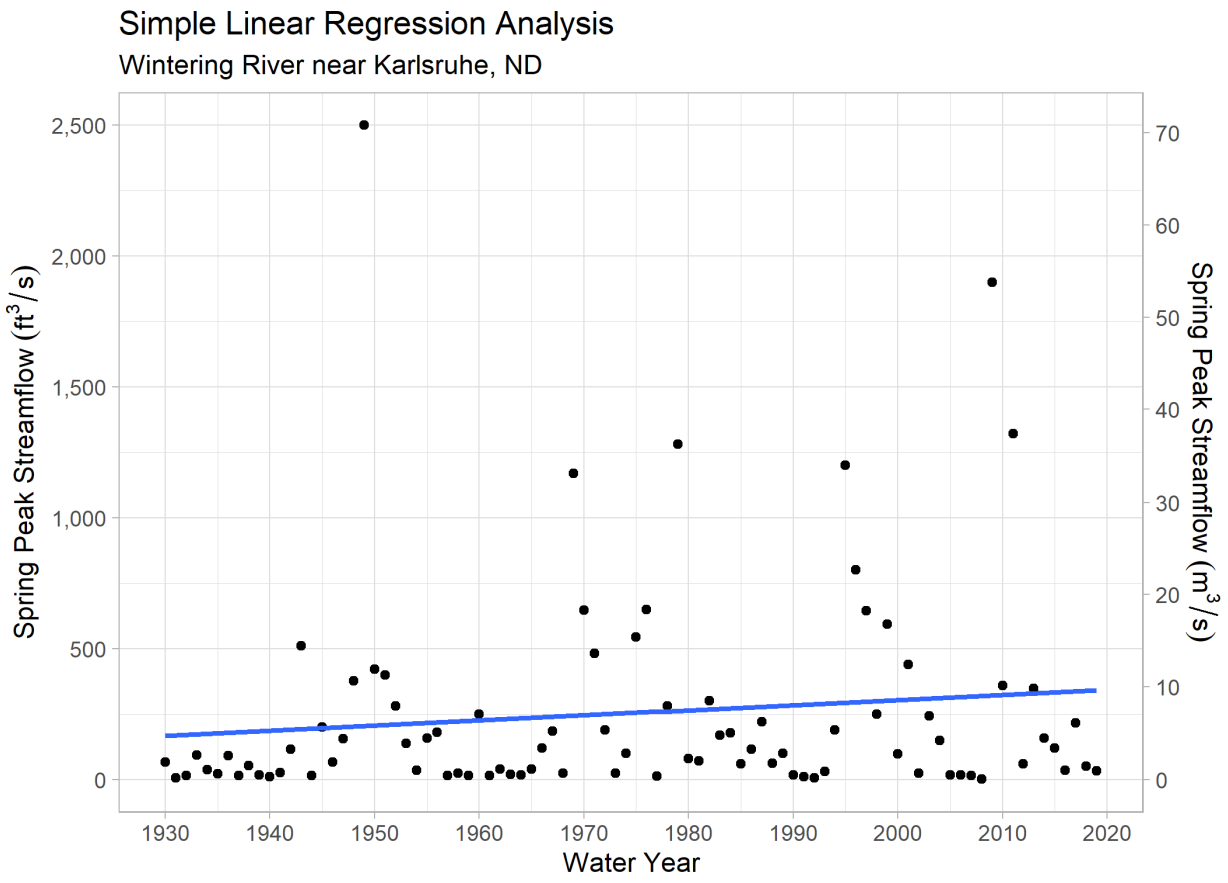

Figure 23. Trend analysis – spring, annual unregulated peak streamflow - Wintering River near Karlsruhe, ND; p-value= 0.1946.

In the summer annual peak flow record, a statistically significant increasing trend is identified by the t-Test (p-value=0.013), Mann-Kendall (p-value= 0.007), Spearman Rank-Order (p-value= 0.008), and simple linear regression (p-value= 0.016) statistical tests. Refer to Figure 24 for a plot of summer peak flows. Further analysis at the strong, 1992 nonstationarity does not indicate a trend in the pre-nonstationarity dataset (1930-1991; p-value= 0.799) or the post-nonstationarity dataset (1993-2017; 0.860).

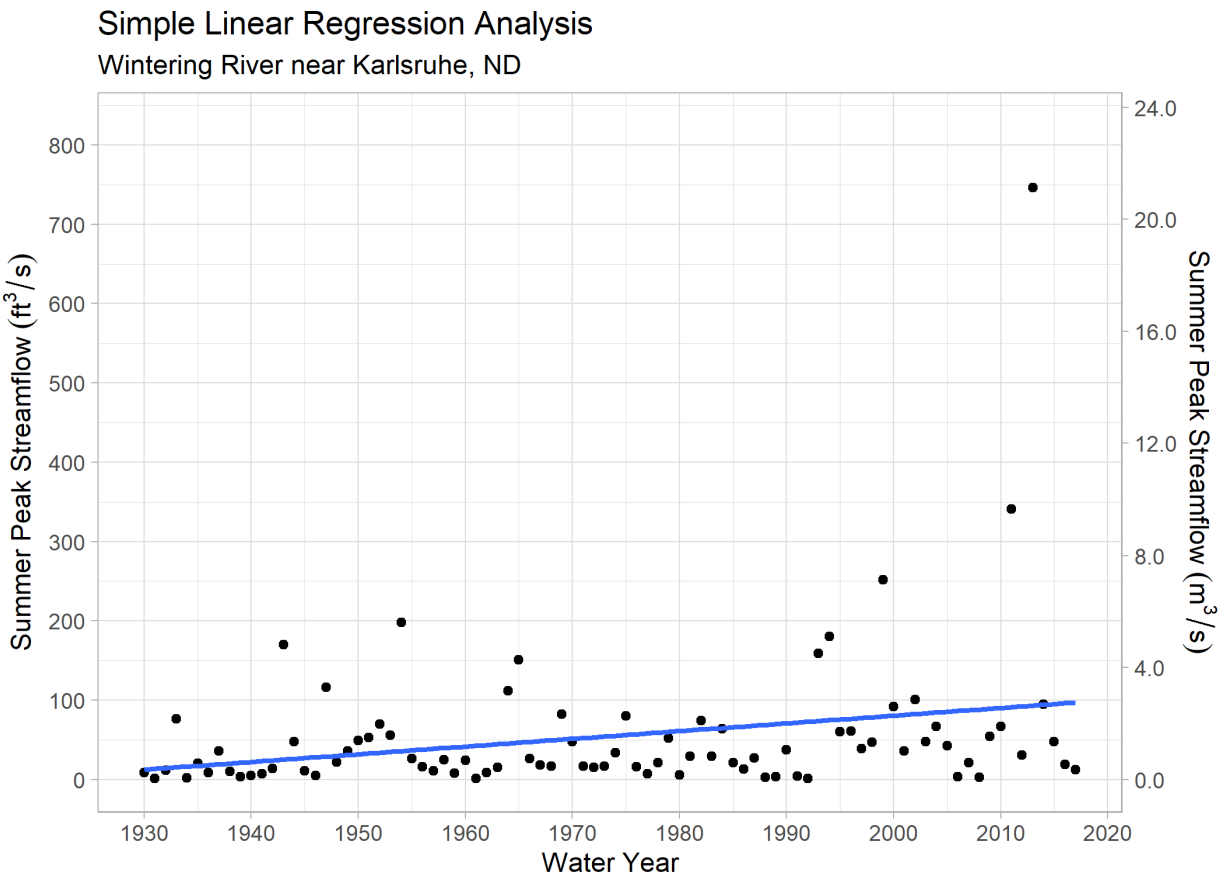

Figure 24. Trend analysis – summer, annual unregulated peak streamflow - Wintering River near Karlsruhe, ND; p-value=0.0157.

Seasonal trend analysis of the fall annual peak streamflow record (1930-2017) indicates a significant, increasing trend. This trend is detected by the t-Test (p-value=0.038), Mann-Kendall (p-value= 0.002), Spearman Rank-Order (p-value= 0.002), and simple linear regression (p-value= 0.043) tests. Additionally, linear regression analysis does not indicate a statistically significant trend in peak flows prior to the 1940 nonstationarity (1930-1939; p-value= 0.389) or after 1940 (1941-2016; p-value= 0.165). See Figure 25 for a plot of the record used in analysis.

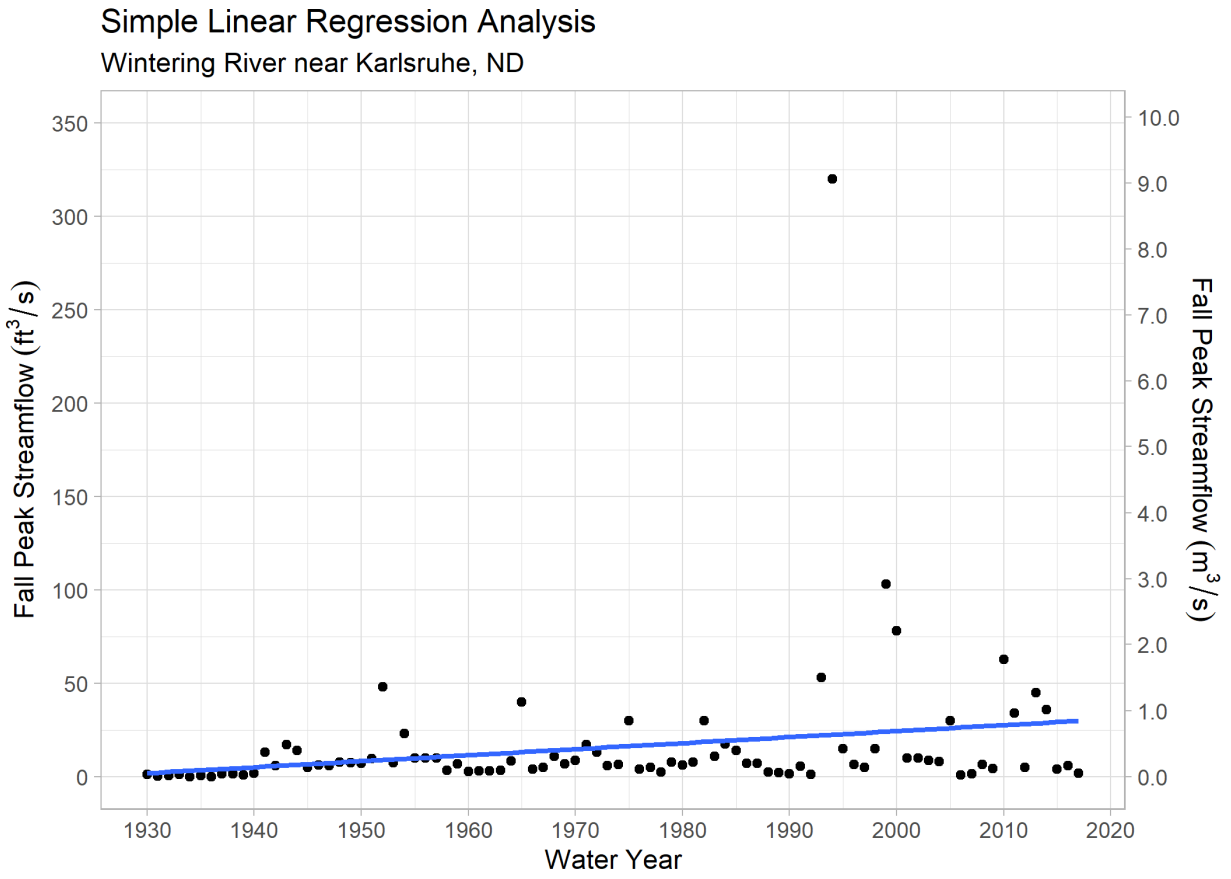

Figure 25. Trend analysis – fall, annual unregulated peak streamflow - Wintering River near Karlsruhe, ND; p-value= 0.0427.

4.1.4.3 Seasonal Trend Analysis – Antler River

Seasonal trend analysis is performed on the annual peak streamflow time series for Antler River near Melita, MB based on mean daily streamflow period of record from 1943 to 2017.

No statistically significant trends for the spring annual peak streamflow were determined by the t-Test (p-value = 0.425), Mann-Kendall Test (p-value = 0.280), Spearman Rank-Order Test (p-value = 0.295), or simple linear regression test (p-value = 0.385). See plotted spring record in the Figure 26.

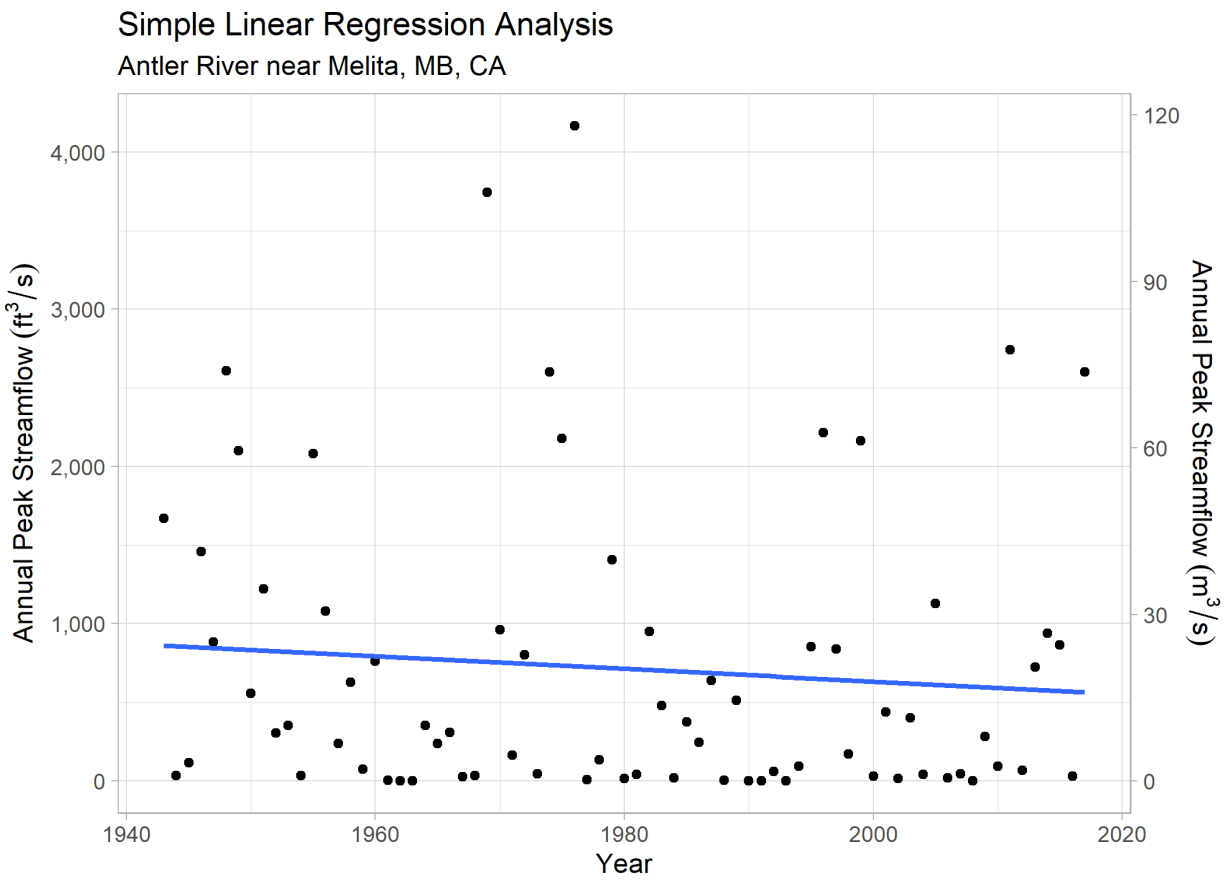

Figure 26. Trend analysis – spring, annual peak streamflow – Antler River near Melita, MB; p-value 0.385

No statistically significant trends for the summer annual peak streamflow were determined by the t-Test (p-value = 0.0827), Mann-Kendall Test (p-value = 0.916), Spearman Rank-Order Test (p-value = 0.859), or simple linear regression test (p-value = 0.088). See plotted summer record in the Figure 27.

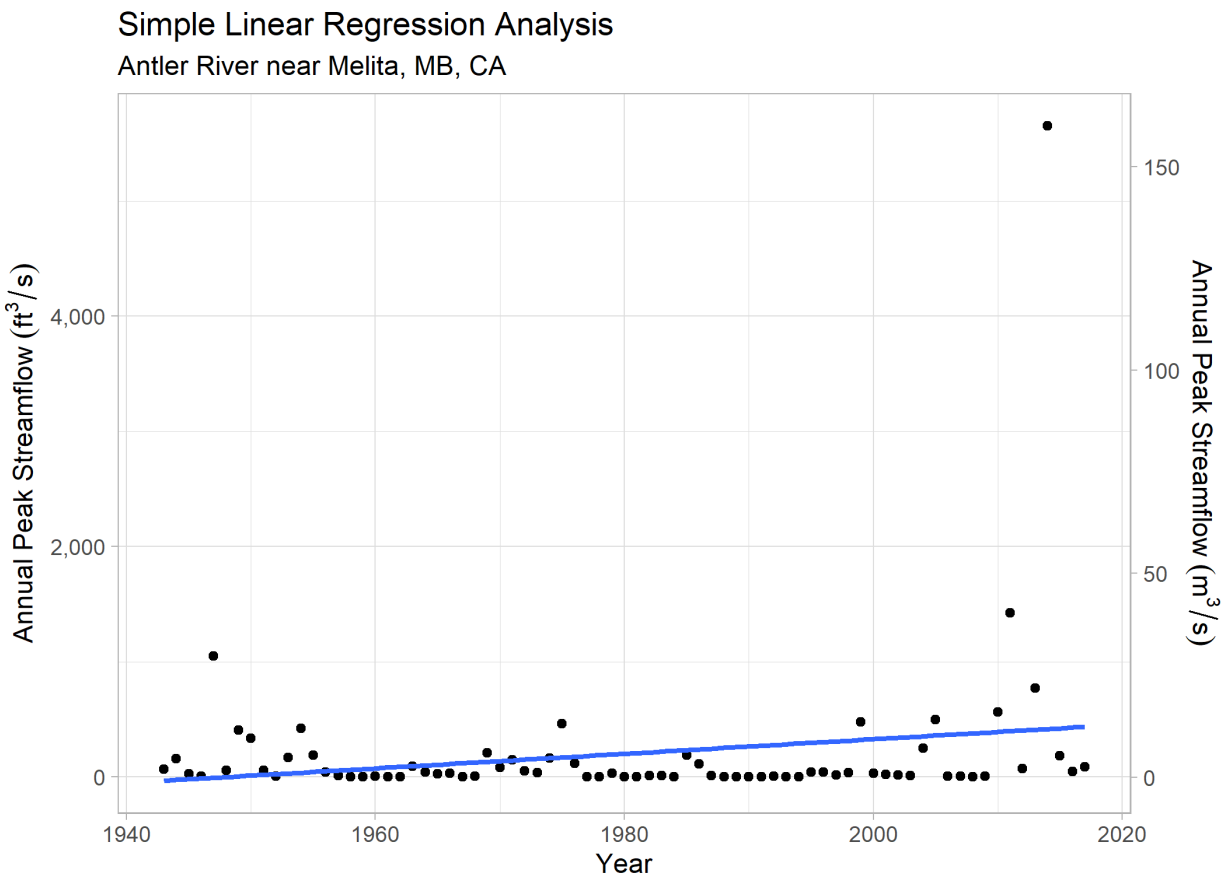

Figure 27. Trend analysis – summer, annual peak streamflow – Antler River near Melita, MB; p-value 0.088

No statistically significant trends for the fall annual peak streamflow were determined by the t-Test (p-value = 0.084), Mann-Kendall Test (p-value = 0.652), Spearman Rank-Order Test (p-value = 0.604), or simple linear regression test (p-value = 0.089). See plotted fall record in the Figure 28. Linear regression analysis of the period prior (1943-2007; p-value = 0.761) to and following (2009-2017; p-value = 0.511) the 2008 nonstationarity do not indicate a statistically significant trend in peak streamflow.

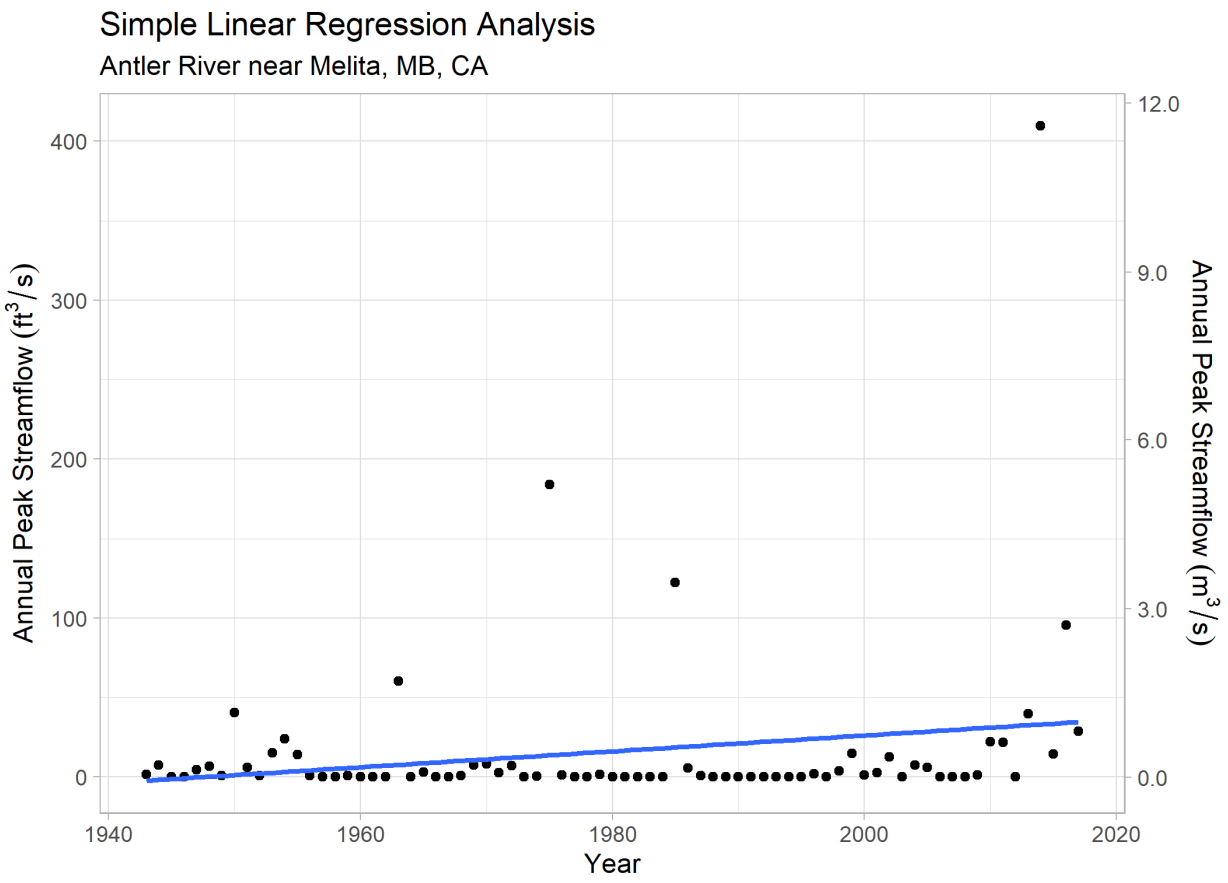

Figure 28. Trend analysis – fall, annual peak streamflow – Antler River near Melita, MB; p-value 0.089

4.2 Trends & Nonstationarities in Annual Average Streamflow Records

In addition to evaluating annual peak streamflow records for trends and nonstationarities, average annual daily streamflow records are also assessed. Average annual daily streamflow records were generated from mean daily streamflow records using the statistics function within HEC-DSSVue (Reference 2) and are quantified in water years (beginning October 1). Average annual daily streamflow records are assessed for USGS gage 05120500 located along the Wintering River near Karlsruhe, ND and for the unregulated record generated for the Souris River at Minot, ND as part of the Plan of Study (Reference 15 & 17).

The average annual daily streamflow records for WSC (05NF002) gage along Antler River near Melita, MB was also assessed. The R software package "tidyhydat" is used to download and process the streamflow data for the Melita gage for the period of record 1943-2017.

4.2.1 Detection of Nonstationarities in Average, Annual Daily Streamflows

4.2.1.1 Nonstationarity Analysis- Average, Annual Daily Unregulated Streamflow– Souris River at Minot, ND

An average annual streamflow timeseries is derived from the daily unregulated streamflow records to analyze the Souris River at Minot, ND for water years 1930-2017, see Figure 29. A nonstationarity is detected for the full period of record in 1941 by the statistical tests Cramer-von-Mises (CVM), Mann Whitney (MW), and LePage (LP in 1946). Additionally, the Smooth Lombard Mood (SLM) test indicates a flux in variance between 1936 and 1938; while the Smooth Lombard Wilcoxon (SLW) test indicates a flux in mean between 1940 and 1942, supporting an abrupt shift in statistical properties in 1941. 1941 is considered a strong nonstationarity because it meets the criteria of consensus, robustness, and magnitude. Consensus is met because multiple distribution-based (CVM and LP) tests detect 1941 as a nonstationarity. 1941 is a robust nonstationarity because multiple tests targeted at detecting shifts in different statistical properties (mean and distribution) detect it as a nonstationary year. Magnitude shift criteria is met because the USACE Timeseries Toolbox (Reference 20) indicates a shift in the magnitude of the mean circa 1941 from 36 cfs in years 1930-1935 to 160 cfs in years 1943-1945. The mean from 1947-1967 is 180 cfs and then another significant shift in mean to 350 cfs occurs in 1969-2017, see Figure 29.

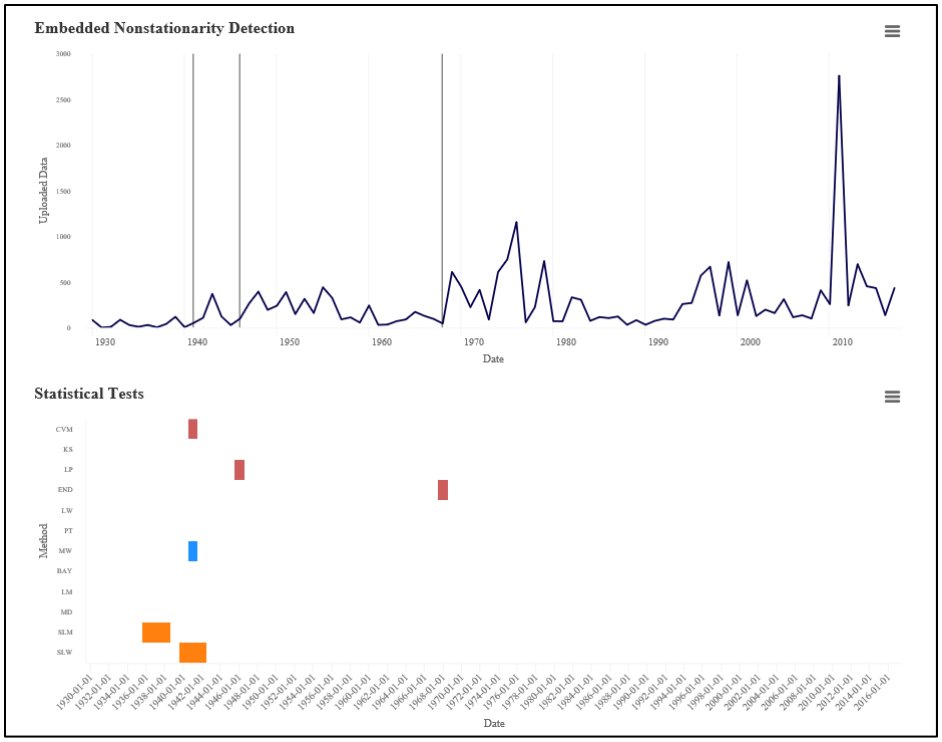

Type: Mean Distribution Variance Smooth

Note: y-axis is annual average flow in cfs

Abbreviation	Statistical Method	Abbreviation	Statistical Method
CVM	Cramer-von-Mises	BAY	Bayesian
KS	Kolmogorov-Smirnov	LM	Lombard Mood
LP	LePage	MD	Mood
END	Energy Divisive	SLM	Smooth Lombard Mood
LW	Lombard Wilcoxon	SLW	Smooth Lombard Wilcoxon
PT	Pettitt	MW	Mann-Whitney

Figure 29. Nonstationarity analysis - average annual streamflow- Souris River at Minot, ND.

4.2.1.2 Nonstationarity Analysis- Average, Annual Daily Streamflow - Wintering River

Nonstationarities in average, annual daily streamflow are analyzed for water years 1930-2017 at a relatively pristine tributary site located along the Wintering River at Karlsruhe, ND. The period of record post-1937 is based on observed data. Data analyzed prior to 1937 was approximated as part of the Plan of Study (Reference 15). Based on the period of record analysis, nonstationarities in average, daily, annual flow are detected in 1941 and 1987 (Figure 30). The 1941 nonstationarity is detected by the following three statistical tests: Cramer-von-Mises (CVM), Mann Whitney (MW), and LePage (LP). The 1987 nonstationarity is identified by five statistical tests: CVM (1987), LP (1989), MW (1987), Lombard Mood (LM; 1988) and Mood

(MD; 1989). Additionally, the Smooth Lombard Wilcoxon (SLW) test indicates that the mean of the dataset is in flux between 1939 and 1942.

These nonstationarities can be considered strong because they demonstrate a degree of consensus, robustness and a significant shift in the magnitude of the dataset's statistical properties. The criteria of consensus are fulfilled because multiple tests targeted at detecting shifts in the overall statistical distribution of the dataset are indicating nonstationarities in 1941 and 1987. The 1941 and 1987 nonstationarities are considered robust because tests targeted at detecting abrupt shifts in multiple types of statistical properties are indicating a nonstationarity (overall distribution and mean). Additionally, the results presented by the USACE Timeseries Toolbox (Reference 20) indicate a significant shift in both the magnitude of the mean and variance around 1941 and 1987. Data collected between 1930 and 1939 has a mean of 3.6 cfs and variance of 7.8. Data collected between 1943 and 1955 has a mean of 18 cfs and variance of 77. For 1987, the subset of data between 1969 and 1986 has a mean of 17 cfs and variance of 92, then shifts to a mean of 29 cfs and variance of 940 for 1990-2017.

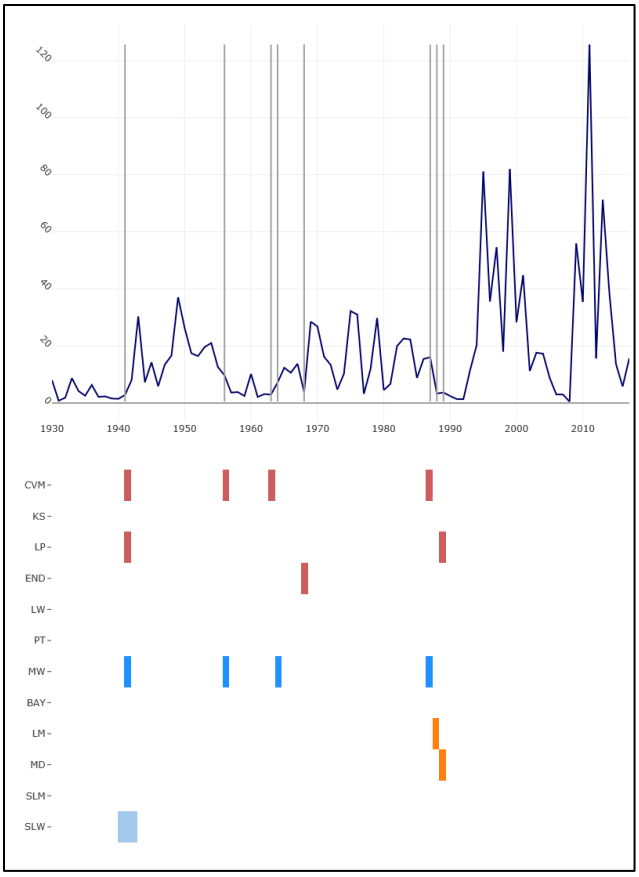

Type: Mean Distribution Variance Smooth

Note: y-axis is annual average flow in cfs

Abbreviation	Statistical Method	Abbreviation	Statistical Method
CVM	Cramer-von-Mises	BAY	Bayesian
KS	Kolmogorov-Smirnov	LM	Lombard Mood
LP	LePage	MD	Mood
END	Energy Divisive	SLM	Smooth Lombard Mood
LW	Lombard Wilcoxon	SLW	Smooth Lombard Wilcoxon
PT	Pettitt	MW	Mann-Whitney

Figure 30. Nonstationarity analysis - average annual streamflow - Wintering River near Karlsruhe, ND

4.2.1.3 Nonstationarity Analysis – Average, Annual Daily Unregulated Streamflow – Antler River near Melita, MB

The USACE Timeseries Toolbox (Reference 20) is used to detect nonstationarity for Antler River near Melita gage (WSC: 05NF002) for the water years 1943 to 2018. As seen in the Figure 31, no statistically significant nonstationarities are detected within the average annual streamflow record at Melita.

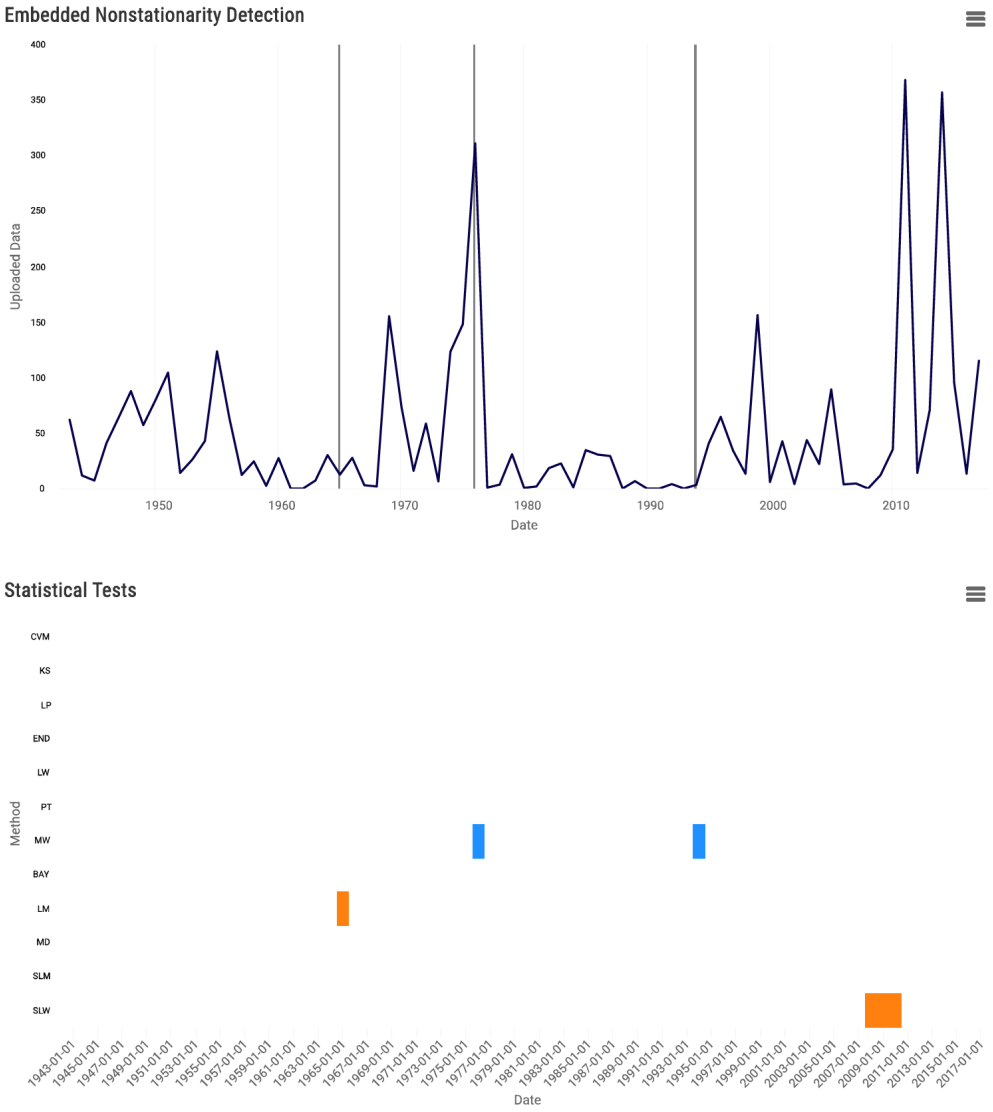

Note: y-axis is annual average flow in cfs

Abbreviation	Statistical Method	Abbreviation	Statistical Method
CVM	Cramer-von-Mises	BAY	Bayesian
KS	Kolmogorov-Smirnov	LM	Lombard Mood
LP	LePage	MD	Mood
END	Energy Divisive	SLM	Smooth Lombard Mood
LW	Lombard Wilcoxon	SLW	Smooth Lombard Wilcoxon
PT	Pettitt	MW	Mann-Whitney

Figure 31. Nonstationarity analysis – average annual streamflow – Antler River near Melita, MB

4.2.2 Detection of Nonstationarities in Seasonal Average Annual Streamflow

Daily flow records are assessed along the Souris River and the Wintering River to identify nonstationarities occurring seasonally. Seasonal, annual average streamflow records are extracted from daily streamflow based on month using Microsoft Excel. Seasons analyzed are spring (March- May), summer (June- August), and fall (September- November). Winter flows are not assessed because flows over the winter months are not large enough to be operationally significant due to frozen basin conditions.

The majority of the period of record for the WSC gage for Antler River near Melita is operated as a seasonal gage from March- October. It is assumed that the majority of the fall flow will occur in September and October, and that the flows occurring in November are not large enough to be operationally significant. Therefore, the fall season will be assessed as September- October for the Melita gage. Seasonal, annual average streamflow records for the Melita gage are extracted from mean daily streamflow records based on month using R.

4.2.2.1 Nonstationarity Analysis- Seasonal Average Annual Streamflow – Souris River at Minot, ND

Seasonal average annual streamflow records for the Souris River at Minot, ND for water years 1930-2017 were analyzed to assess the stationarity of the records. In the spring, a nonstationarity is detected in 1945 by the statistical tests Cramer-von-Mises (CVM), Energy Divisive (END), and detection by Mann Whitney (MW) in 1941 (Figure 32). Additionally, the Smooth Lombard Wilcoxon (SLW) test indicates a flux in mean between 1935 and 1946.

The 1945 nonstationarity detected for spring average annual streamflow is considered strong because it meets the criteria of consensus, robustness, and magnitude. The criterion of consensus is fulfilled because multiple tests targeted at detecting shifts in distribution (CVM, LP) indicate a nonstationarity in 1945. It is robust because tests targeted at identifying changes in different statistical properties (mean and overall distribution) detect a nonstationarity in around 1945. The USACE Timeseries Toolbox (Reference 20) indicates a shift in magnitude of the mean for the subsets of data collected between 1930-1934 (110 cfs) and 1947-1972 (600 cfs).

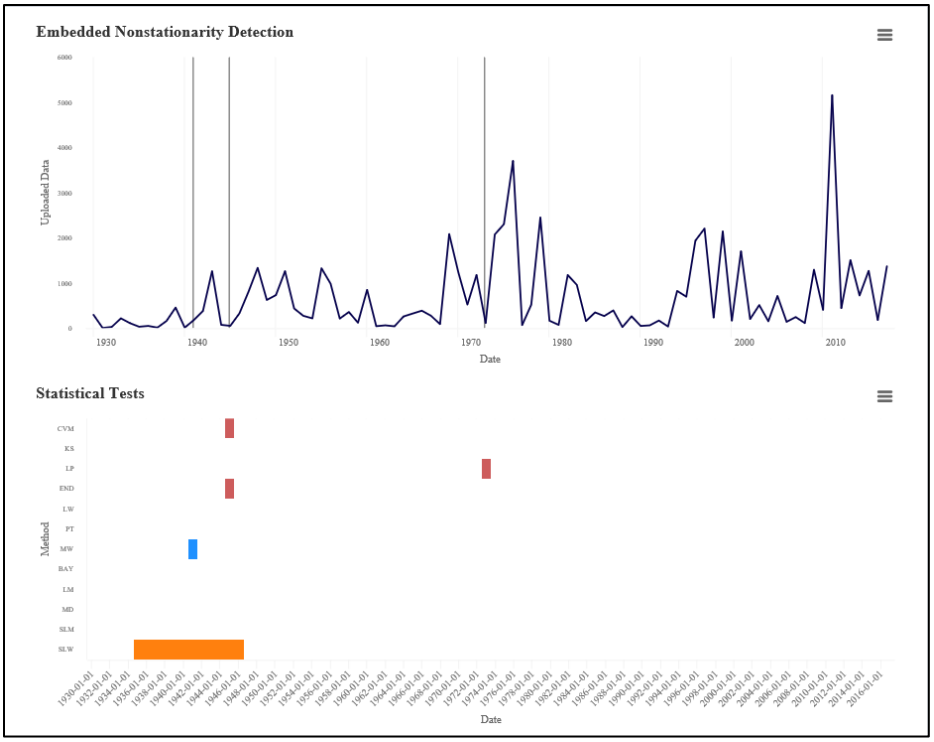

Type: Mean Distribution Variance Smooth

Note: y-axis is spring average flow in cfs

Abbreviation	Statistical Method	Abbreviation	Statistical Method
CVM	Cramer-von-Mises	BAY	Bayesian
KS	Kolmogorov-Smirnov	LM	Lombard Mood
LP	LePage	MD	Mood
END	Energy Divisive	SLM	Smooth Lombard Mood
LW	Lombard Wilcoxon	SLW	Smooth Lombard Wilcoxon
PT	Pettitt	MW	Mann-Whitney

Figure 32. Nonstationarity analysis – spring, annual average streamflow - Souris River at Minot, ND.

For summer annual average streamflow period of record, a nonstationarity is detected in 1942 by the statistical tests CVM, LP, MW, and a 1945 detection by MD, see Figure 33. Additionally, the SLW test indicates a flux in mean between 1939 and 1942, supporting an abrupt shift in 1942 (Reference 4). The nonstationarity meets the criteria of consensus because multiple distribution-based (CVM, LP) tests indicate 1942 as a nonstationary year. 1942 can be considered robust because multiple tests that detect changes in distribution, mean, and variance identify 1942 as a nonstationarity. Finally, the Timeseries Toolbox indicates a shift in the magnitude of the mean from 1930-1938 (mean=24 cfs) to 1943-1944 (mean=190 cfs) and 1946-1967 (mean=160 cfs).

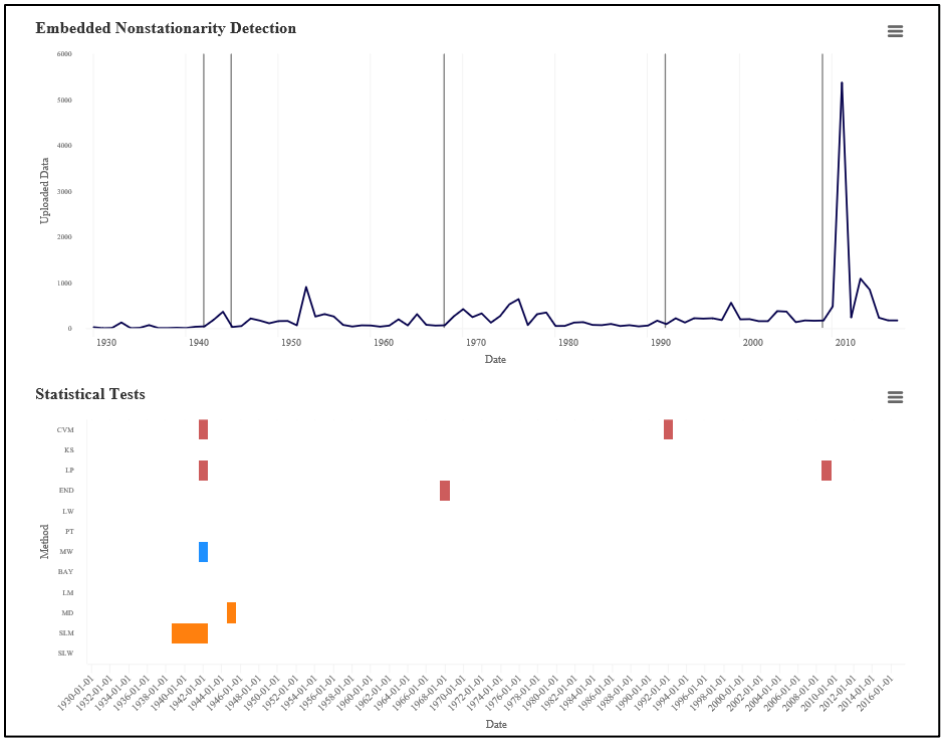

Type: Mean Distribution Variance Smooth

Note: y-axis is summer average flow in cfs

Abbreviation	Statistical Method	Abbreviation	Statistical Method
CVM	Cramer-von-Mises	BAY	Bayesian
KS	Kolmogorov-Smirnov	LM	Lombard Mood
LP	LePage	MD	Mood
END	Energy Divisive	SLM	Smooth Lombard Mood
LW	Lombard Wilcoxon	SLW	Smooth Lombard Wilcoxon
PT	Pettitt	MW	Mann-Whitney

Figure 33. Nonstationarity analysis – summer, annual average streamflow - Souris River at Minot, ND.

For the fall annual average streamflow record, nonstationarities are detected in the years 1940 (CVM, LP in 1941, MW, MD) and 1990 (CVM, LP, END, MW, LW in 1989), as shown Figure 34. The Smooth Lombard Mood (SLM) test indicates a flux in variance between 1930 and 1945; while the SLW test indicates a flux in mean between 1930 and 2012. 1940 and 1990 are strong nonstationarities because several distribution-based statistics tests indicate a degree of consensus. The criterion of robustness is met because both distribution and mean-based tests detect 1940 and 1990 as nonstationarities. The Timeseries Toolbox indicates a gradual shift in the mean over most of the period (SLW 1930-2012).

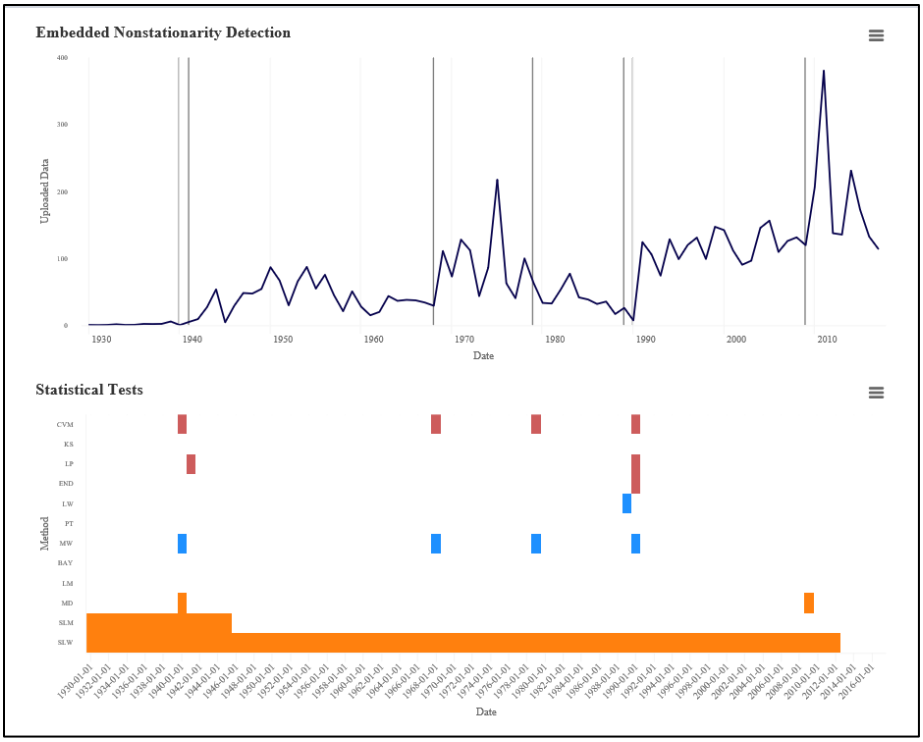

Type: Mean Distribution Variance Smooth

Note: y-axis is fall average flow in cfs

Abbreviation	Statistical Method	Abbreviation	Statistical Method
CVM	Cramer-von-Mises	BAY	Bayesian
KS	Kolmogorov-Smirnov	LM	Lombard Mood
LP	LePage	MD	Mood
END	Energy Divisive	SLM	Smooth Lombard Mood
LW	Lombard Wilcoxon	SLW	Smooth Lombard Wilcoxon
PT	Pettitt	MW	Mann-Whitney

Figure 34. Nonstationarity analysis – fall, annual average streamflow - Souris River at Minot, ND.

4.2.2.2 Nonstationarity Analysis- Seasonal Streamflow - Wintering River

The streamflow record recorded along the Wintering River is analyzed for nonstationarities in average, seasonal flows between water years 1930 and 2017. For the spring, average annual flow record, a nonstationarity is detected in 1989, see Figure 35. The nonstationarity is detected by the following statistical tests: Cramer-von-Mises (CVM), Lombard Mood (LM in 1988), and Mood (MD). Additionally, the Smooth Lombard Wilcoxon (SLW) test indicates a flux in the mean between 1940 and 1942.

1989 is considered a strong nonstationarity because it demonstrates a degree of consensus, robustness and a significant shift in the magnitude of the dataset's statistical properties. Multiple tests targeted at detecting shifts in the overall variance (LM, MD) of the dataset are

indicating a nonstationarity in 1989, thus meeting the criteria of consensus. The nonstationarity is considered robust because tests targeted at detecting changes in multiple statistical properties are indicating nonstationarities in 1989 (overall statistical distribution and variance). The USACE Timeseries Toolbox (Reference 20) indicates that there is a significant shift in the magnitude of the mean circa the 1989 nonstationarity. The means associated with the various subsets of data analyzed by the Timeseries Toolbox are 1930-1939 (mean= 11 cfs), 1943-1967 (mean= 31 cfs), 1969-1987 (mean=50 cfs), 1990-1993 (mean= 11 cfs), and 1995-2017 (mean= 85 cfs).

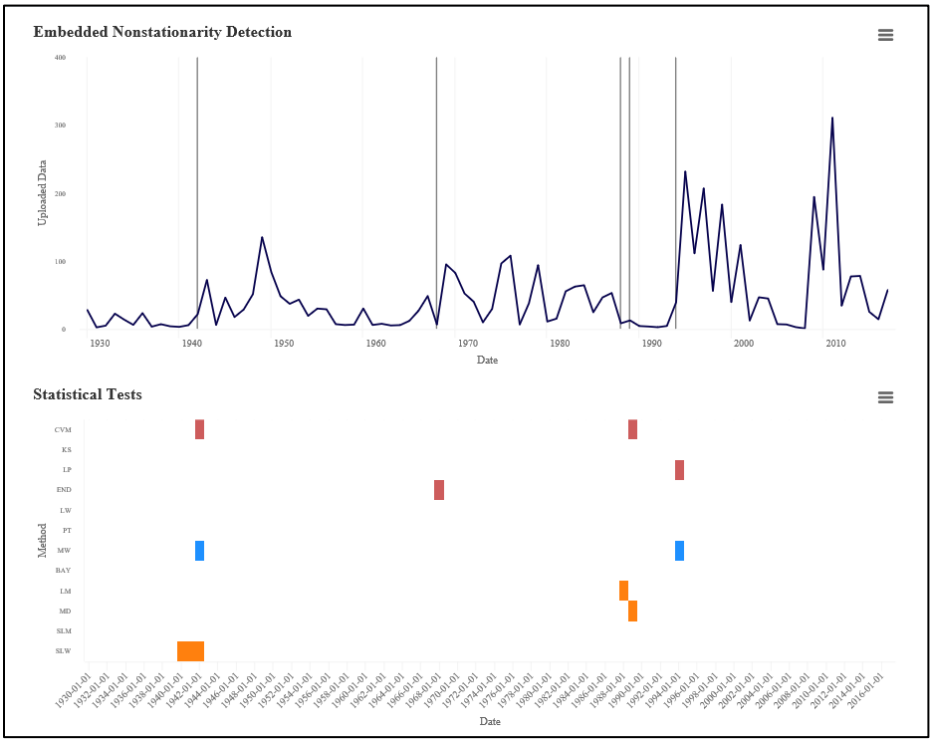

Type: Mean Distribution Variance Smooth

Note: y-axis is spring average flow in cfs

Abbreviation	Statistical Method	Abbreviation	Statistical Method
CVM	Cramer-von-Mises	BAY	Bayesian
KS	Kolmogorov-Smirnov	LM	Lombard Mood
LP	LePage	MD	Mood
END	Energy Divisive	SLM	Smooth Lombard Mood
LW	Lombard Wilcoxon	SLW	Smooth Lombard Wilcoxon
PT	Pettitt	MW	Mann-Whitney

Figure 35. Nonstationarity analysis – spring, annual average flows - Wintering River near Karlsruhe, ND.

A nonstationarity is detected in 1992 within the summer, annual average streamflow record; see Figure 36 for results. Statistical tests detecting the 1992 nonstationarity include CVM,

LePage (LP), Energy Divisive (END), Mann Whitney (MW), and Lombard Wilcoxon (LW) in 1991. The nonstationarity is considered strong because it meets the criteria of consensus (detected by multiple distribution-based statistical tests), robustness (mean and distribution based tests), and changes in magnitude. The Timeseries Toolbox shows shifts in magnitude of the mean between the subsets of data analyzed: 1942-1985 (mean=11 cfs), 1987-1990 (mean=2.6 cfs), and 1993-2017 (mean= 35 cfs).

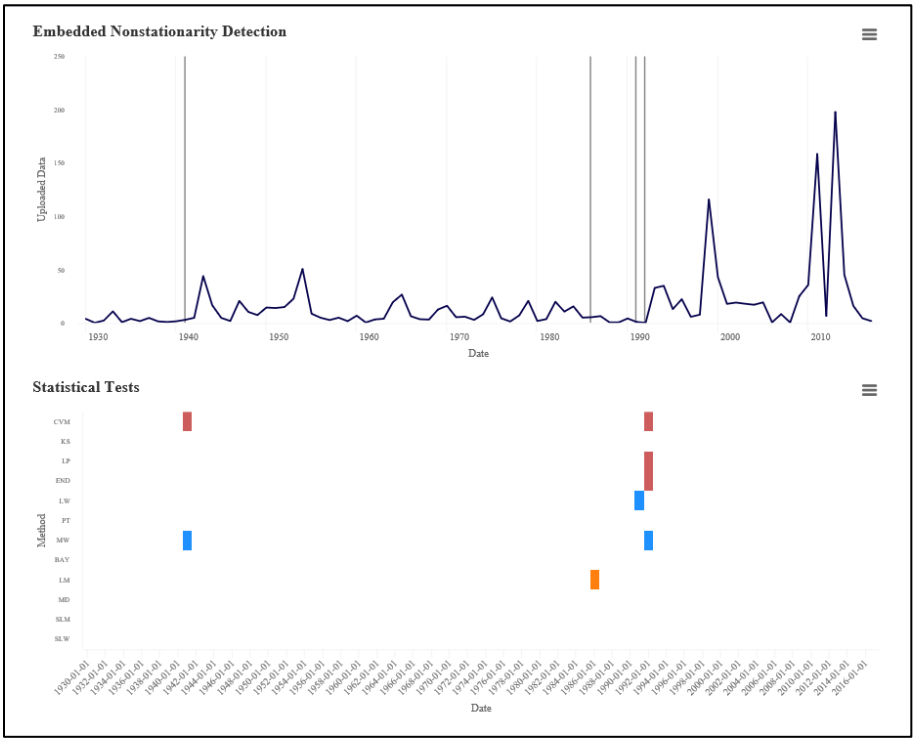

Type: Mean Distribution Variance Smooth

Note: y-axis is summer average flow in cfs

Abbreviation	Statistical Method	Abbreviation	Statistical Method
CVM	Cramer-von-Mises	BAY	Bayesian
KS	Kolmogorov-Smirnov	LM	Lombard Mood
LP	LePage	MD	Mood
END	Energy Divisive	SLM	Smooth Lombard Mood
LW	Lombard Wilcoxon	SLW	Smooth Lombard Wilcoxon
PT	Pettitt	MW	Mann-Whitney

Figure 36. Nonstationarity analysis – summer, annual average flows - Wintering River near Karlsruhe, ND.

Nonstationarities are detected in 1940 and 1987 within the fall, average streamflow record (Figure 37). The 1940 nonstationarity is detected by the following statistical tests: LP, END, MW, and MD, with an additional detection by CVM in 1939. The 1987 nonstationarity is detected by

the CVM, LP, MW, and MD statistical tests. Additionally, the Smooth Lombard Mood (SLM) indicates a flux in variance between the years 1935 and 1940.

These nonstationarities can be considered strong because they demonstrate a degree of consensus, robustness and a significant shift in the magnitude of the dataset's statistical properties. The criterion of consensus is fulfilled because multiple tests targeted at detecting shifts in the overall statistical distribution are indicating nonstationarities in 1940 and 1987. Both nonstationarities are considered robust because tests targeted at detecting abrupt shifts in multiple types of statistical properties are indicating nonstationarities (overall distribution, mean, and variance). Additionally, the results presented by the Timeseries Toolbox (Reference 20) indicates a significant shift in both the magnitude of the mean and standard deviation (variance) in the subsets of data analyzed by the tool: 1930-1934 (mean=0.28 cfs; variance=0.094), 1941-1956 (mean=5.4 cfs; variance=12), 1958-1962 (mean=1.7 cfs; variance=0.12 cfs), 1964-1986 (mean=4.8 cfs; variance=9), and 1988-2017 (mean=9.8 cfs; variance=230).

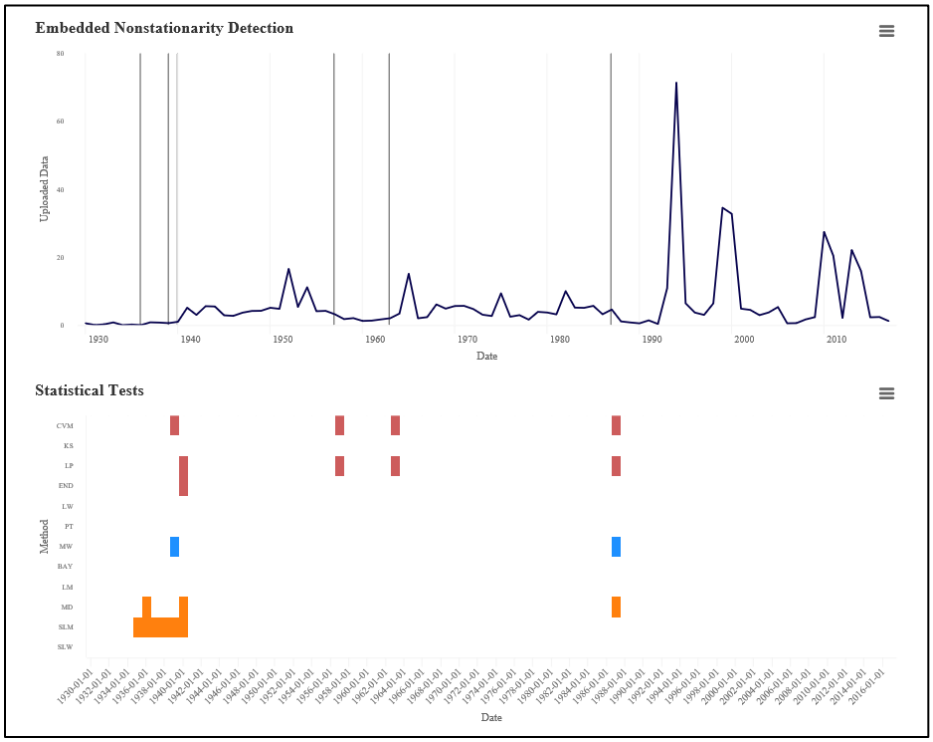

Type: Mean Distribution Variance Smooth

Note: y-axis is fall average flow in cfs

Abbreviation	Statistical Method	Abbreviation	Statistical Method
CVM	Cramer-von-Mises	BAY	Bayesian
KS	Kolmogorov-Smirnov	LM	Lombard Mood
LP	LePage	MD	Mood
END	Energy Divisive	SLM	Smooth Lombard Mood
LW	Lombard Wilcoxon	SLW	Smooth Lombard Wilcoxon
PT	Pettitt	MW	Mann-Whitney

Figure 37. Nonstationarity analysis – fall, annual average flows - Wintering River near Karlsruhe, ND.

4.2.2.3 Nonstationarity Analysis – Seasonal Average Annual Streamflow – Antler River

The USACE Timeseries Toolbox (Reference 20) is used to detect nonstationarities in the seasonal annual average streamflow between 1943 and 2018 for Antler River near Melita, MB. For the spring peak streamflow, no statistically significant nonstationarities are detected.

For the summer annual average streamflow, no strong nonstationarities were detected. Several tests indicate change points in: 1956 (CVM and MW), 1968 (CVM and MW), 1976 (CVM and MW), 1994 (CVM and MW), and 2009 (LP). However, none of these meet the criteria of consensus, and robustness; see Figure 38.

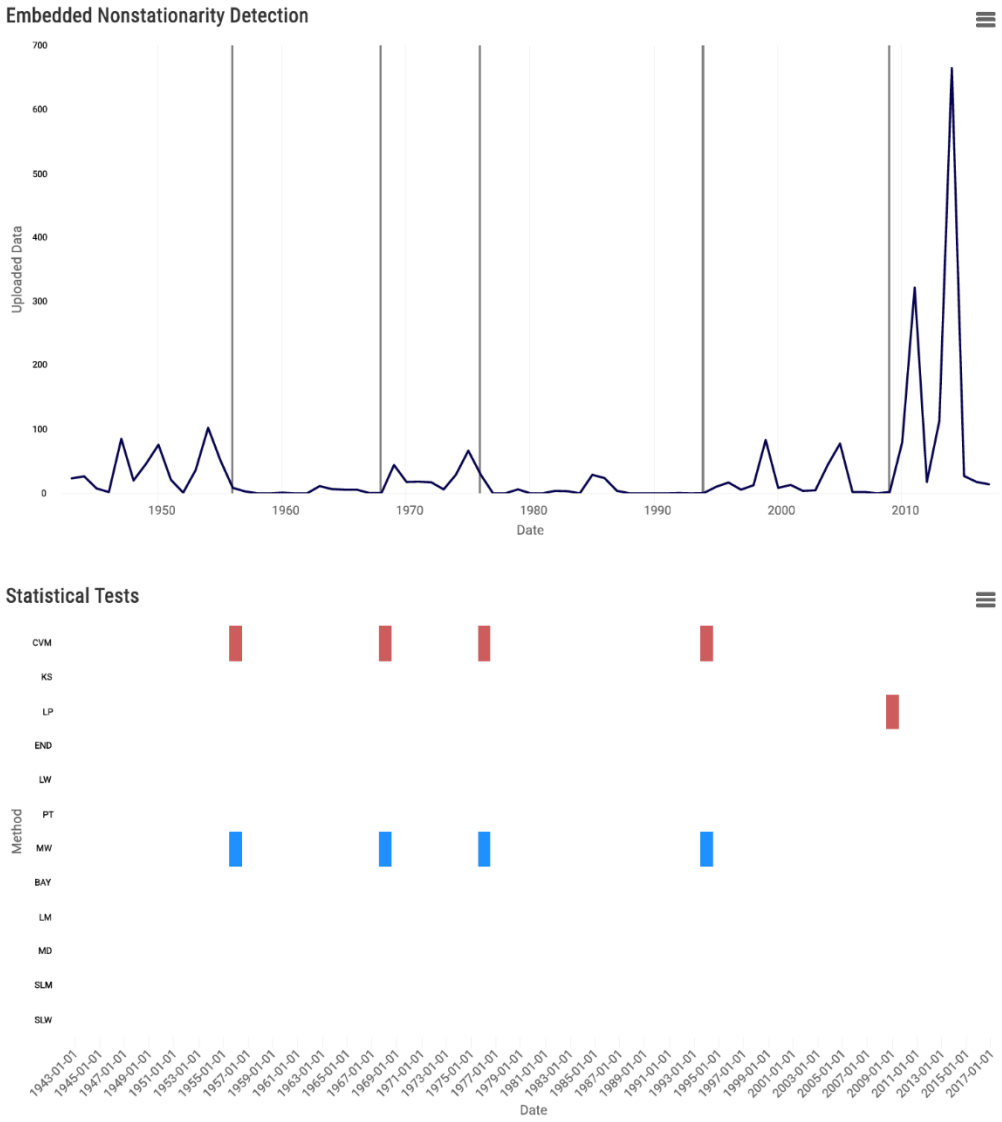

Note: y-axis is summer average flow in cfs

Abbreviation	Statistical Method	Abbreviation	Statistical Method
CVM	Cramer-von-Mises	BAY	Bayesian
KS	Kolmogorov-Smirnov	LM	Lombard Mood
LP	LePage	MD	Mood
END	Energy Divisive	SLM	Smooth Lombard Mood
LW	Lombard Wilcoxon	SLW	Smooth Lombard Wilcoxon
PT	Pettitt	MW	Mann-Whitney

Figure 38. Nonstationarity analysis – summer, annual average streamflow – Antler River near Melita, MB

For fallfall average annual streamflow, a strong nonstationarity is detected in 2008 by the Cramer-von-Mises (CVM; 2009 detection), LePage (LP; 2003 detection), Lombard Wilcoxon (LW; 2008 detection), Mann-Whitney (MW; 2009 detection), and Lombard Mood (LM; 2008 detection), see Figure 39. This nonstationarity exhibits consensus because multiple tests targeted at detecting changes in mean are detecting nonstationarity within a 5 year span. It shows robustness because multiple test targeted at different statistical properties are detecting nonstationarity within a 5 year span.

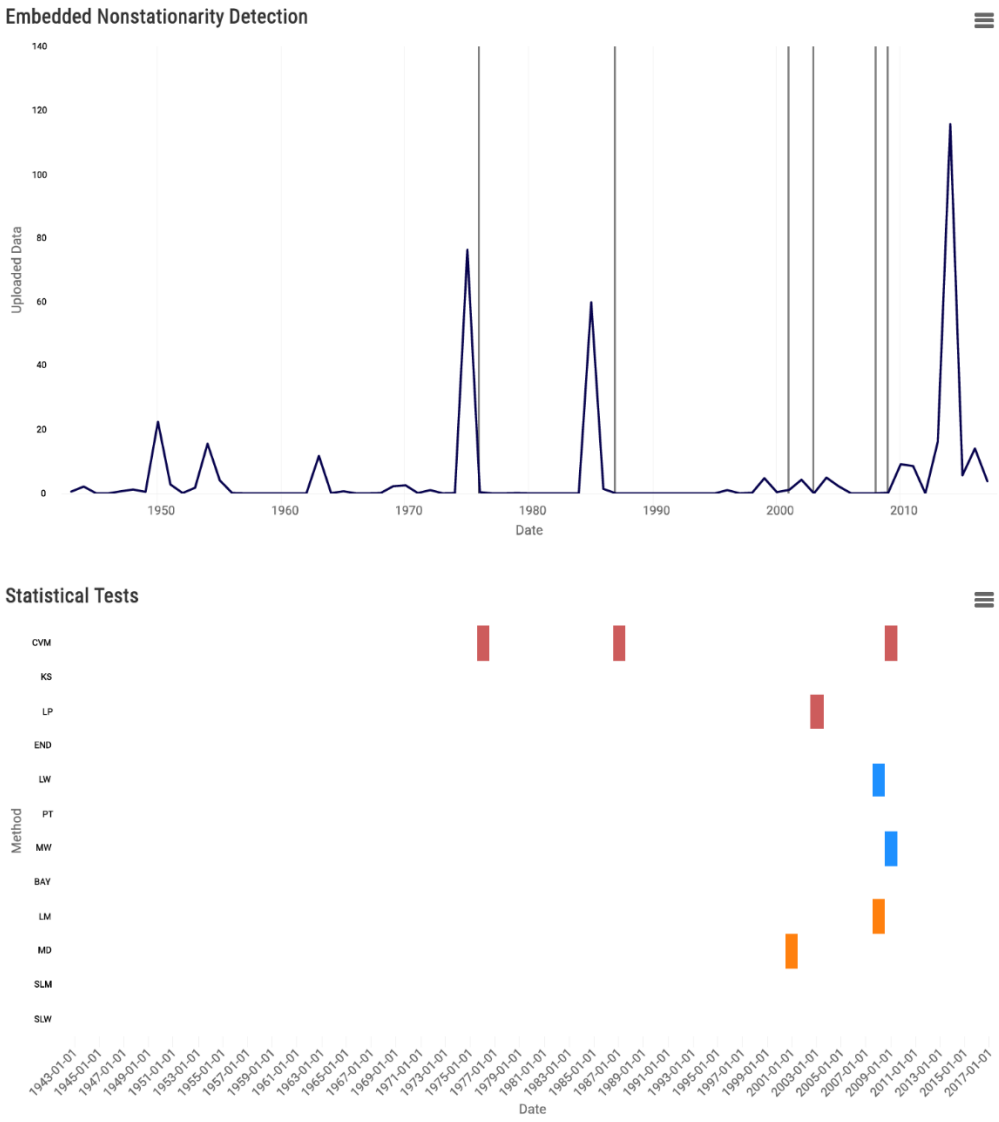

Type: Mean Distribution Variance Smooth

Note: y-axis is fall average flow in cfs

Abbreviation	Statistical Method	Abbreviation	Statistical Method
CVM	Cramer-von-Mises	BAY	Bayesian
KS	Kolmogorov-Smirnov	LM	Lombard Mood
LP	LePage	MD	Mood
END	Energy Divisive	SLM	Smooth Lombard Mood
LW	Lombard Wilcoxon	SLW	Smooth Lombard Wilcoxon
PT	Pettitt	MW	Mann-Whitney

Figure 39. Nonstationarity analysis – fall, annual average streamflow – Antler River near Melita, MB

4.2.3 Detection of Trends in Average, Annual Daily Streamflows

In addition to assessing the nonstationarity of the average annual daily flow records for Wintering River, Antler River, and the Souris River, trend analysis is applied using t-Test, Mann-Kendall, Spearman Rank-Order and linear regression. The generally accepted p-value<0.05 (linear regression) and α =.05 level of significance (monotonic trend analysis) are used as the thresholds for statistical significance.

4.2.3.1 Trend Analysis- Unregulated Average, Annual Daily Streamflow – Souris River-Minot, ND

Average, annual daily unregulated streamflow is analyzed for monotonic trends for the Souris River at Minot, ND. A significant increasing trend is identified by the t-Test (p-value=0.002), Mann-Kendall (p-value=1.60×10^{-5}), Spearman Rank-Order (p-value=1.55×10^{-5}), and linear regression (p-value=0.003) tests. Linear regression at the detected nonstationarity in 1941 does not indicate a significant trend pre-1941 (1930-1940; p-value= 0.979) or post-1941 (1942-2017; p-value=0.063). Figure 40 displays the plotted data with an observable, increasing trend in average, annual daily unregulated streamflow.

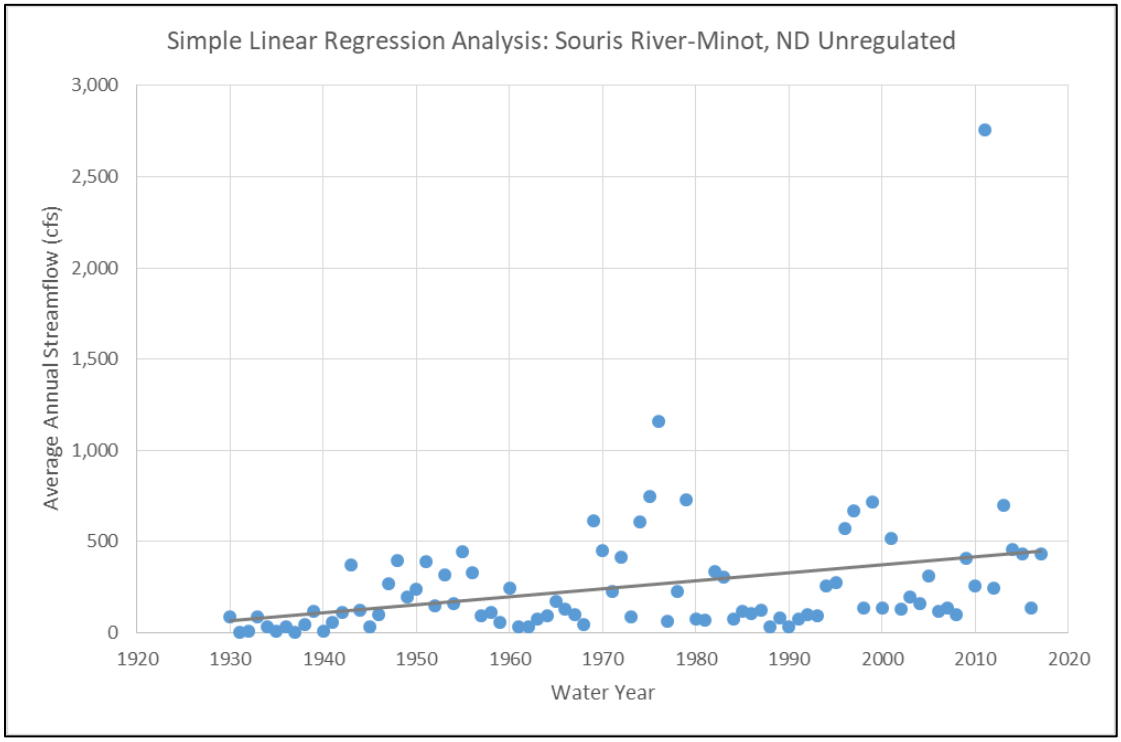

Figure 40. Trend analysis - unregulated annual streamflow at the Souris River at Minot, ND; p-value =0.0031.

4.2.3.2 Trend Analysis- Average Annual Daily Streamflow - Wintering River

As indicated within Figure 41, trend analysis for the average, annual daily streamflow record for the Wintering River at Karlsruhe, ND identifies a significant increasing trend for the period of analysis: 1930-2017. There is concurrence between all three statistical tests applied: t-Test (p-value=1.26×10^{-4}, Mann-Kendall (p-value= 5.40×10^{-4}), Spearman Rank-Order (p-value= 3.71×10^{-4}), and linear regression (p-value= 1.86×10^{-4}).

Additionally, linear regression is analyzed for the periods prior to and after the detected 1941 and 1987 nonstationarities. When the period of record between 1930 and 1940 is analyzed, there is no statistically significant trend in the data (p-value= 0.191). When the period of record between 1942 and 2017 is analyzed, a significant increasing trend is present (p-value 0.008). A statistically significant, increasing trend exists in the dataset collected between 1930 and 1986 (p-value =0.012). Post the 1987 nonstationarity, there is no statistically significant trend in the data (1988-2017; p-value=0.314).

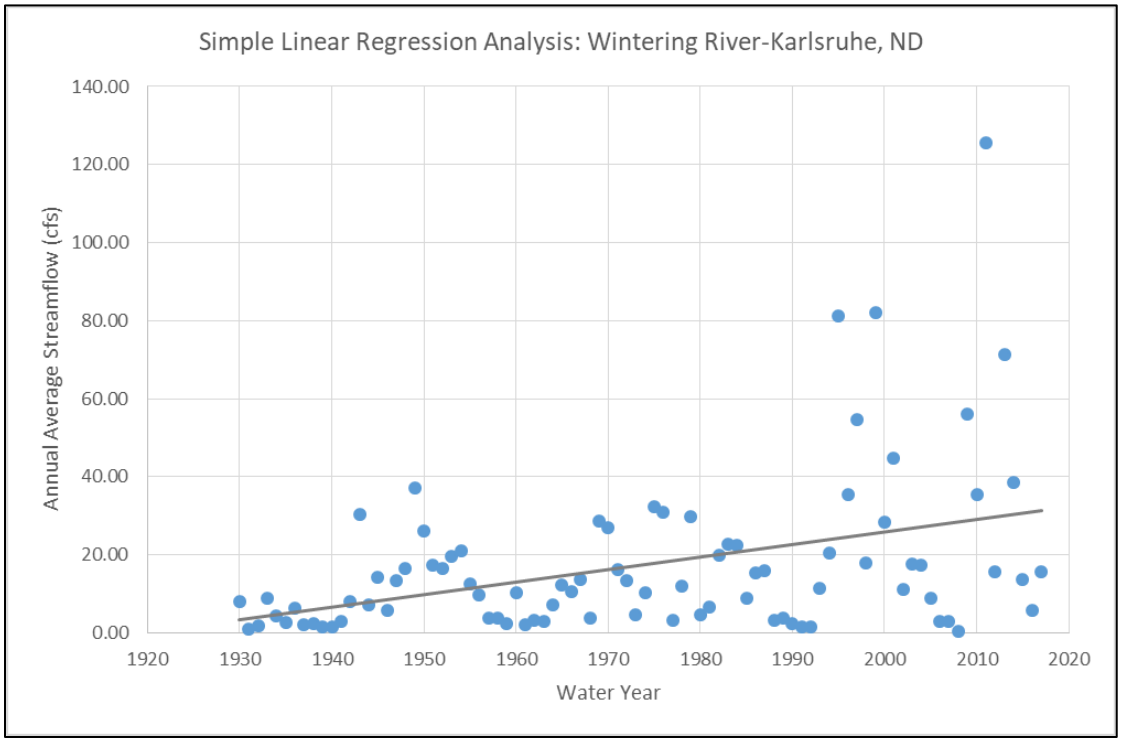

Figure 41. Trend analysis – Average Annual streamflow at the Wintering River near Karlsruhe, ND; p-value $1.86x10^{-4}$.

4.2.3.3 Trend Analysis – Average Annual Daily Streamflow - Antler River

For the tributary gage analyzed at Antler River near Melita, the results of the linear regression analysis are displayed in the Figure 42. The p-value determined for the trend line is 0.295. This indicates that the trend line does not have a statistically significant slope at a 95% level of confidence, since the p-value is greater than 0.05. The USACE Time Series Toolbox (Reference 20) was also used to perform the t-Test (p-value =0.267), Mann Kendall Test (p-value = 0.840), and Spearman Rank-Order Test (p-value = 0.790) on the Melita gage. These results are consistent with the results of the simple linear regression. There is no trend in the annual peak streamflow data set observed along Antler River near Melita, MB.

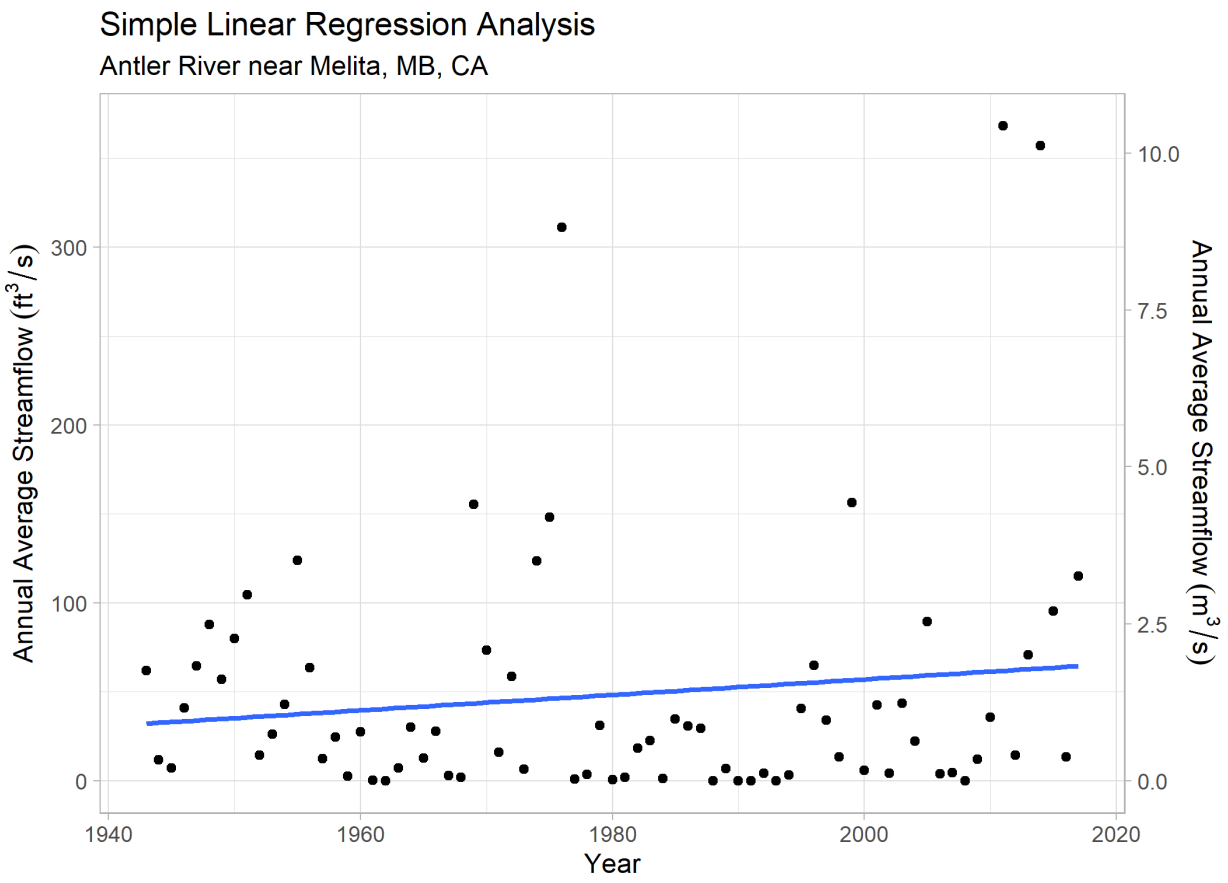

Figure 42. Trend analysis – annual average streamflow – Antler River near Melita, MB; p-value 0.295

4.2.4 Detection of Trends in Seasonal Average Streamflow

Daily flow records are assessed along the Souris River and the Wintering River to identify trends occurring seasonally. Seasonal, annual average streamflow records are extracted from daily streamflow based on month using Microsoft Excel. Seasons analyzed are spring (March- May), summer (June- August), and fall (September- November). Trends in winter flows are not assessed because flows over the winter months are not large enough to be operationally significant due to frozen basin conditions. The generally accepted p-value<0.05 is used as the threshold for statistical significance.

The majority of the period of record for the WSC gage for Antler River near Melita is operated as a seasonal gage from March- October. It is assumed that the majority of the fall flow will occur in September and October, and that the flows occurring in November are not large enough to be operationally significant. Therefore, the fall season will be assessed as September- October for the Melita gage. Seasonal, annual peak streamflow records for the Melita gage are extracted from mean daily streamflow records based on month using R.

4.2.4.1 *Trend Analysis- Seasonal Unregulated Average Streamflow - Souris River at Minot, ND*

A trend analysis on the average, spring streamflow record for Minot, ND (1930-2017) identifies a statistically significant increasing trend using the t-Test (p-value=0.013), Mann-Kendall (p-value= 0.008), Spearman Rank-Order (p-value=0.006), and linear regression (p-value 0.016) tests. Figure 43 displays the spring, annual average streamflow record.

Linear regression trends are also analyzed for portions of the period of record prior to and after the identified strong nonstationarity in 1945. No trends are indicated in the pre-nonstationarity dataset for 1945 (1930-1944; p-value= 0.130) or post-nonstationarity (1946-2017; p-value= 0.322).

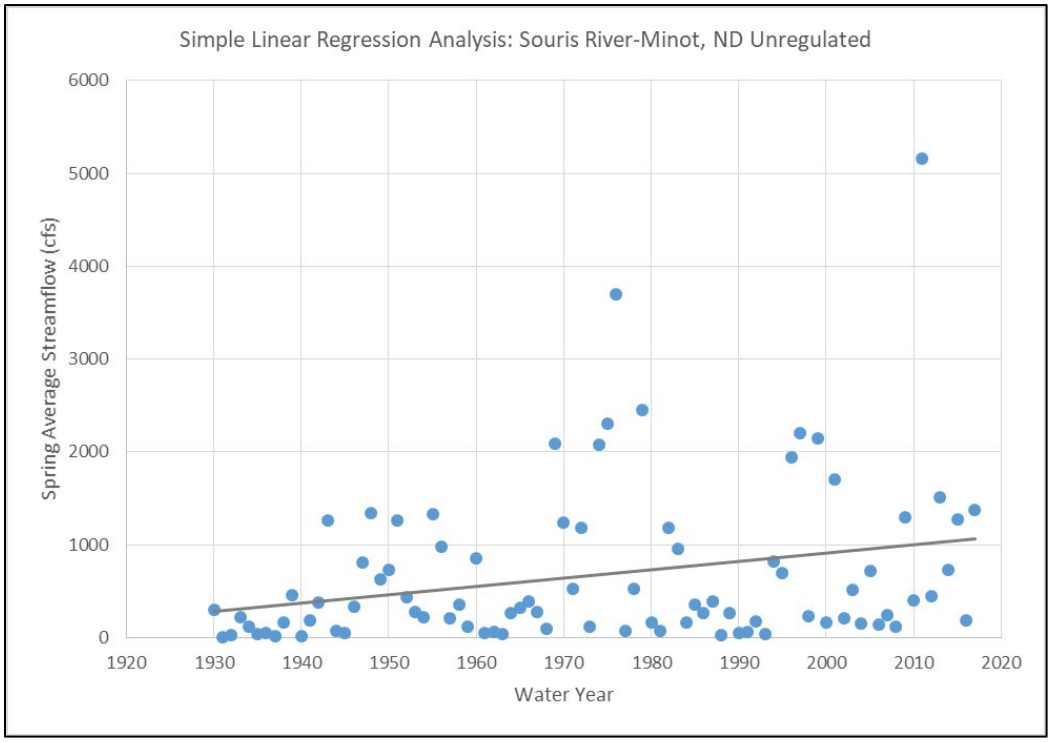

Figure 43. Trend analysis - unregulated spring streamflow at the Souris River at Minot, ND; p-value 0.0162.

In the average, summer streamflow record (1930-2017), trend analysis identifies a statistically significant increasing trend using the t-Test (p-value= 0.011), Mann-Kendall (p-value 3.58×10^{-7}), Spearman Rank-Order (p-value 3.92×10^{-7}), and linear regression (p-value 0.013) tests (see Figure 44). Trend analysis is also conducted for the portion of the period of record prior to and after the strong nonstationarity detected in 1941. The average summer streamflow record exhibits no trend prior to the nonstationarity indicated in 1941 (1931-1940; p-value= 0.685). The post-nonstationarity dataset (1943-2017) does not indicated a statistically significant increasing trends, however, the p-value of 0.059 calculated is near the accepted threshold for statistical significance.

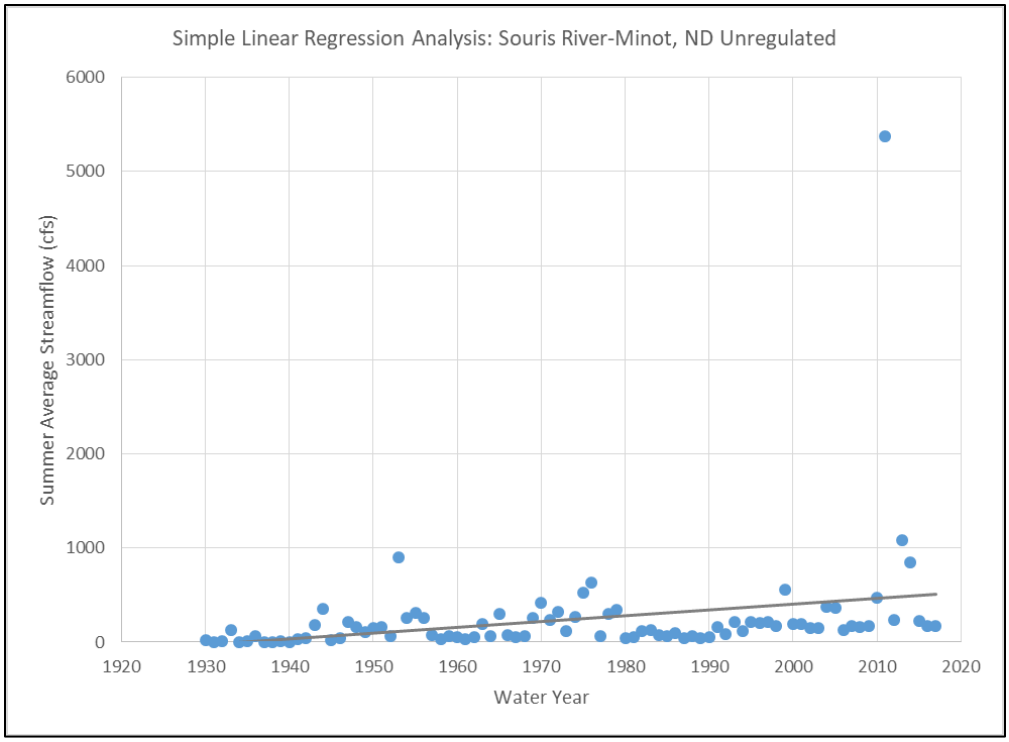

Figure 44. Trend analysis - average summer streamflow at the Souris River at Minot, ND; p-value 0.0127.

As can be seen from the plot in Figure 45, there exists a statistically significant, increasing trend in the fall, unregulated streamflow record at Minot (1930-2017). The trend is identified by the t-Test (p-value= 2.89×10^{-15}), Mann-Kendall (p-value < 2.2×10^{-16}), Spearman Rank-Order (p-value 2.18×10^{-19}), and linear regression (p-value 7.23×10^{-15}) statistical tests. Trend analysis is also conducted for the portions of the period of record prior to and after the strong nonstationarities identified within the fall streamflow record: 1940 and 1990. Analysis of the 1940 nonstationarity identifies a significant increasing trend in the record approximated prior to 1940 (1930-1939; p-value= 0.009) and after 1940 (1941-2017; p-value=5.47×10^{-10}). When the portions of the period of record prior to and after 1990 are analyzed, there are significant increasing trends in the data collected prior to 1990 dataset (1930-1989; p-value=3.25×10^{-4}) and the data collected post 1990 (1991-2017; p-value=0.031).

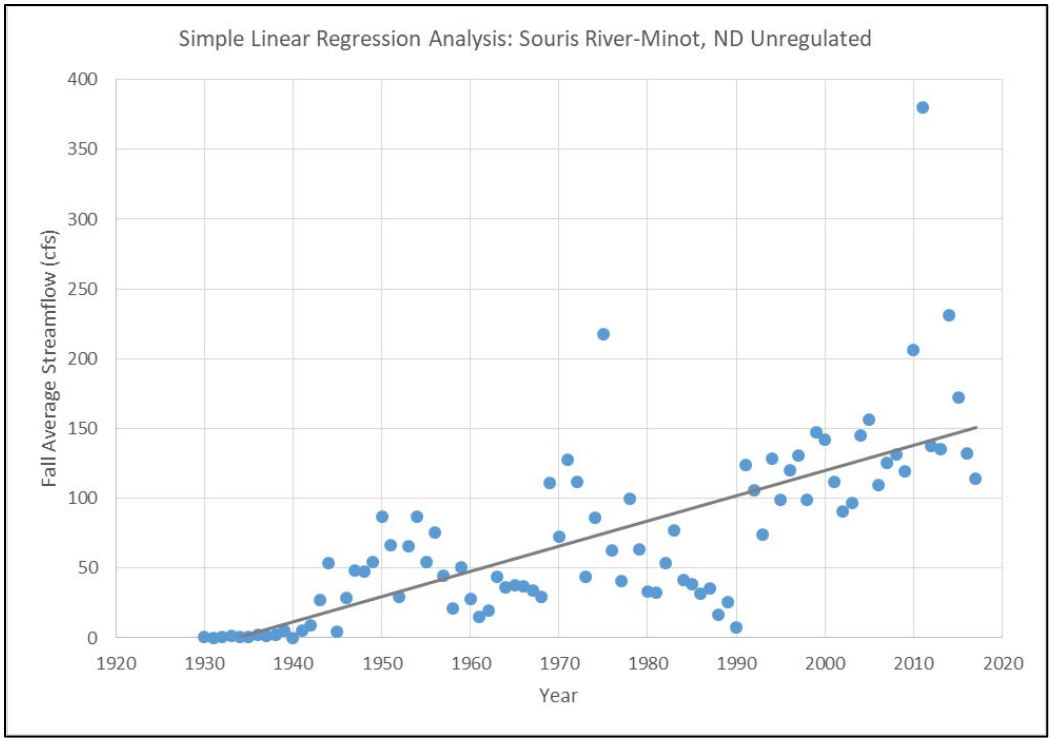

Figure 45. Trend analysis - average fall streamflow - Souris River at Minot, ND; p-value $7.23x10^{-15}$.

4.2.4.2 Trend Analysis- Seasonal Unregulated Average Streamflow - Wintering River

When spring, average daily flows are analyzed for the period of record between water years 1930 and 2017 a significant, increasing trend is detected by the t-Test (p-value=0.001), Mann-Kendall (p-value=0.004), Spearman Rank-Order (p-value= 0.004), and linear regression (p-value=0.002) tests (see Figure 46). Further linear regression analysis is applied to the subsets of data collected prior to and after the nonstationarity detected in 1989. For the 1989 nonstationarity, linear regression analysis suggests a significant increasing trend in the data prior to 1989 (1930-1988; p-value= 0.026) with no trend identified post-nonstationarity (1990-2017; p-value=0.840).

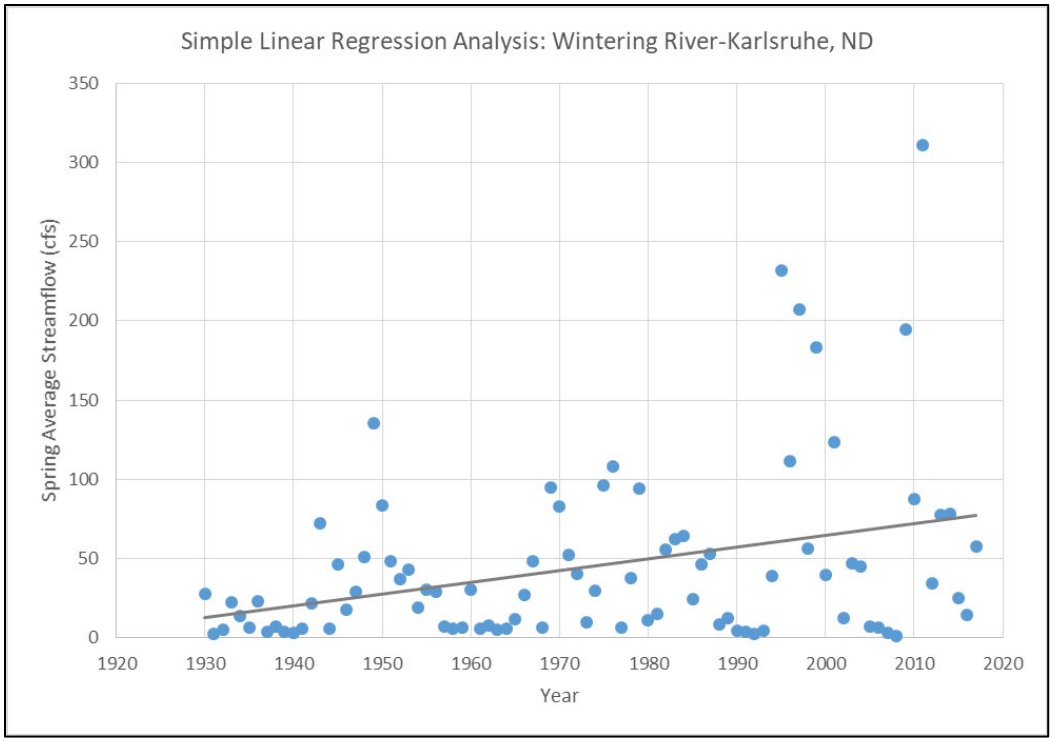

Figure 46. Trend analysis - average spring annual streamflow - Wintering River near Karlsruhe, ND; p-value 0.0016.

A statistically significant increasing trend is identified by the t-Test (p-value=0.002), Mann-Kendall (p-value= 0.002), Spearman Rank-Order (p-value= 0.003), and linear regression (p-value= 0.003) tests for the summer, annual average streamflows collected at Karlsruhe between 1930 and 2017 (Reference 12). Figure 47 displays the summer, annual average streamflow record collected along the Wintering River, along with the increasing trend line produced using linear regression in Microsoft Excel.

Further linear regression analysis is performed using the periods of record collected prior to and after the strong nonstationarities identified in 1992. There are no statistically significant trends in the datasets collected prior to (1930-1991; p-value= 0.880) and after the 1992 nonstationarity (1993-2017; p-value=0.516).

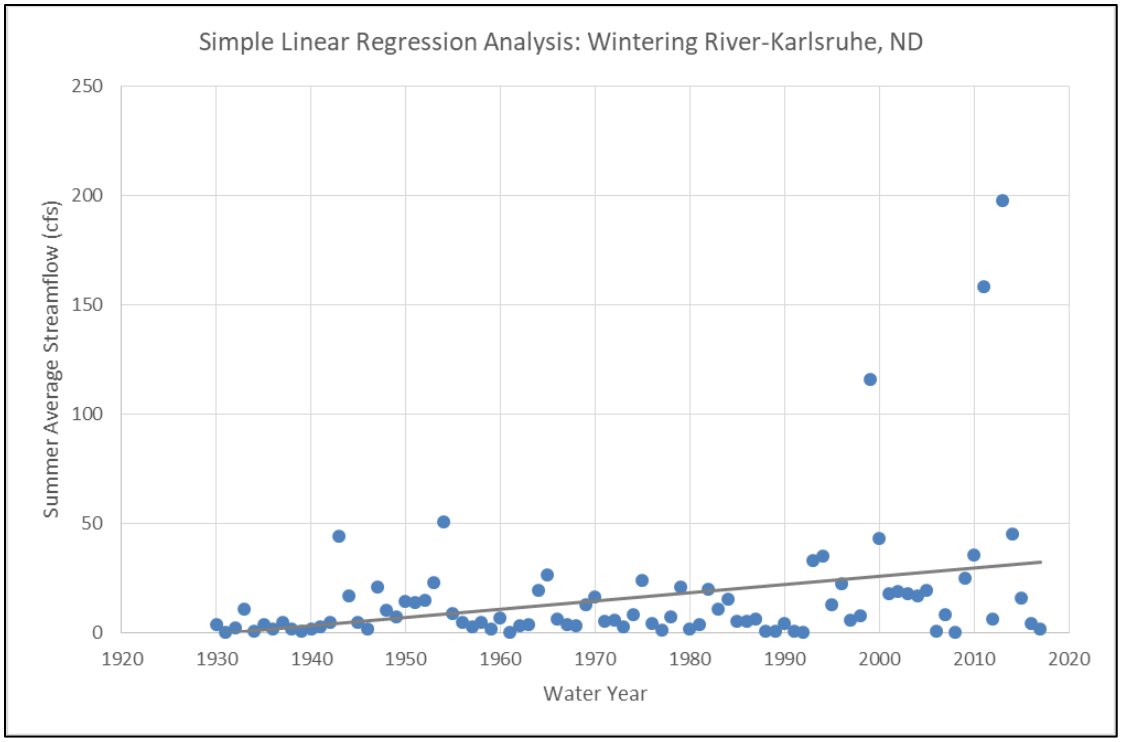

Figure 47. Trend analysis - average summer annual streamflow - Wintering River near Karlsruhe, ND; p-value 0.0026.

Within the fall, annual average streamflow record, a statistically significant increasing trend is identified by the t-Test (p-value=0.008), Mann-Kendall (p-value= 0.007), Spearman Rank-Order (p-value= 0.007), and linear regression (p-value=0.009) tests. See Figure 48 for a plot of the data. The record prior to the 1940 nonstationarity is analyzed and no significant trend is detected between 1930 and 1939 (p-value=0.340) or the record between 1941 and 2017 (p-value 0.093). A statistically significant increasing trend is present in the dataset collected prior to the 1987 nonstationarity (1930-1986, p-value= 0.016), but in the data collect post-1987 (1988-2017; p-value=0.828).

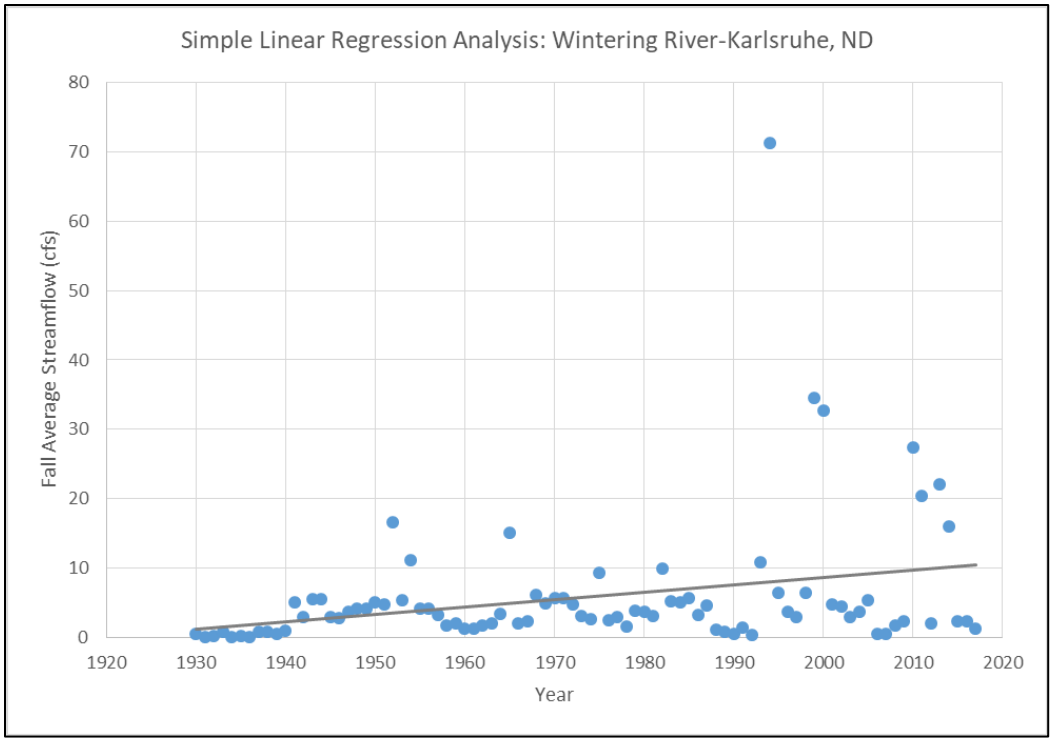

Figure 48. Trend analysis - average fall annual streamflow - Wintering River near Karlsruhe, ND; p-value 0.0094.

4.2.4.3 Trend Analysis – Seasonal Unregulated Average Streamflow – Antler River

Seasonal trend analysis is performed on the annual average streamflow time series for Antler River near Melita, MB based on mean daily streamflow period of record from 1943 to 2017.

No statistically significant trends for the spring annual average streamflow were determined by the t-Test (p-value = 0.787), Mann-Kendall Test (p-value = 0.647), Spearman Rank-Order Test (p-value = 0.667), or simple linear regression test (p-value = 0.838). See plotted spring record in the Figure 49.

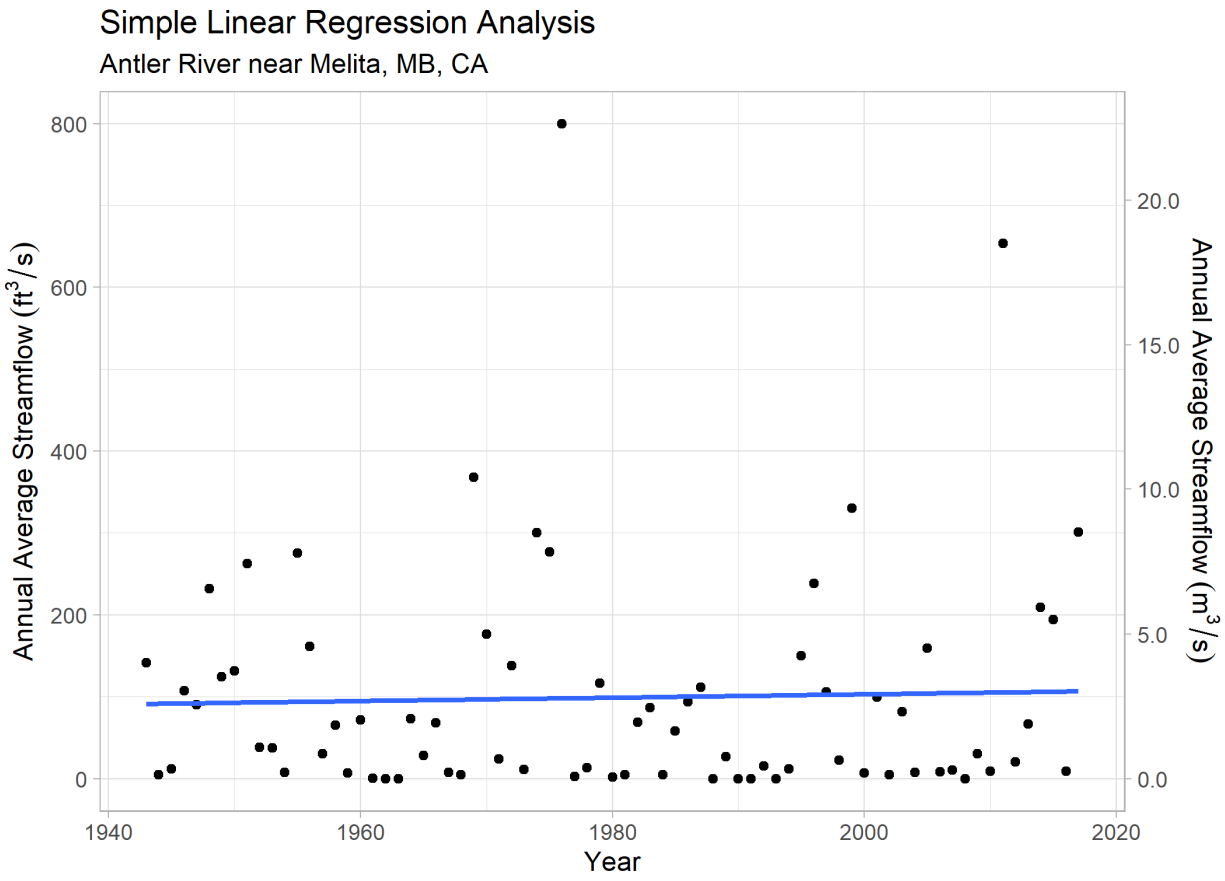

Figure 49. Trend analysis – spring, annual average streamflow – Antler River near Melita, MB; p-value 0.838

No statistically significant trends for the summer annual average streamflow were determined by the t-Test (p-value = 0.058), Mann-Kendall Test (p-value = 0.898), Spearman Rank-Order Test (p-value = 0.867), or simple linear regression test (p-value = 0.063). See plotted spring record in the Figure 50.

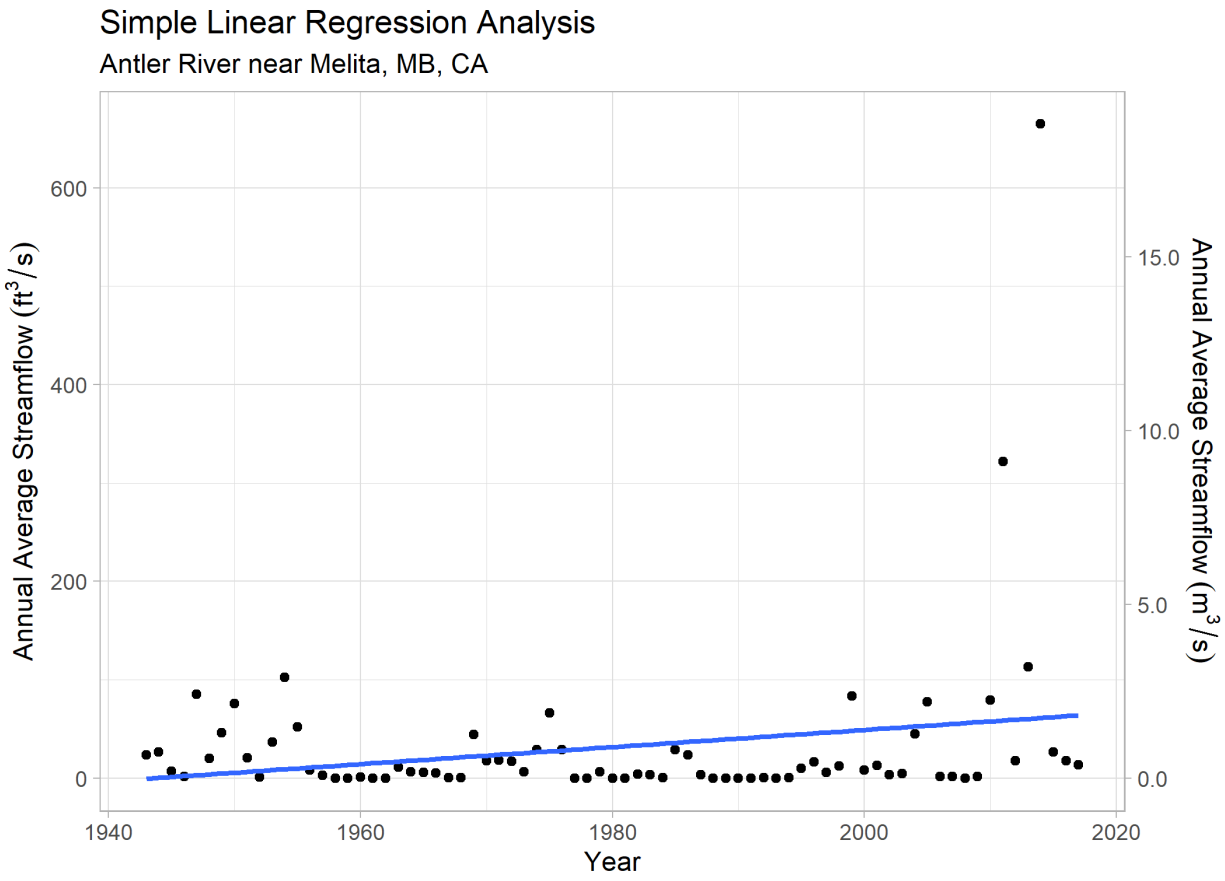

Figure 50. Trend analysis – summer, annual average streamflow – Antler River near Melita, MB; p-value 0.063

No statistically significant trends for the fall annual average streamflow were determined by the t-Test (p-value = 0.175), Mann-Kendall Test (p-value = 0.625), Spearman Rank-Order Test (p-value = 0.568), or simple linear regression test (p-value = 0.185). See plotted spring record in the Figure 51. Linear regression analysis of the period prior (1943-2007; p-value = 0.861) to and following (2009-2017; p-value = 0.656) the 2008 nonstationarity do not indicate a statistically significant trend in average streamflow.

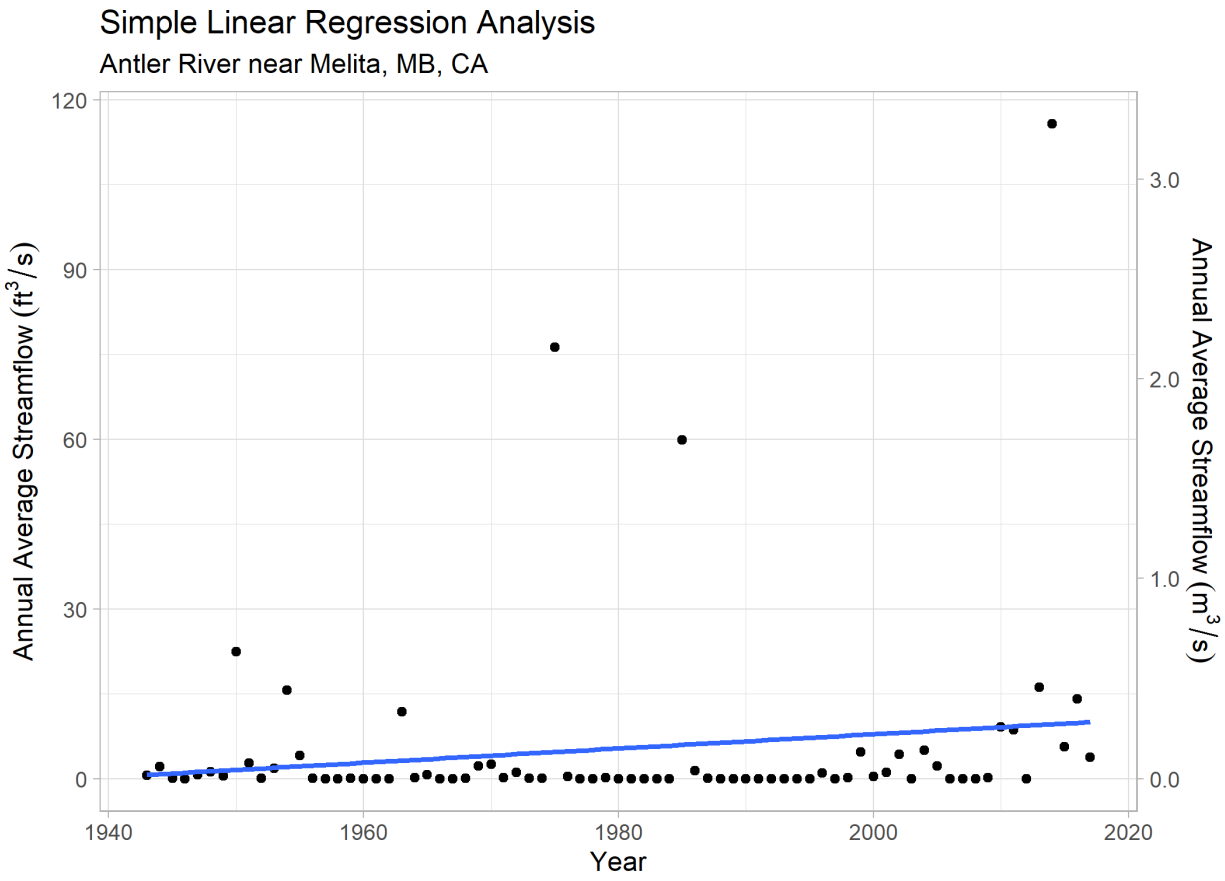

Figure 51. Trend analysis – fall, annual average streamflow – Antler River near Melita, MB; p-value 0.185

5 First Order Statistical Analysis of Historic Temperature Records

As part of the climate assessment for the Souris River Basin, trends in observed temperature records are analyzed. The NCEI's Minot Experimental Station, ND (Reference 10) is used to assess trends in observed maximum and minimum annual temperatures, as well as seasonal variation in temperature extremes in the U.S portion of the basin. The station has a daily period of record from June 1905 to present (2019). The station has 99% coverage over the period record. Three stations were utilized to fill in data gaps larger than 9 consecutive days; the Minot International Airport (Reference 11), Foxholm, ND (Reference 8), and Velva, ND (Reference 12). All stations used to fill the data gaps are within a 25-mile radius of the Minot Experimental Station. For shorter data gaps, missing values are approximated using linear interpolation in HEC-DSSVue (Reference 2). Data are analyzed from 1906-2018 in calendar years, both annually and seasonally. Data from 1905 are excluded from analysis because the temperature record only starts in June of 1905 for the Minot Experimental Station.

Observed, daily, average temperature data are not available at the Minot Experimental Station, so the Minot International Airport Station is used to analyze average temperature trends

annually and seasonally in the U.S portion of the basin. One hour temperature data from the Iowa Environment Mesonet (IEM; Reference 6) are used to calculate average annual, daily temperatures at the Minot International Airport using Microsoft Excel. Four missing values in late November and early December 1985 are accounted for with linear interpolation in HEC-DSSVue. The period of record available for analysis is 1949-2018, assessed in calendar years (beginning January 1).

The Yellow Grass climate station is used to assess trends in observed temperature in the Canadian portion of the basin. The Yellow Grass climate station is located approximately 50 miles southeast of Regina, Canada, within the Souris River Basin. The station has a relatively long period of continuous observations of daily temperature, spanning from August 1, 1911 to present. Data are available online from the Canadian Historical Climate Data Archive (Reference 5). Of the long-term climate stations in the Saskatchewan portion of the Souris River Basin, the Yellow Grass station has the most complete set of observations (1,687 missing values, approximately 95% availability). A simple method for gap-filling was used, in which all missing observations were replaced with a nearest neighbor observation from one of three stations. The three stations chosen to gap-fill missing observations were, in order of preference based on their distance from Yellow Grass: Weyburn, Francis, and Regina.The R software package "weathercan" (Reference 8) is used to download and process the temperature data. These stations were selected for their proximity to the Yellow Grass station, and for their consistency of record. No additional adjustments were applied. Ideally, a weighted approach, such as Theisen polygons would be applied to fill-in the temperature record. However, given the available resources and that data are being considered at the annual and seasonal scale rather than daily records, the nearest neighbor approach is sufficient for this analysis. Source data are provided in Celsius and then converted to Fahrenheit using a Microsoft Excel conversion function to be consistent with other temperature analysis in this report.

A first order statistical analysis of variation in seasonal temperature is carried out for the winter (December-February), spring (March- May), summer (June- August), and fall (September-November) months based on the calendar year. For the winter temperature datasets, the month of December is accounted for by including it in the same analysis year as the consecutive January and February. For example, the year 2010 includes data from December 2009, January 2010, and February 2010. HEC-DSSVue is used to convert the daily minimum and maximum temperature record into the annual timeseries used in this analysis.

5.1 Trends & Nonstationarities in Annual Maximum Temperature

5.1.1 Detection of Nonstationarities in Annual Maximum Temperatures

5.1.1.1 Nonstationarity Analysis- Annual Maximum Temperatures- Minot Experimental Station

The USACE Timeseries Toolbox (Reference 20) is used to assess trends and nonstationarities in annual maximum temperature at the Minot Experimental Station in North Dakota. Results indicate a strong nonstationarity in 1942, with detections by the statistical tests Cramer-von-Mises (CVM), LePage (LP), Mann-Whitney (MW), and a 1941 detection by the Lombard

Wilcoxon (LW) test. Figure 52 displays the output from the Timeseries Toolbox for the data primarily collected at the Minot Experimental Station gage.

1942 is considered a strong nonstationarity because it meets the criteria of consensus, robustness, and magnitude. The criterion of consensus is met with multiple distribution-based (CVM, LP) and mean-based (MW, LW) tests detecting 1942 as a nonstationarity. With different statistical based tests (mean and distribution) detecting 1942, the nonstationarity is considered robust. There is a significant shift in the magnitude of the variance between the subsets of temperature data analyzed: 1906-1940 (mean=100 degrees Fahrenheit (F); variance= 13), 1943-1948 (mean=99 degrees F; variance=24), and 1950-2018 (mean= 98 degrees F; variance=9).

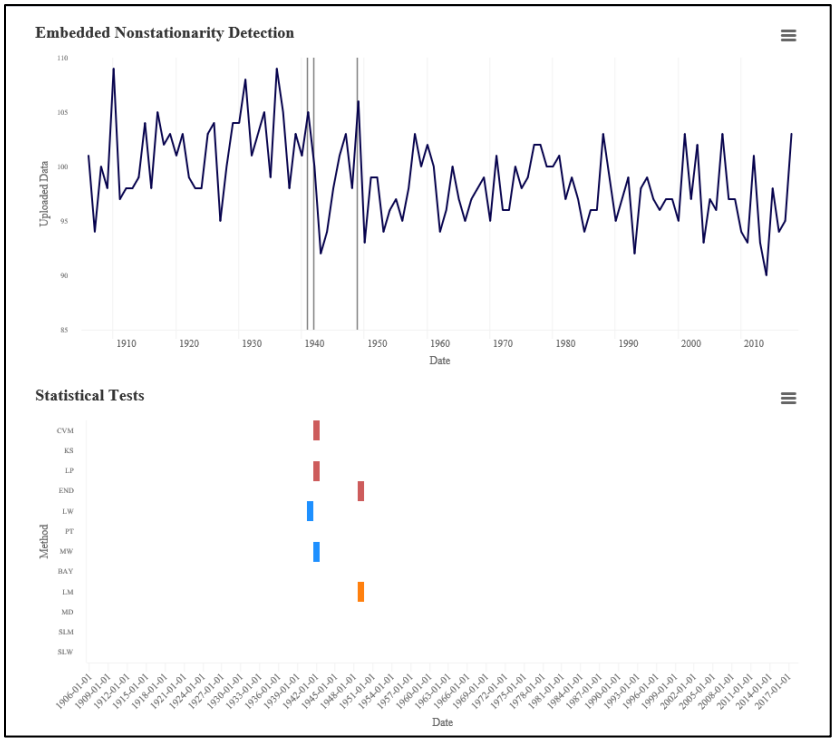

Type: Mean Distribution Variance Smooth

Note: y-axis is annual maximum temperature in degrees Fahrenheit

Abbreviation	Statistical Method	Abbreviation	Statistical Method
CVM	Cramer-von-Mises	BAY	Bayesian
KS	Kolmogorov-Smirnov	LM	Lombard Mood
LP	LePage	MD	Mood
END	Energy Divisive	SLM	Smooth Lombard Mood
LW	Lombard Wilcoxon	SLW	Smooth Lombard Wilcoxon
PT	Pettitt	MW	Mann-Whitney

Figure 52. Nonstationarity analysis – annual maximum temperatures –Minot Experimental Station, ND

5.1.1.2 Nonstationarity Analysis- Annual Maximum Temperatures- Yellow Grass, SK Station

The USACE Timeseries Toolbox is used to analyze nonstationarities in annual maximum temperatures at Yellow Grass, SK, Canada (period of record 1912-2018). No strong nonstationarities are identified in the annual maximum temperature timeseries using the Timeseries Toolbox. Nonstationarities detected are identified by two or less statistical tests.

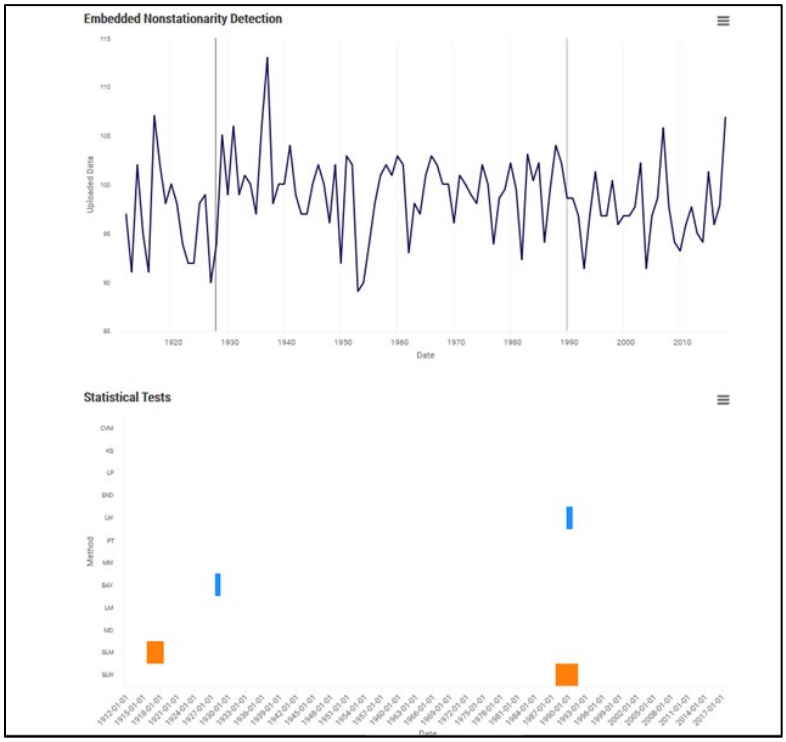

Type: Mean Distribution Variance Smooth

Note: y-axis is annual maximum temperature in degrees Fahrenheit

Abbreviation	Statistical Method	Abbreviation	Statistical Method
CVM	Cramer-von-Mises	BAY	Bayesian
KS	Kolmogorov-Smirnov	LM	Lombard Mood
LP	LePage	MD	Mood
END	Energy Divisive	SLM	Smooth Lombard Mood
LW	Lombard Wilcoxon	SLW	Smooth Lombard Wilcoxon
PT	Pettitt	MW	Mann-Whitney

Figure 53. Nonstationarity analysis- annual maximum temperatures-Yellow Grass, SK

5.1.2 Detection of Trends in Annual Maximum Temperatures

5.1.2.1 Trend Analysis- Annual Maximum Temperatures- Minot Experimental Station

In addition to assessing the stationarity of the maximum temperature record at the Minot Experimental Station, the USACE Timeseries Toolbox (Reference 20) is used to analyze the dataset for monotonic trends. A statistically significant decreasing trend is indicated by the t-Test (p-value=8.85×10^{-6}), Mann-Kendall (p-value=2.35×10^{-5}) and Spearman Rank-Order (p-value=1.09×10^{-5}) test. A linear regression analysis is also performed using Microsoft Excel. As can be seen in Figure 54, results of linear regression show a statistically significant decreasing trend in the dataset (p-value of 1.64×10^{-16}) for the full period of record (1906-2018). Linear regression analysis for subset data at the 1942 nonstationarity does not indicate a significant trend prior to the detection (1906-1941; p-value=0.214) and a significant decreasing trend post-nonstationarity (1943-2018; p-value=6.06×10^{-5}).

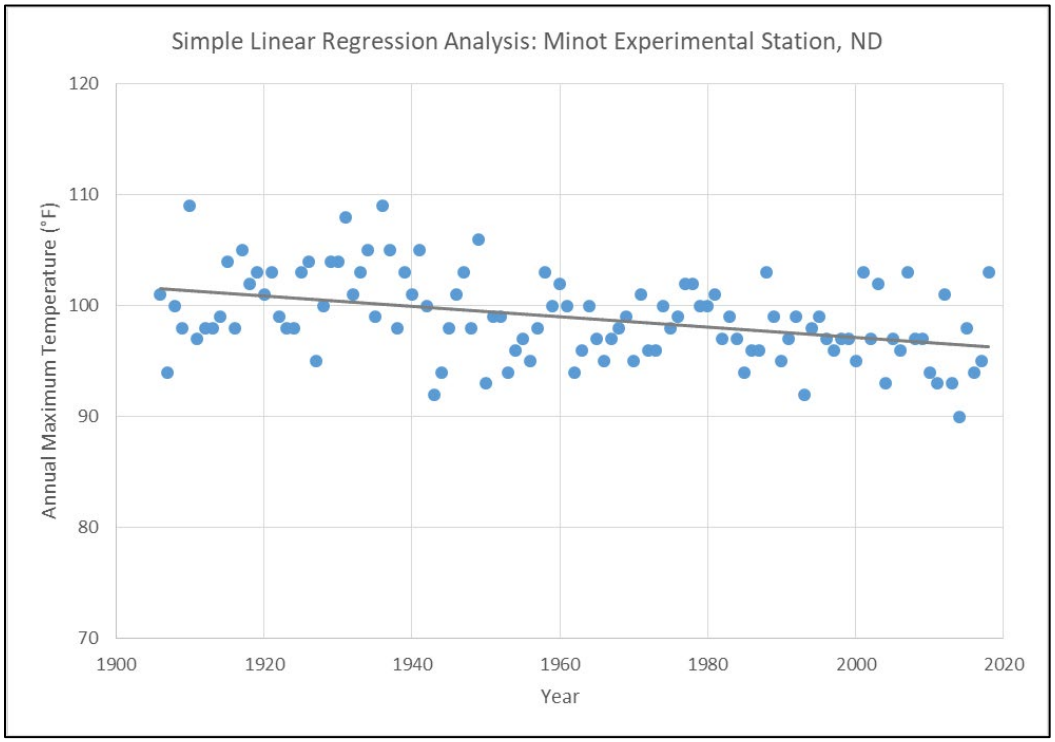

Figure 54. Trend analysis - annual maximum temperatures - Minot Experimental Station, ND; p-value= 1.64×10^{-16}.

5.1.2.2 Trend Analysis- Annual Maximum Temperatures- Yellow Grass Station, SK

Trends in annual maximum temperatures are also analyzed at the Yellow Grass Station in Saskatchewan. No significant trends are present in the annual maximum temperatures using the t-Test (p-value= 0.7114), Mann-Kendall (p-value= 0.4375), and Spearman-Rank Order (p-value= 0.5045) test. Linear regression analysis in Microsoft Excel suggests a statistically significant decreasing trend, with a p-value= 5.91×10^{-5}.

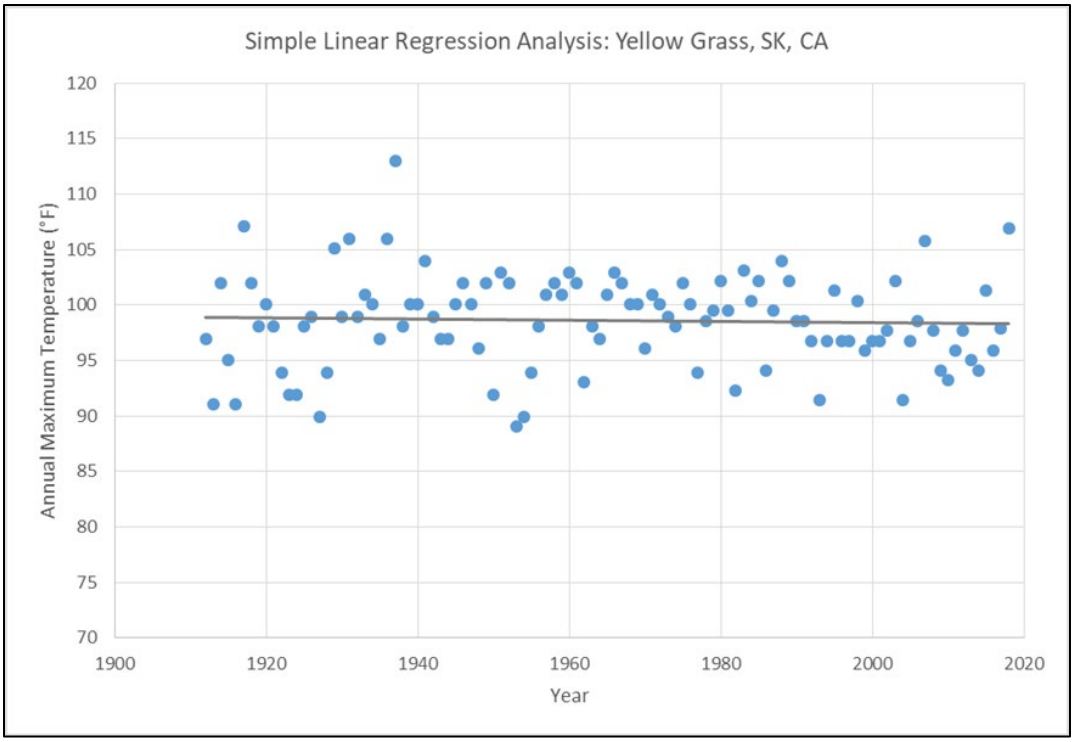

Figure 55. Trend analysis- annual maximum temperatures- Yellow Grass, SK; p-value= 5.91×10^{-5}

5.2 Trends & Nonstationarities in Maximum Seasonal Temperatures

Along with looking at trends in the annual maximum temperature record, a nonstationarity analysis and a trend analysis is performed on the maximum seasonal temperatures.

5.2.1 Detection of Nonstationarities in Maximum Seasonal Temperatures

5.2.1.1 Nonstationarity Analysis- Seasonal Maximum Temperatures- Minot Experimental Station

In spring maximum temperatures recorded at Minot Experimental Station, a strong nonstationarity is detected in 1994 by the following three statistical tests: the Cramer-von-Mises (CVM), the Lombard Wilcoxon (LW, 1993), and the Mann-Whitney (MW) tests. Because two different tests (LW and MW) targeted at identifying a shift in mean indicate a nonstationarity there is consensus. Tests identifying changes in overall distribution (CVM) and mean identify 1994 as a nonstationarity, meeting the criteria of robustness. The USACE Timeseries Toolbox (Reference 20) output indicates that there is a shift in both the mean and the variance between the subsets of data analyzed: 1950-1992 (mean=88 degrees Fahrenheit (F); variance=20), 1995-2006 (mean=85 degrees F; variance=19), and 2008-2018 (mean=83 degrees F; variance= 35). Results are displayed in Figure 56.

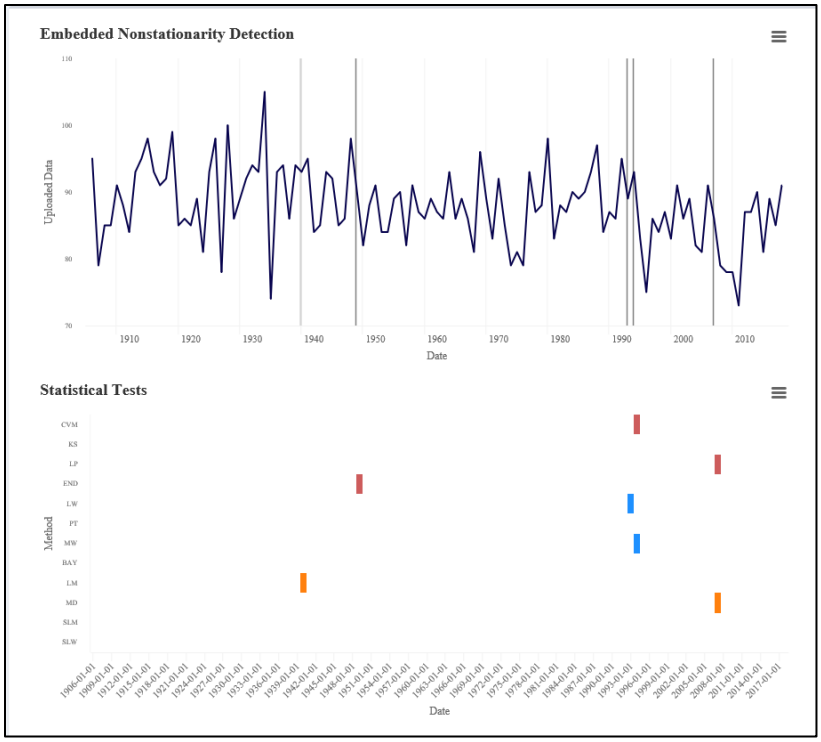

Type: Mean Distribution Variance Smooth

Note: y-axis is spring maximum temperature in degrees Fahrenheit

Abbreviation	Statistical Method	Abbreviation	Statistical Method
CVM	Cramer-von-Mises	BAY	Bayesian
KS	Kolmogorov-Smirnov	LM	Lombard Mood
LP	LePage	MD	Mood
END	Energy Divisive	SLM	Smooth Lombard Mood
LW	Lombard Wilcoxon	SLW	Smooth Lombard Wilcoxon
PT	Pettitt	MW	Mann-Whitney

Figure 56. Nonstationarity analysis – spring, annual maximum temperatures –Minot Experimental Station, ND

In the summer annual maximum temperatures, a strong nonstationarity is detected in 1942. The 1942 nonstationarity is detected by the statistical tests: CVM, MW, and LW (1941). 1942 is considered a strong nonstationarity because it demonstrates a degree of consensus, robustness and a significant shift in the magnitude of the dataset's overall variance. The criterion of consensus is fulfilled because multiple tests targeted at detecting shifts in the mean (MW and LW) of the dataset are indicating a nonstationarities. It is considered robust because tests targeted at detecting nonstationarities in multiple types of statistical properties are indicating nonstationarities (overall distribution and mean). Additionally, the Timeseries Toolbox indicates a shift in the variance within the subsets of data analyzed by the tool: 1906-1940 (mean=100

degrees F; variance=15), 1943-1948 (mean=99 degrees F; variance=24), and 1950-2018 (mean=97 degrees F; variance=9.9).

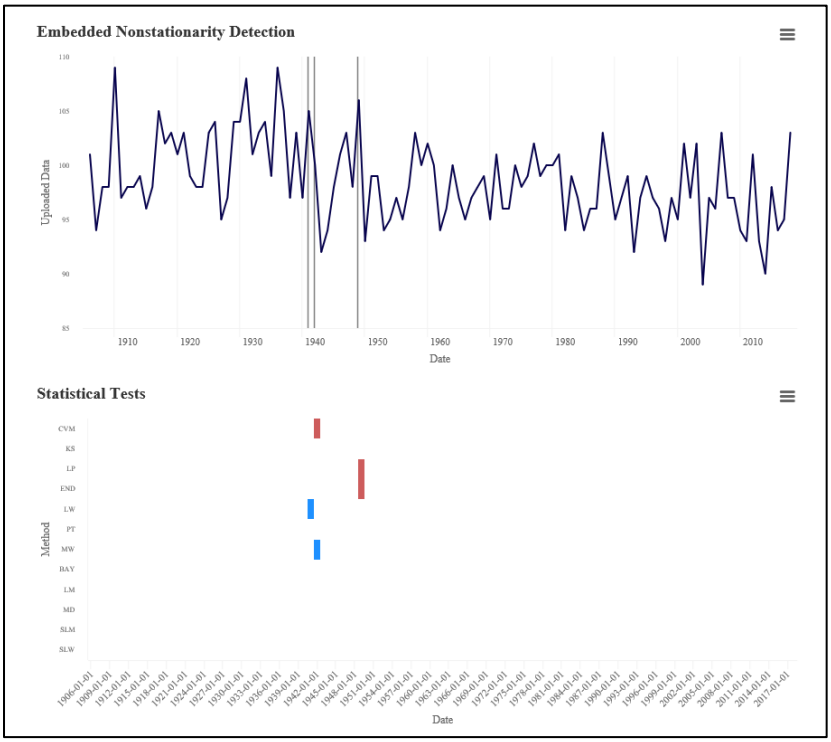

Type: Mean Distribution Variance Smooth

Note: y-axis is summer maximum temperature in degrees Fahrenheit

Abbreviation	Statistical Method	Abbreviation	Statistical Method
CVM	Cramer-von-Mises	BAY	Bayesian
KS	Kolmogorov-Smirnov	LM	Lombard Mood
LP	LePage	MD	Mood
END	Energy Divisive	SLM	Smooth Lombard Mood
LW	Lombard Wilcoxon	SLW	Smooth Lombard Wilcoxon
PT	Pettitt	MW	Mann-Whitney

Figure 57. Nonstationarity analysis – summer, annual maximum temperatures –Minot Experimental Station, ND.

No strong nonstationarities are detected in the annual maximum fall temperatures or annual maximum winter temperatures for the period of records (1906-2018).

5.2.1.2 Nonstationarity Analysis- Seasonal Maximum Temperatures- Yellow Grass, SK Station

Nonstationarity analysis for seasonal maximum temperatures recorded at the Yellow Grass, SK station does not indicate strong nonstationarities in the spring, summer, or fall maximum temperature timeseries. For the winter maximum temperatures, the Timeseries Toolbox detects a strong nonstationarity in 1986 by the Cramer von Mises (CVM), LePage (LP), and

Mann Whitney (MW) statistical tests. The 1986 nonstationarity is considered strong because it meets the criteria of consensus, robustness, and magnitude. Consensus is met because two distribution-based statistical tests (CVM and LP) detect 1986 as a nonstationary within the period of record. Robustness is met because 1986 is detected as a nonstationarity by statistical tests based on different statistical properties (mean and distribution). There is a shift in magnitude of statistical properties starting in 1986, as detected by the Timeseries Toolbox. The segment mean, variance, and standard deviation (std. dev.) increase between the segmented datasets 1912-1985 (mean=45 degrees Fahrenheit, variance= 28, std. dev. = 5.3) and 1987-2018 (mean= 48 degrees F, variance= 31, std. dev. =5.6).

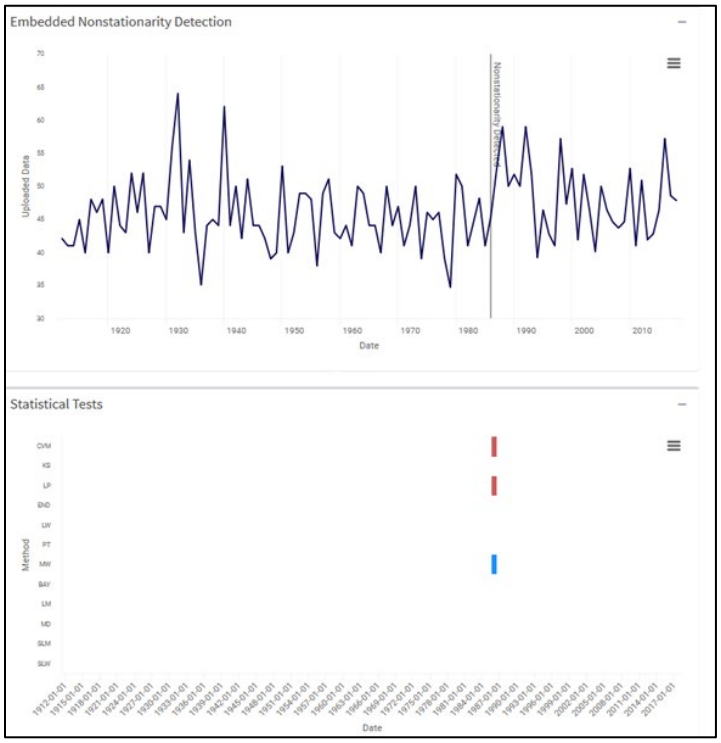

Note: y-axis is winter maximum temperature in degrees Fahrenheit

Abbreviation	Statistical Method	Abbreviation	Statistical Method
CVM	Cramer-von-Mises	BAY	Bayesian
KS	Kolmogorov-Smirnov	LM	Lombard Mood
LP	LePage	MD	Mood
END	Energy Divisive	SLM	Smooth Lombard Mood
LW	Lombard Wilcoxon	SLW	Smooth Lombard Wilcoxon
PT	Pettitt	MW	Mann-Whitney

Figure 58. Nonstationarity analysis- winter, annual maximum temperatures- Yellow Grass, SK

5.2.2 Detection of Trends in Maximum Seasonal Temperatures

5.2.2.1 Trend Analysis- Annual Maximum Temperatures- Minot Experimental Station

In addition to carrying out an assessment of nonstationarities, trend analysis is evaluated for seasonal, maximum temperature records at the Minot Experimental Station (1906-2018). Within the spring, maximum temperature record, a statistically significant decreasing trend is identified using the t-Test (p-value=0.002), Mann-Kendall (p-value 0.003), Spearman Rank-Order (p-value 0.003) and linear regression tests (p-value=2.10×10^{-8}), see Figure 59. The spring maximum temperature record is also evaluated for the pre-nonstationarity dataset (1906-1993) and the post-nonstationarity dataset (1995-2018). The p-values computed for the subsets of data are 0.003 and 0.710, respectively. Only the pre- 1994 nonstationarity portion of the data exhibits a statistically significant, decreasing trend (p-value< 0.05).

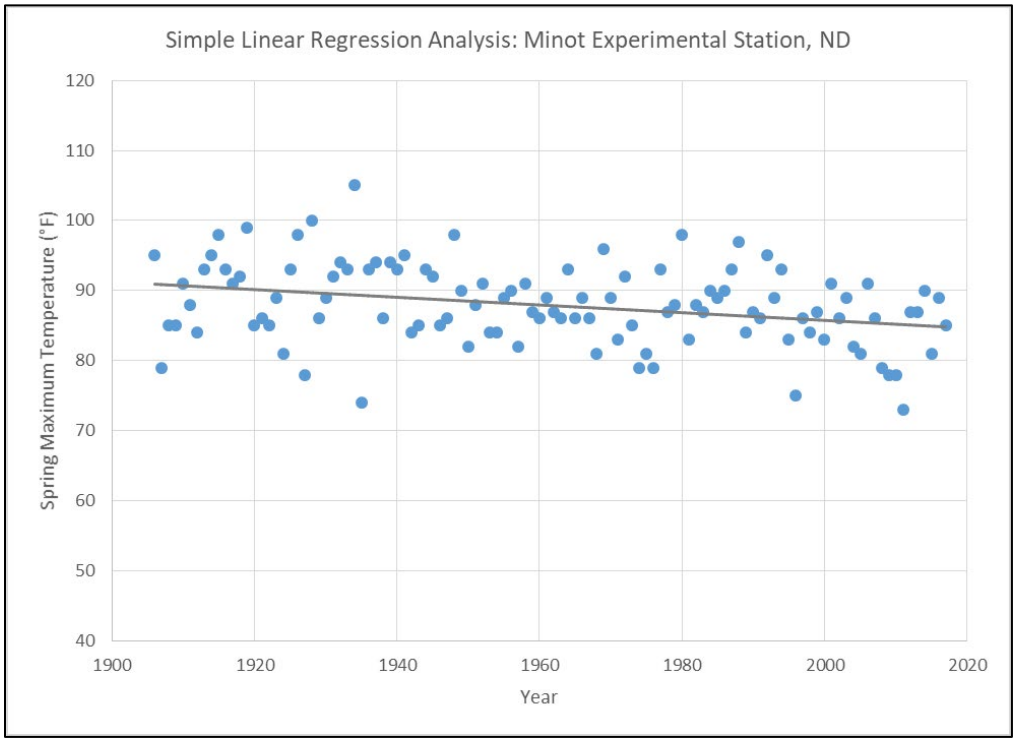

Figure 59. Trend analysis – spring, annual maximum temperatures - Minot Experimental Station, ND; p-value= 2.01×10^{-8}.

There is a statistically significant decreasing trend present in the summer annual maximum temperature record (1906-2018). This trend is identified by the t-Test (p-value 3.56×10^{-5}), Mann-Kendall (p-value 1.66×10^{-4}), Spearman Rank-Order (p-value 8.44×10^{-5}), and linear regression (p-value= 2.79×10^{-15}) tests. The summer maximum temperature dataset is also evaluated for trends within the portions of the period of record prior to and after the 1942 nonstationarity using simple linear regression analysis. No trend is indicated in the pre-nonstationarity dataset (1906-1941; p-value=0.392). Linear regression suggests a significant decreasing trend in the post-nonstationarity dataset (1943-2018; p-value=3.26×10^{-5}).

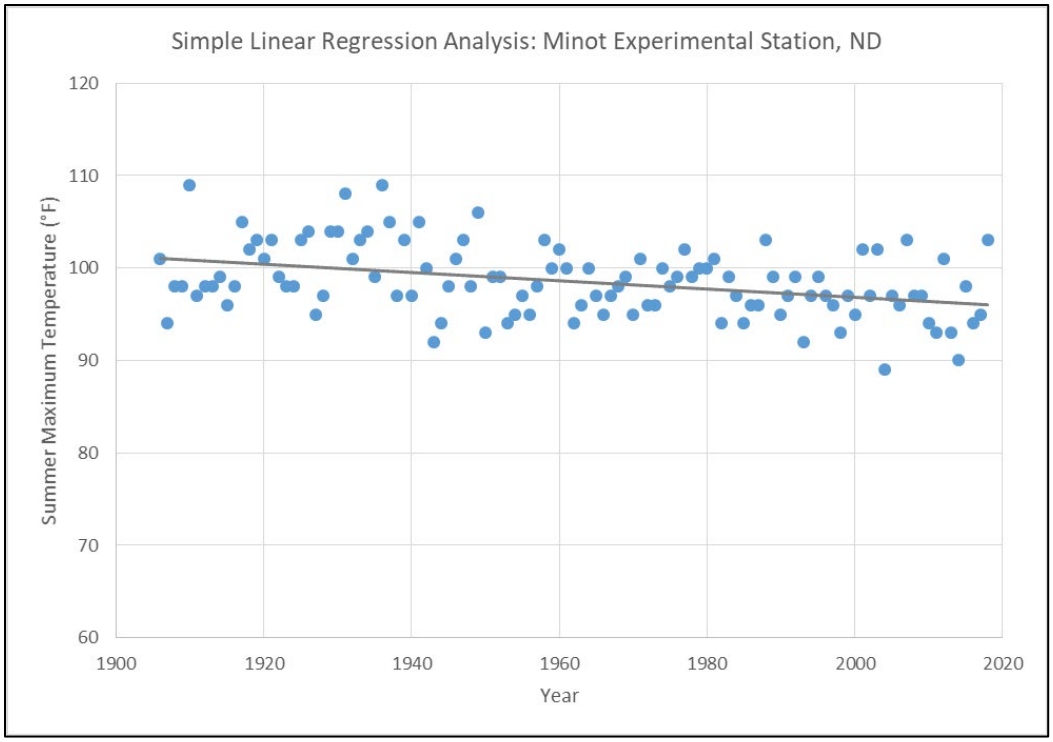

Figure 60. Trend analysis – summer, annual maximum temperatures - Minot Experimental Station, ND; p-value=2.79x10^{-15}.

The fall, annual maximum temperature dataset does not exhibit a statistically significant trend by the t-Test (p-value=0.100), Mann-Kendall (p-value 0.087), and Spearman Rank-Order (p-value 0.088) tests. Linear regression analysis indicates a statistically significant decreasing trend, with a p-value of 2.46x10^{-5} (see Figure 61). No nonstationarities are detected in the fall maximum temperature data for further analysis.

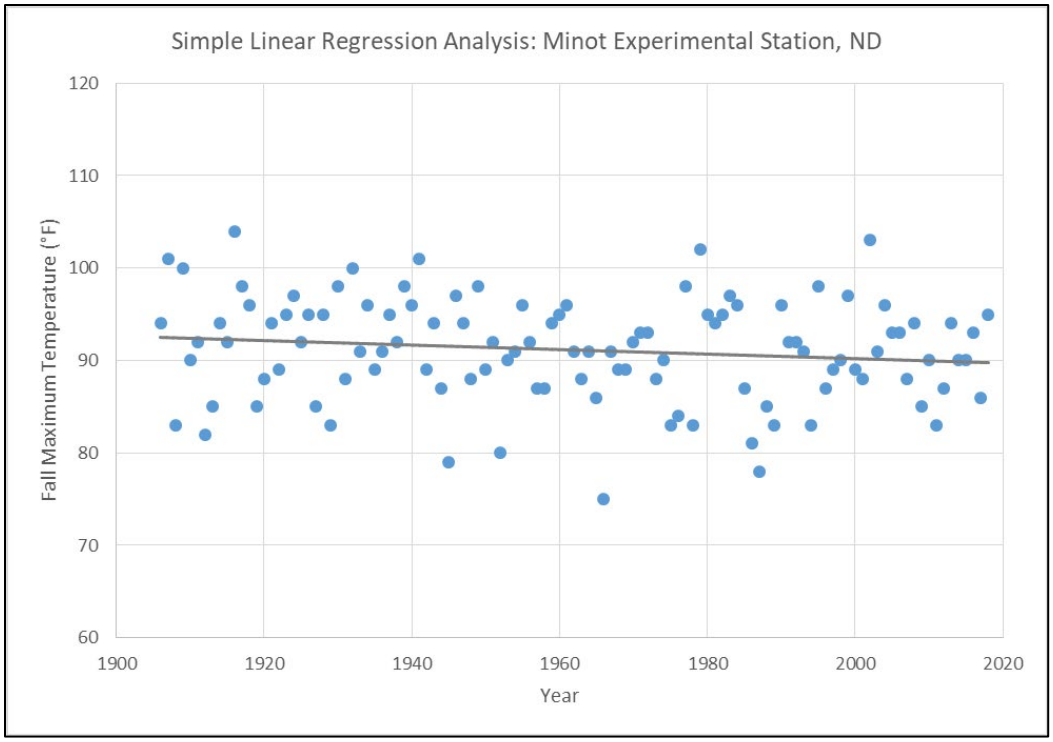

Figure 61. Trend analysis – fall, annual maximum temperatures - Minot Experimental Station, ND; p-value $2.46x10^{-5}$.

For the winter annual maximum temperature data (1906-2018), a statistically significant decreasing trend is detected by the Mann-Kendall (p-value 0.048), Spearman Rank-Order (p-value 0.041), and linear regression (p-value= 0.002) tests. The t-Test does not indicate a statistically significant trend, but the calculated p-value of 0.053 is just above the cutoff for accepted significance. See Figure 62 for a plot of the annual winter maximum data.

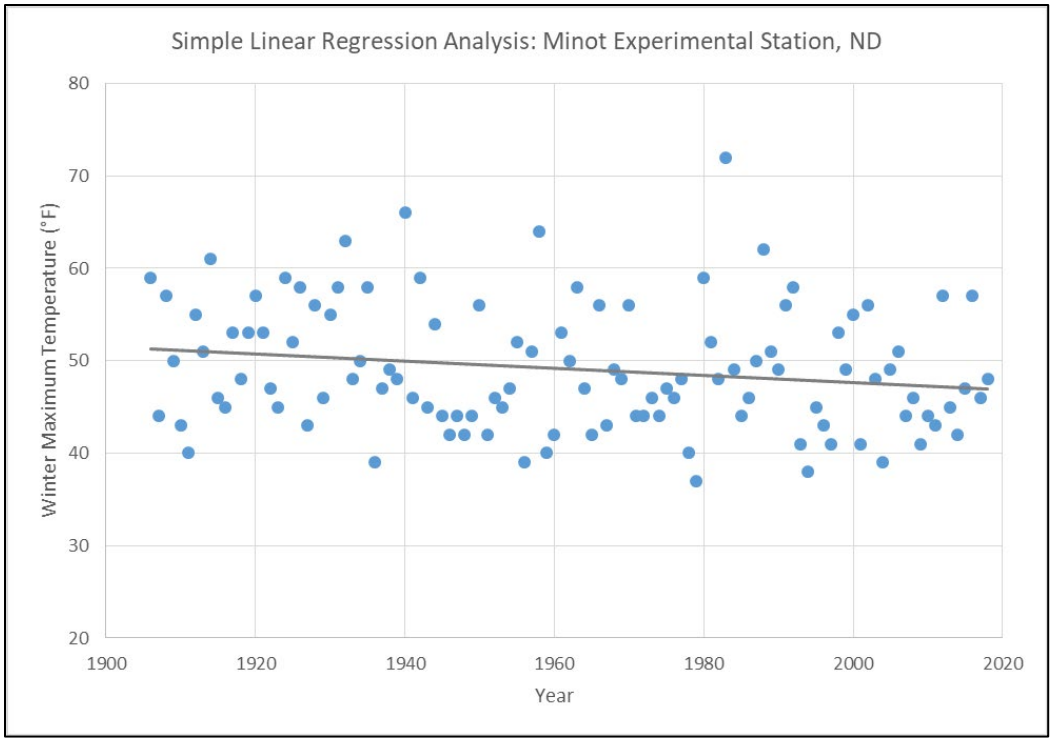

Figure 62. Trend analysis – winter, annual maximum temperatures - Minot Experimental Station, ND; p-value= 0.0015.

5.2.2.2 Trend Analysis- Annual Maximum Temperatures- Yellow Grass, SK Station

In addition to carrying out an assessment of nonstationarities, trend analysis is evaluated for seasonal, maximum temperature records at the Yellow Grass, SK Station (1912-2018). In the spring, annual maximum temperature record (1912-2018), the Timeseries Toolbox does not indicate a statistically significant monotonic trend by the t-Test (p-value= 0.853), Mann-Kendall (p-value=0.597), and Spearman Rank-Order (p-value=0.567) statistical tests. Linear regression analysis using Microsoft Excel does suggest a statistically significant trend, with a p-value=0.005 (see Figure 63).

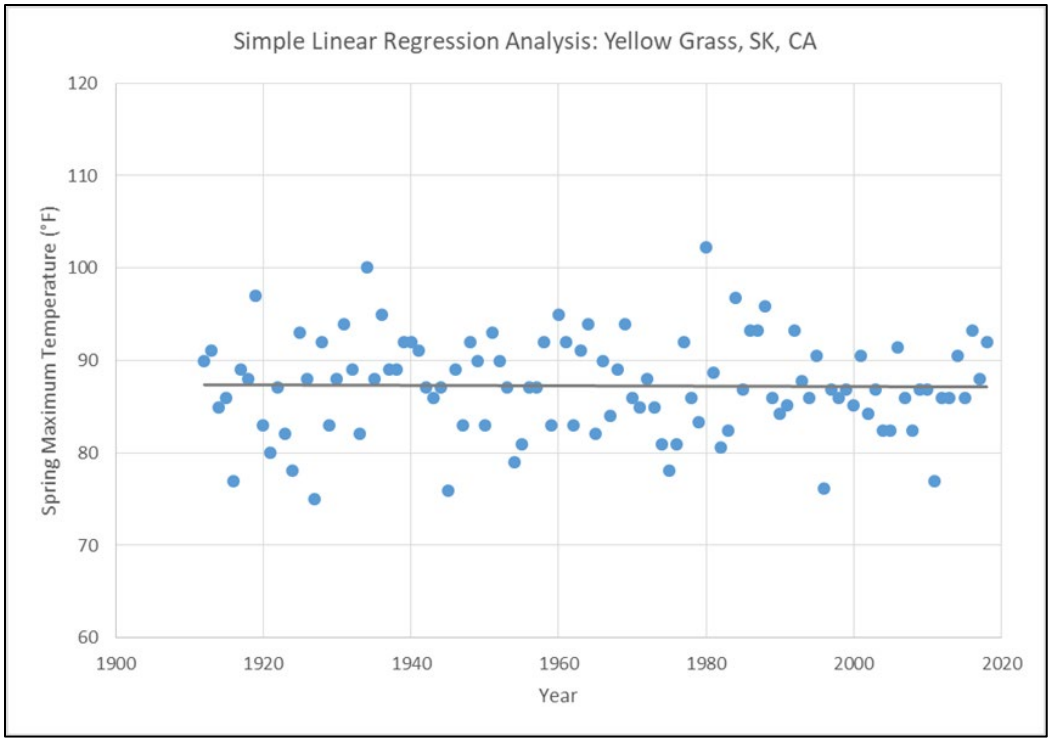

Figure 63. Trend analysis- spring, annual maximum temperatures- Yellow Grass, SK; p-value= 0.0046

In the summer, annual maximum temperature record, the Timeseries Toolbox does not indicate a significant monotonic trend by the t-Test (p-value= 0.660), Mann-Kendall (p-value= 0.362), and Spearman Rank-Order (p-value= 0.457) statistical tests. Linear regression analysis for the full period of record suggests a significant, decreasing trend in summer maximum temperatures (p-value= 6.34×10^{-5}; see Figure 64).

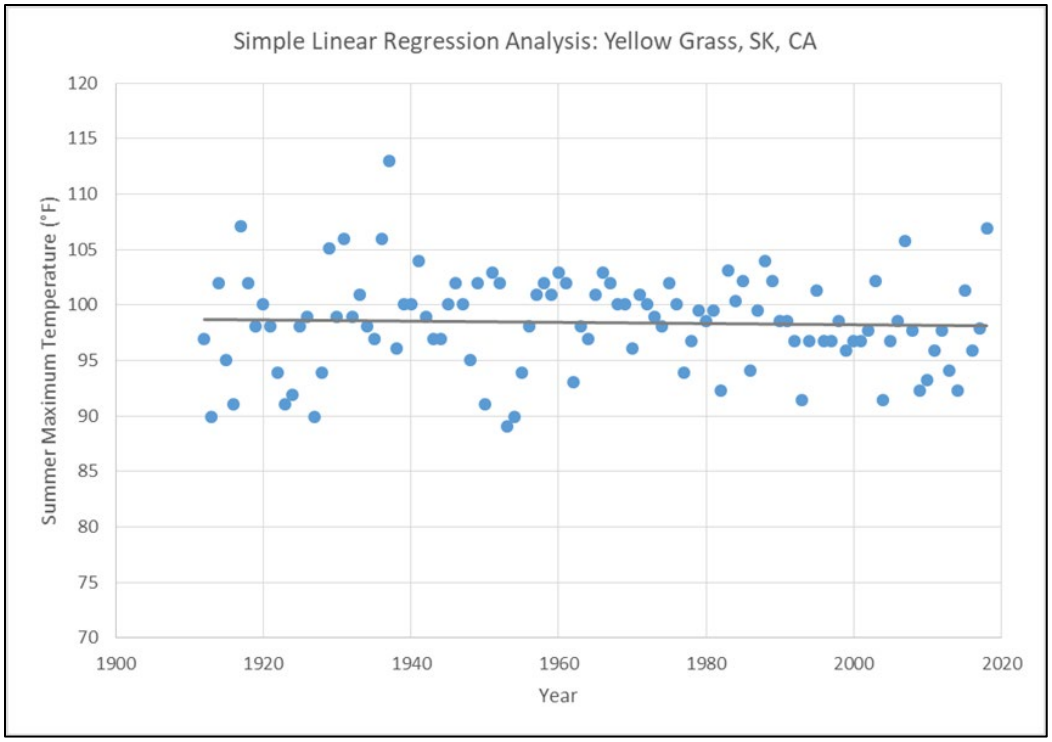

Figure 64. Trend analysis- summer, annual maximum temperatures- Yellow Grass, SK; p-value= 6.34×10^{-5}

In the fall, annual maximum temperature timeseries, the Timeseries Toolbox detects significant increasing trends with the Mann-Kendall (p-value= 0.033) and Spearman Rank-Order (p-value= 0.028) statistical tests, but not the t-Test (p-value=0.069). Linear regression does not indicate a significant trend, with a p-value=0.327 (see Figure 65).

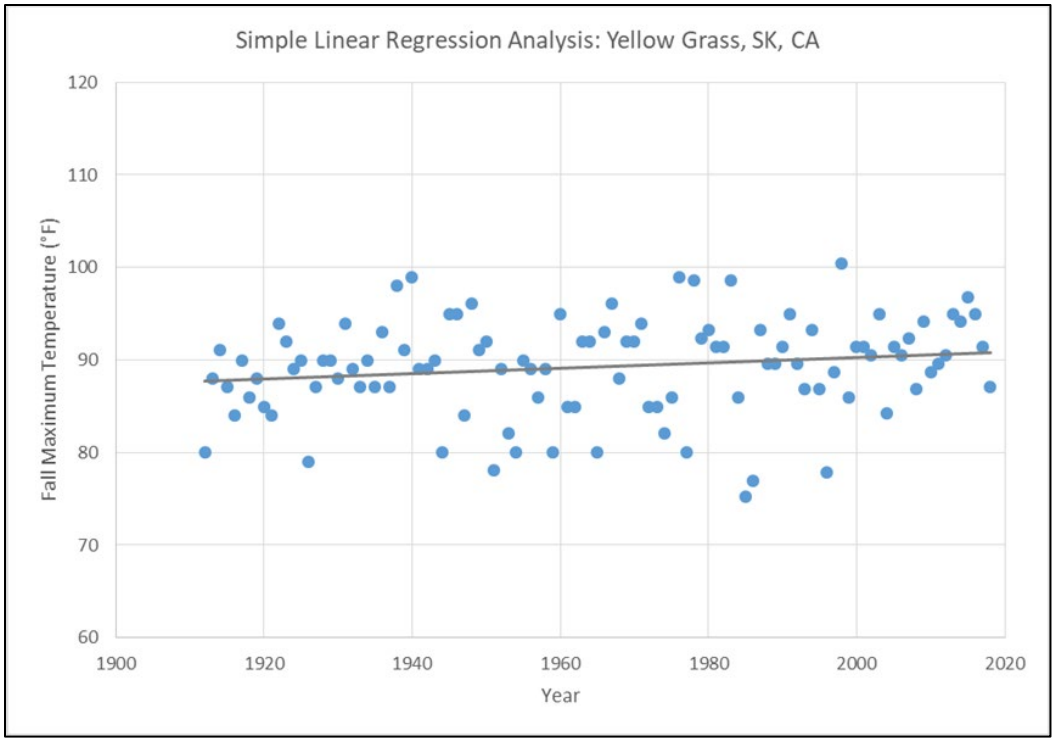

Figure 65. Trend analysis- fall, annual maximum temperatures, Yellow Grass, SK; p-value= 0.3269

In the winter, annual maximum temperatures timeseries, the Timeseries Toolbox does not detect statistically significant trends in the period of record (1912-2018) using the t-Test (p-value=0.261), Mann-Kendall (p-value= 0.182), and Spearman Rank-Order (p-value= 0.184). Linear regression analysis using Microsoft Excel does not indicate a significant trend, with a p-value of 0.808 (see Figure 66). Analysis based upon the detected nonstationarity in 1986 does not indicate significant trends in the datasets pre-1986 (1912-1985; p-value=0.112) or post-1986 (1987-2018; p-value= 0.079).

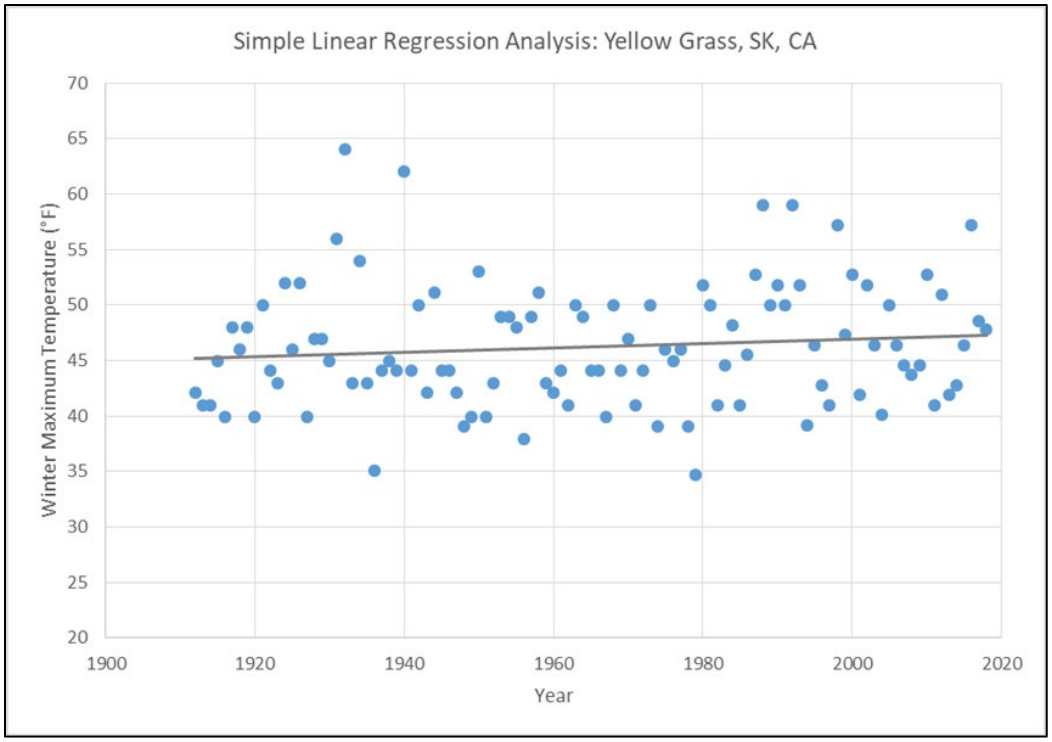

Figure 66. Trend analysis- winter, annual maximum temperatures- Yellow Grass, SK; p-value= 0.8075

5.3 Trends and Nonstationarities in Annual Minimum Temperatures

5.3.1 Detection of Nonstationarities in Annual Minimum Temperatures

5.3.1.1 Nonstationarity Analysis- Annual Minimum Temperatures- Minot Experimental Station

The USACE Timeseries Toolbox (Reference 20) is used to assess trends and nonstationarities in observed annual minimum temperatures collected primarily at the Minot Experimental Station, ND. Results indicate a strong nonstationarity in 1939. Figure 67 displays the nonstationarity detection output from the Timeseries Toolbox. Statistical tests that detect 1939 as a nonstationarity are the Cramer-von-Misses (CVM) and Energy Divisive (END) tests. The Lombard Wilcoxon (LW) test also detects a nonstationarity in 1938. The nonstationarity demonstrates consensus by being identified by two tests that detect changes in the overall statistical distribution (CVM and END) of the dataset. The 1939 nonstationarity is considered robust because it is identified by tests that indicate a change in the overall distribution and the sample mean. Results from the Timeseries Toolbox also indicate a significant shift in the magnitude of the mean and variance between the subsets of data analyzed by the tool: 1906-1922 (mean= -38 degrees Fahrenheit (F); variance=42), 1925-1937 (mean= -32 degrees F; variance= 64), and 1940-2018 (mean=-28 degrees F; variance=28).

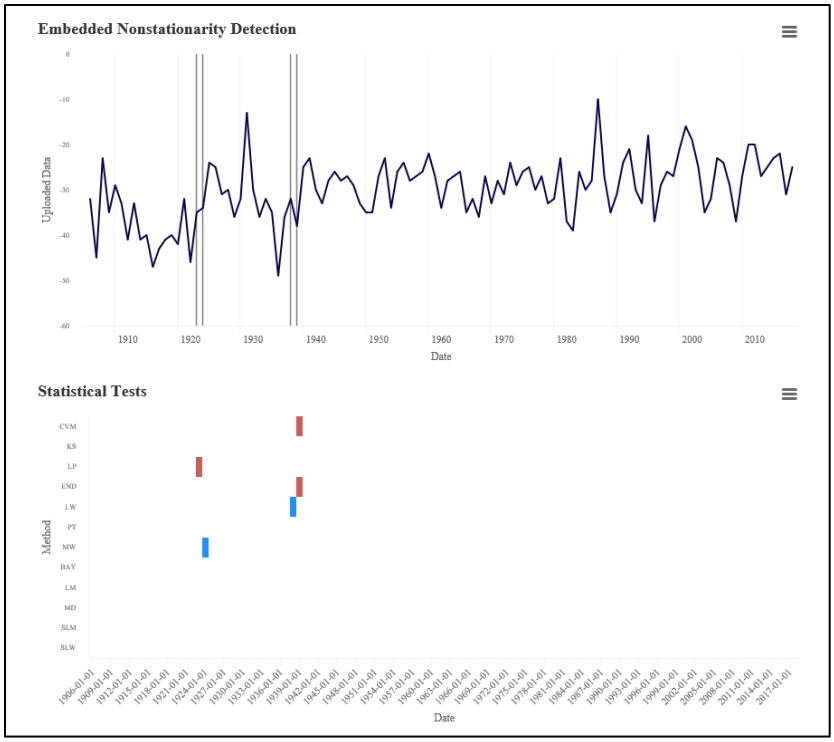

Type: Mean Distribution Variance Smooth

Note: y-axis is annual minimum temperature in degrees Fahrenheit

Abbreviation	Statistical Method	Abbreviation	Statistical Method
CVM	Cramer-von-Mises	BAY	Bayesian
KS	Kolmogorov-Smirnov	LM	Lombard Mood
LP	LePage	MD	Mood
END	Energy Divisive	SLM	Smooth Lombard Mood
LW	Lombard Wilcoxon	SLW	Smooth Lombard Wilcoxon
PT	Pettitt	MW	Mann-Whitney

Figure 67. Nonstationarity analysis - annual minimum temperatures - Minot Experimental Station, ND

5.3.1.2 Nonstationarity Analysis- Annual Minimum Temperatures- Yellow Grass, SK Station

The USACE Timeseries Toolbox is used to analyze nonstationarities in annual minimum temperatures at Yellow Grass, SK, Canada. The period of record used for the Yellow Grass station is calendar years 1912-2018. No strong nonstationarities are present in the annual minimum temperature timeseries detected using the Timeseries Toolbox. However, the Smooth Lombard Wilcoxon test detects a gradual shift in the mean in the years 1915 to 1920.

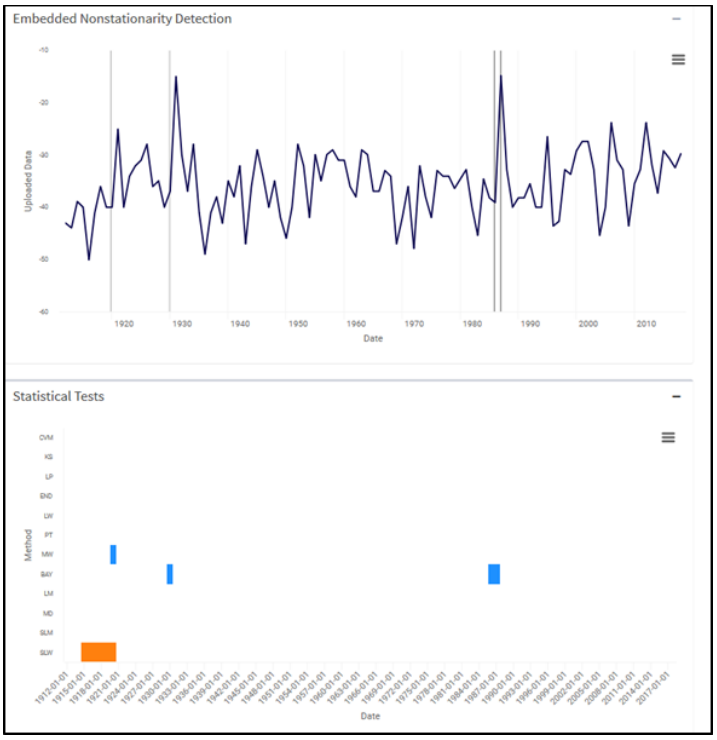

Type: Mean Distribution Variance Smooth

Note: y-axis is annual minimum temperature in degrees Fahrenheit

Abbreviation	Statistical Method	Abbreviation	Statistical Method
CVM	Cramer-von-Mises	BAY	Bayesian
KS	Kolmogorov-Smirnov	LM	Lombard Mood
LP	LePage	MD	Mood
END	Energy Divisive	SLM	Smooth Lombard Mood
LW	Lombard Wilcoxon	SLW	Smooth Lombard Wilcoxon
PT	Pettitt	MW	Mann-Whitney

Figure 68. Nonstationarity analysis- annual minimum temperatures-Yellow Grass, SK

5.3.2 Detection of Trends in Annual Minimum Temperatures

5.3.2.1 Trend Analysis- Annual Minimum Temperatures- Minot Experimental Station

Annual minimum temperature recorded at the Minot Experimental Station in North Dakota are evaluated for the presence of statistically significant trends. Based on the results of the t-Test (p-value=9.01×10^{-8}), Mann-Kendall (p-value 3.58×10^{-7}) and Spearman Rank-Order (p-value=1.65×10^{-7}) monotonic trend tests, the USACE Timeseries Toolbox (Reference 20) identifies a statistically significant, increasing trend in annual minimum temperature. Linear regression analysis, performed in Microsoft Excel, also indicates an increasing trend with a p-value of 1.50×10^{-9} (see Figure 69).

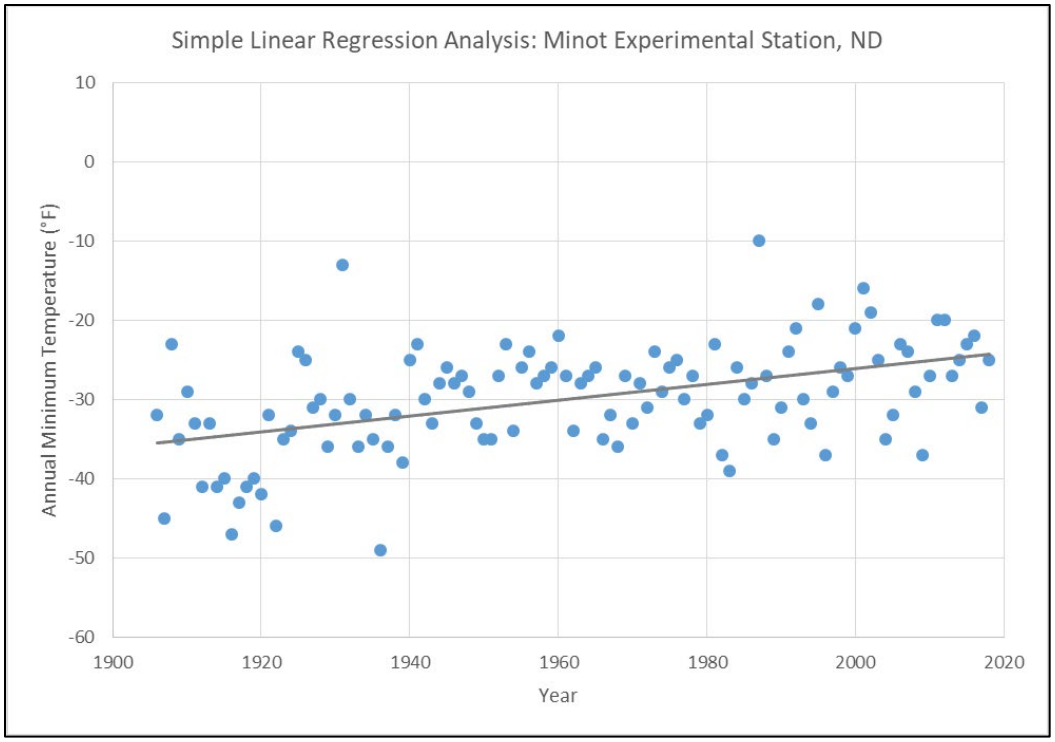

Figure 69. Trend analysis - annual minimum temperatures - Minot Experimental Station, ND; p-value 1.50×10^{-9}.

The annual minimum temperature record is segmented into the pre- and post- nonstationarity portions of the period of record at the 1939 nonstationarity. There is no statistically significant trend in the dataset collected prior to 1939 (1906-1938; p-value=0.305). Linear regression analysis carried out for the period of record between 1940 and 2018 indicates a statistically significant, increasing trend in annual minimum temperatures, with a p-value of 0.021.

5.3.2.2 Trend Analysis- Annual Minimum Temperatures- Yellow Grass Station, SK

The USACE Timeseries Toolbox (Reference 20) is used to assess monotonic trends in the annual minimum temperature timeseries at Yellow Grass, SK, Canada (period of record 1912-2018). A statistically significant increasing trend is present in the annual minimum temperature record and is detected using the t-Test (p-value= 0.045), Mann-Kendall (p-value= 0.029), and Spearman-Rank Order (p-value= 0.024) test. Linear regression analysis in Microsoft Excel suggests a statistically significant increasing trend, with a p-value= 0.004.

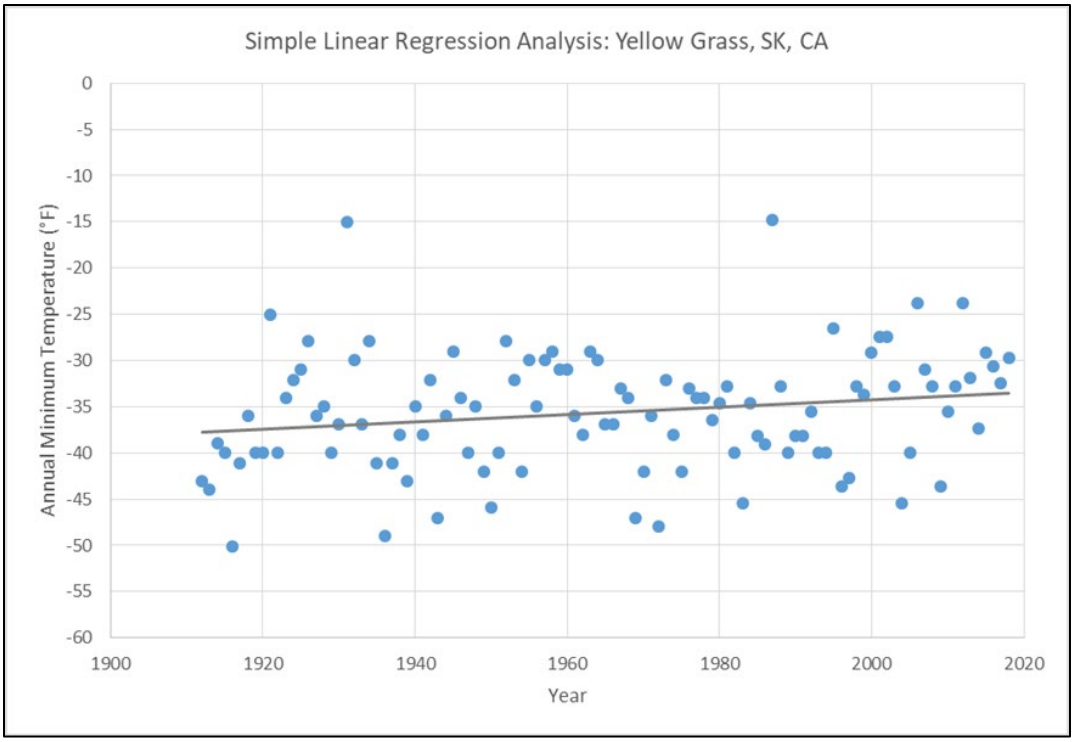

Figure 70. Trend analysis- annual minimum temperatures- Yellow Grass, SK; p-value= 0.0039

5.4 Trends & Nonstationarities in Minimum Seasonal Temperatures

5.4.1 Detection of Nonstationarities in Minimum Seasonal Temperatures

5.4.1.1 Nonstationarity Analysis- Seasonal Minimum Temperatures – Minot Experimental Station

A nonstationarity assessment is carried out using seasonal minimum temperature data primarily collected at the Minot Experimental Station. No strong nonstationarities are detected in the spring and fall annual minimum temperatures datasets. For the summer annual minimum temperature record, strong nonstationarities are detected in the years 1929 and 2004, see Figure 71. The year 1929 is detected as a nonstationarity by the Cramer-von-Mises (CVM), LePage (LP), and Mann Whitney (MW) statistical tests. The nonstationarity in 2004 is detected by the CVM and LP tests, while the Lombard Mood (LM) detects the year 2003. Additionally, the Smooth Lombard Wilcoxon (SLW) test indicates a flux in the mean between the years 1916 and 2016. These nonstationarities are considered strong because 1929 and 2004 meet the criteria of consensus and robustness. Consensus is met because multiple tests that detect abrupt changes in distribution (CVM and LP) indicate 1929 and 2004 as nonstationarities. Robustness is met because tests detecting changes in different statistical properties (distribution, mean, and variance) detect these years as nonstationary.

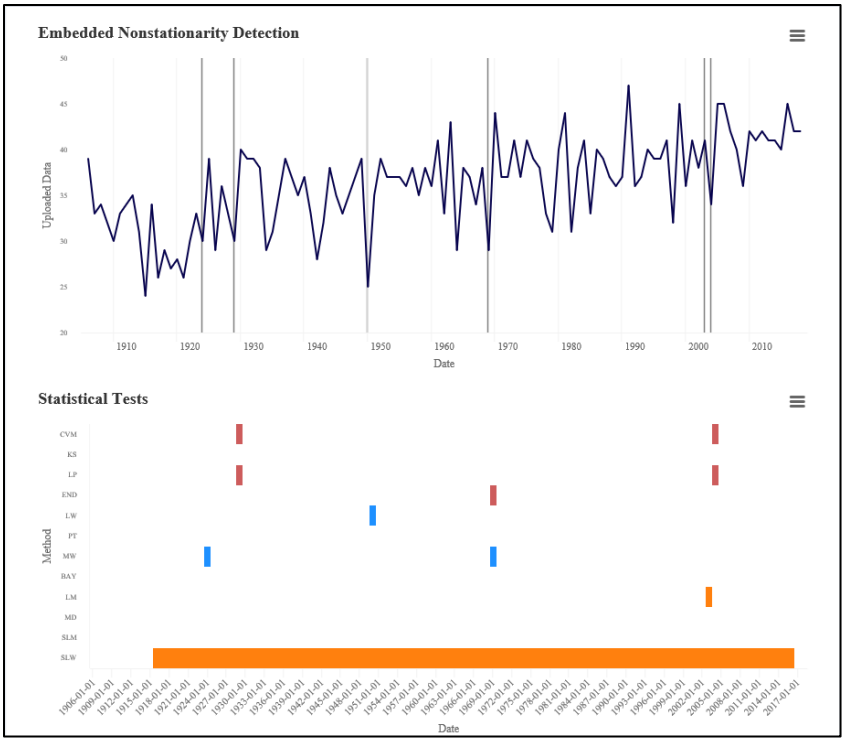

Type: Mean Distribution Variance Smooth

Note: y-axis is summer minimum temperature in degrees Fahrenheit

Abbreviation	Statistical Method	Abbreviation	Statistical Method
CVM	Cramer-von-Mises	BAY	Bayesian
KS	Kolmogorov-Smirnov	LM	Lombard Mood
LP	LePage	MD	Mood
END	Energy Divisive	SLM	Smooth Lombard Mood
LW	Lombard Wilcoxon	SLW	Smooth Lombard Wilcoxon
PT	Pettitt	MW	Mann-Whitney

Figure 71. Nonstationarity analysis – summer, annual minimum temperatures - Minot Experimental Station, ND.

For the winter annual minimum temperatures, a strong nonstationarity is detected in 1939, see Figure 72. Statistical tests detecting 1939 as a nonstationary year are the CVM, LP, Energy Divisive (END), Lombard Wilcoxon (LW; 1938), and MW. Water year 1939 (to account for December 1938) is considered a strong nonstationarity because multiple distribution based statistical tests (CVM, LP, and END) indicate that 1939 as a nonstationarity. The nonstationarity detected in 1939 is robust because statistical tests targeted at identifying a shift in the overall distribution and the mean (LW and MW) indicate a nonstationarity. The USACE Timeseries Toolbox (Reference 20) results indicated a shift in the magnitude of the mean and variance between the subsets of data collected in 1906-1937 (mean= -35 degrees Fahrenheit (F); variance= 58) and 1940-2018 (mean= -28 degrees F; variance= 30).

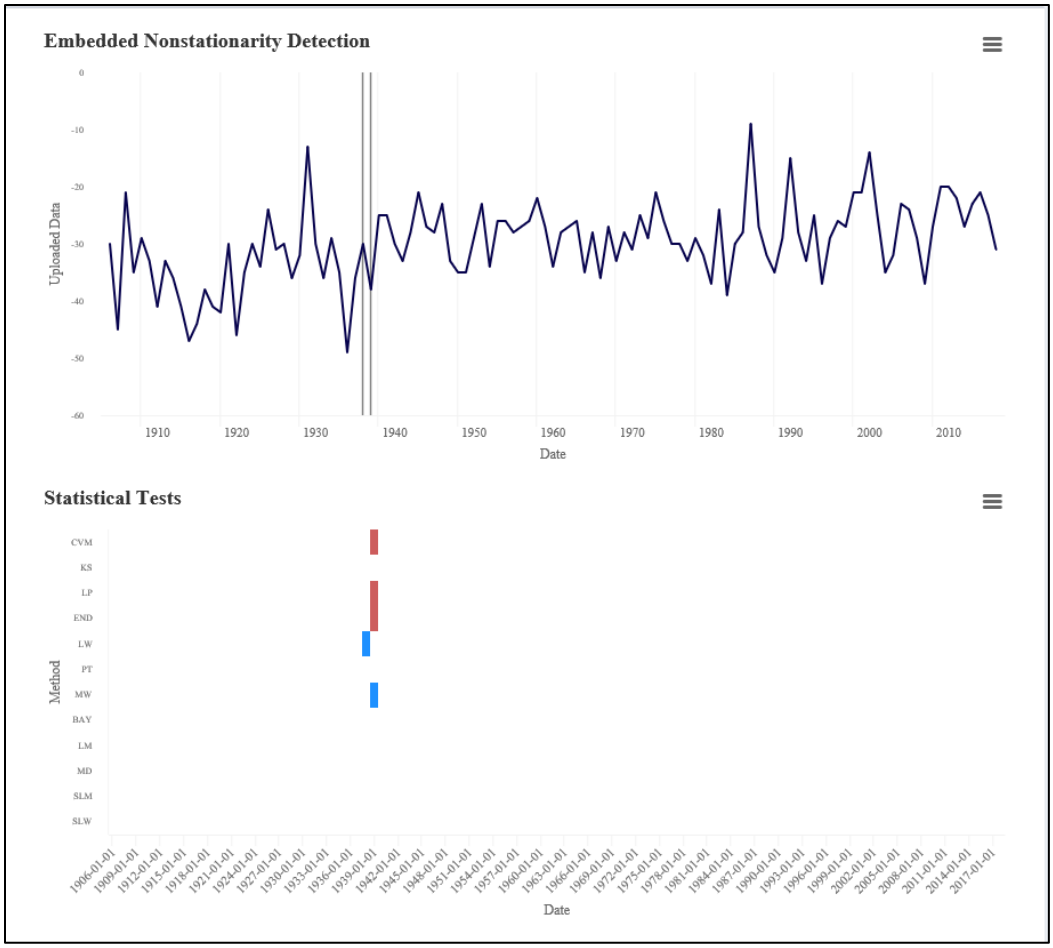

Type: Mean Distribution Variance Smooth

Note: y-axis is winter annual minimum temperature in degrees Fahrenheit

Abbreviation	Statistical Method	Abbreviation	Statistical Method
CVM	Cramer-von-Mises	BAY	Bayesian
KS	Kolmogorov-Smirnov	LM	Lombard Mood
LP	LePage	MD	Mood
END	Energy Divisive	SLM	Smooth Lombard Mood
LW	Lombard Wilcoxon	SLW	Smooth Lombard Wilcoxon
PT	Pettitt	MW	Mann-Whitney

Figure 72. Nonstationarity analysis – winter, annual minimum temperatures - Minot Experimental Station, ND.

5.4.1.2 Nonstationarity Analysis- Seasonal Minimum Temperatures- Yellow Grass Station, SK

Seasonal minimum temperatures collected at the Yellow Grass, SK station are analyzed for nonstationarities using the USACE Timeseries Toolbox (Reference 20). No strong nonstationarities are detected in the spring, summer, fall, or winter minimum temperature timeseries.

5.4.2 Detection of Trends in Minimum Seasonal Temperatures

5.4.2.1 Trend Analysis- Seasonal Minimum Temperatures- Minot Experimental Station

For spring minimum temperatures at the Minot Experimental Station, trend analysis using the t-Test (p-value= 0.022), Mann-Kendall (p-value=0.035), Spearman Rank-Order (p-value= 0.034), and linear regression (p-value= 0.015) tests indicate a statistically significant, increasing trend. Figure 73 displays a plot of spring annual minimum temperatures.

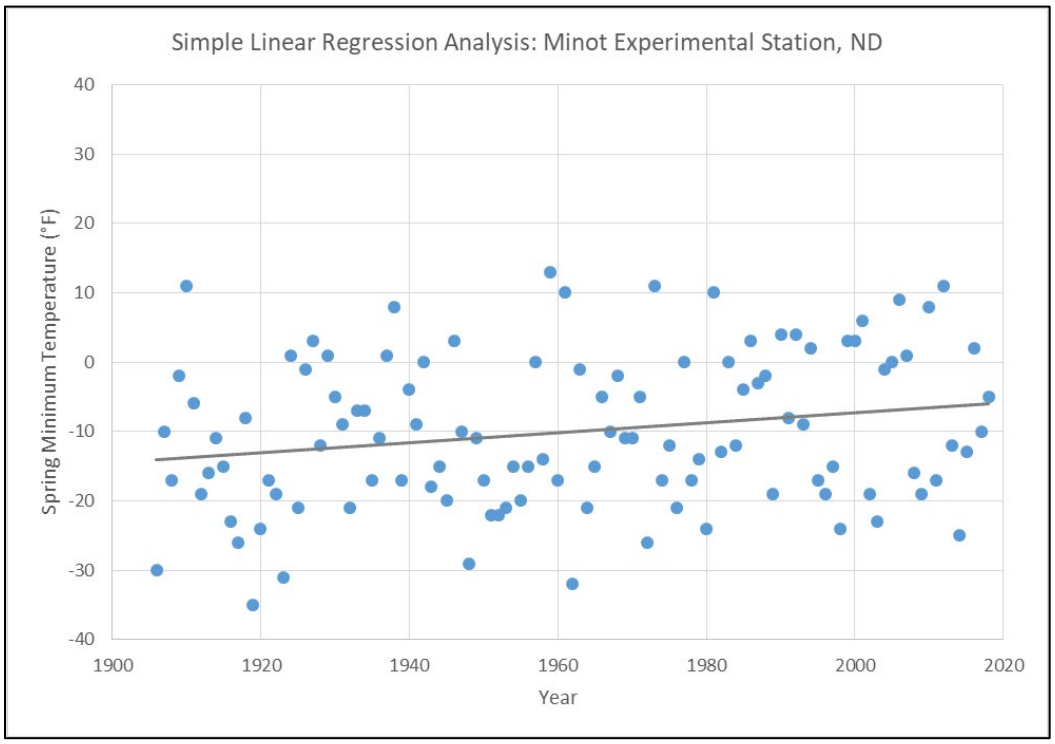

Figure 73. Trend analysis – spring, annual minimum temperatures - Minot Experimental Station, ND; p-value= 0.0146.

Trend analysis for the summer, annual minimum temperatures indicates a statistically significant increasing trend by the t-Test (p-value= 3.24×10^{-13}), Mann-Kendall (p-value< 2.2×10^{-16}), Spearman Rank-Order (p-value= 1.05×10^{-13}), and linear regression (p-value= 1.57×10^{-9}) statistical tests for the full period of record (1906-2018). Further linear regression analysis is carried out for the subsets of data collected prior to and after the 1929 and 2004 nonstationarities. The record prior to 1929 does not indicate a trend in minimum summer temperatures (1906-1928; p-value=0.414), while the record after 1929 indicates a statistically significant increasing trend (1930-2018; p-value= 3.82×10^{-4}). For the 2004 nonstationarity, the record pre-detection indicates a significant increasing trend (1906-2003, p-value=5.27×10^{-6}), but the record post-detection does not (2005-2018; p-value= 0.679). See Figure 74 for a plot of annual minimum temperatures in the summer.

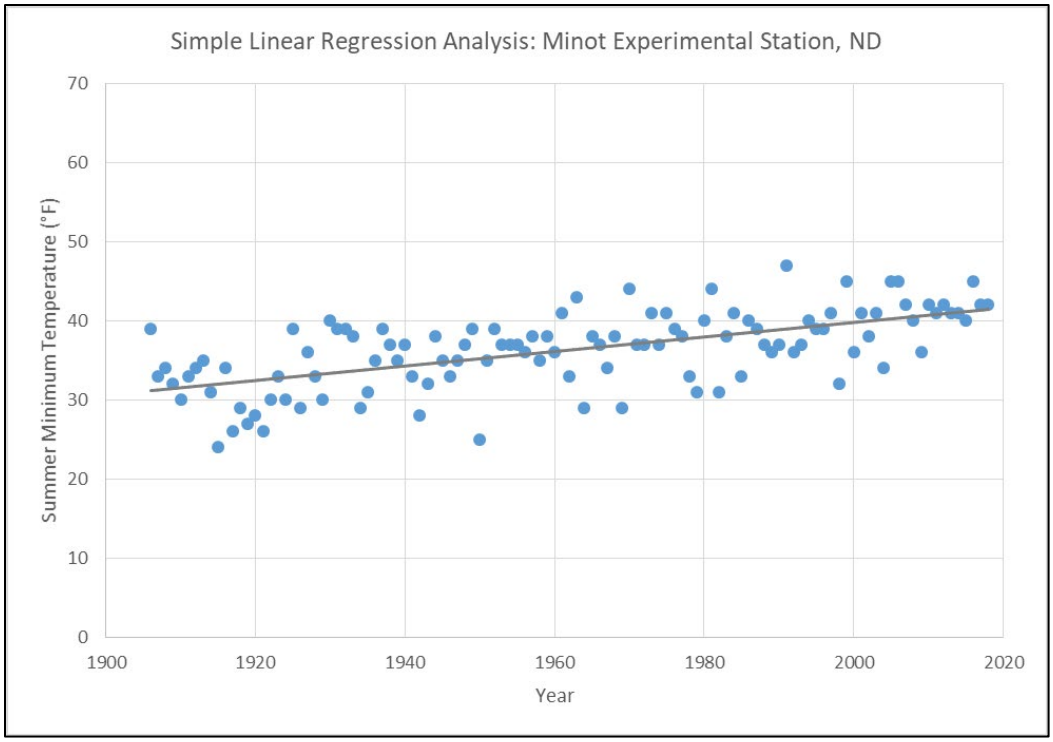

Figure 74. Trend analysis – summer, annual minimum temperatures - Minot Experimental Station, ND; p-value= $1.57x10^{-9}$.

For fall, annual minimum temperatures, trend analysis does not indicate a statistically significant trend over the period of record (1906-2018) using the t-Test (p-value= 0.100) Mann-Kendall (p-value= 0.134), Spearman Rank-Order (p-value= 0.128), and linear regression (p-value= 0.082) tests. Figure 75 displays the fall annual minimum temperature dataset for Minot.

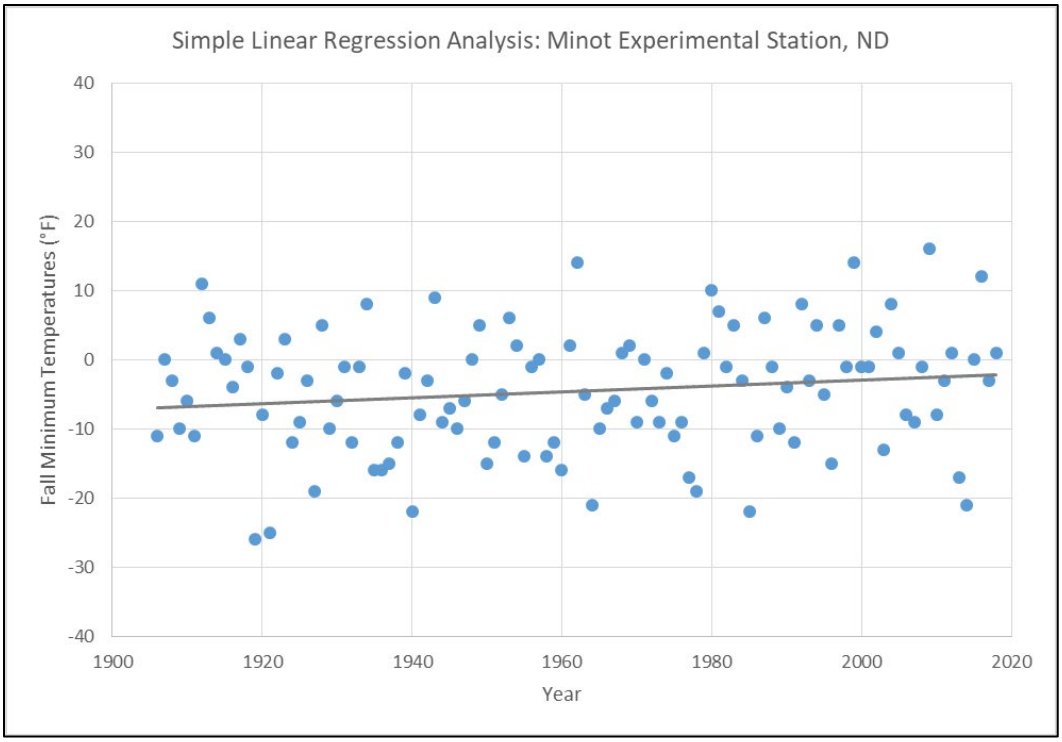

Figure 75. Trend analysis – fall, annual minimum temperatures - Minot Experimental Station, ND; p-value= 0.082.

Trend analysis on winter annual minimum temperatures is carried out using the t-test (p-value= 5.89×10^{-7}), Mann-Kendall (p-value= 1.19×10^{-6}), Spearman Rank-Order (p-value= 6.51×10^{-7}) and linear regression (p-value= 1.27×10^{-8}) tests over the full period of record (1906-2018). All tests indicate a statistically significant, increasing trend. Trends are also assessed for the portions of the period of record prior to and after the strong nonstationarity detected in 1939. There is no statistically significant trend in the dataset collected prior to 1939 (1906-1938; p-value= 0.368). In the dataset collected between 1940 and 2018 there is evidence of a statistically, significant increasing trend with a calculated p-value of 0.04.

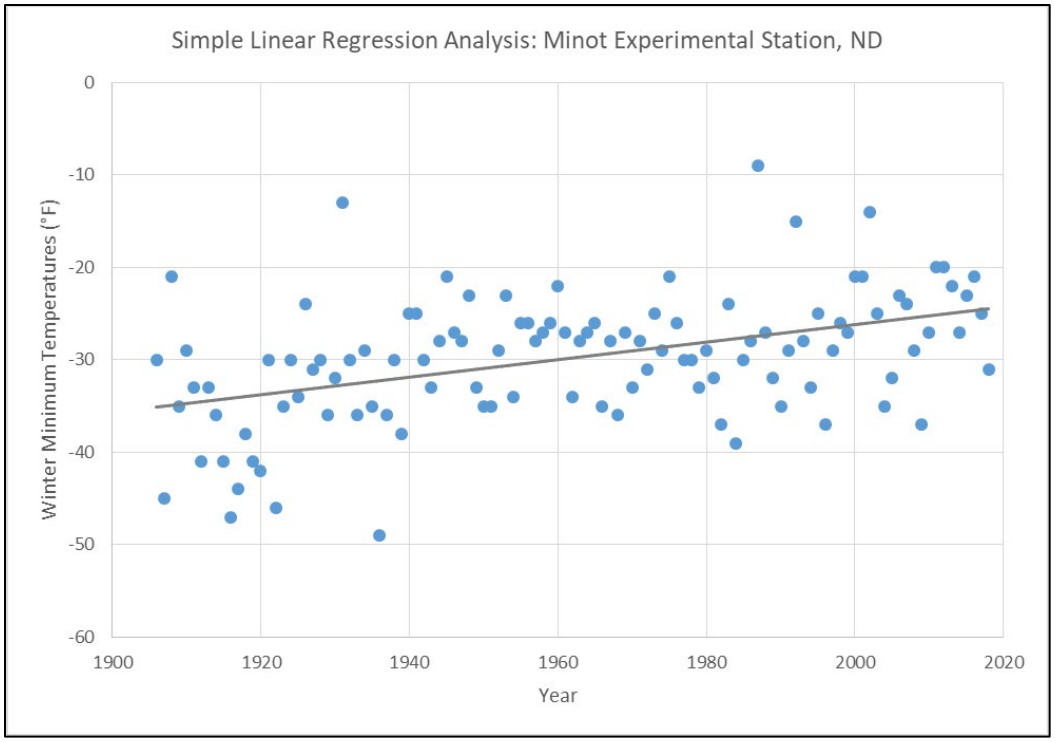

Figure 76. Trend analysis – winter, annual minimum temperatures - Minot Experimental Station, ND; p-value= 1.27×10^{-8}.

5.4.2.2 Trend Analysis- Seasonal Minimum Temperatures- Yellow Grass, SK Station

In the spring, annual minimum temperature record in Yellow Grass, SK(1912-2018), the Timeseries Toolbox does not indicate a statistically significant monotonic trend by the t-Test (p-value= 0.477), Mann-Kendall (p-value=0.504), and Spearman Rank-Order (p-value=0.494) statistical tests. Linear regression analysis using Microsoft Excel also does not suggest a statistically significant trend, with a p-value=0.353. Results of the trend analysis are displayed in Figure 77.

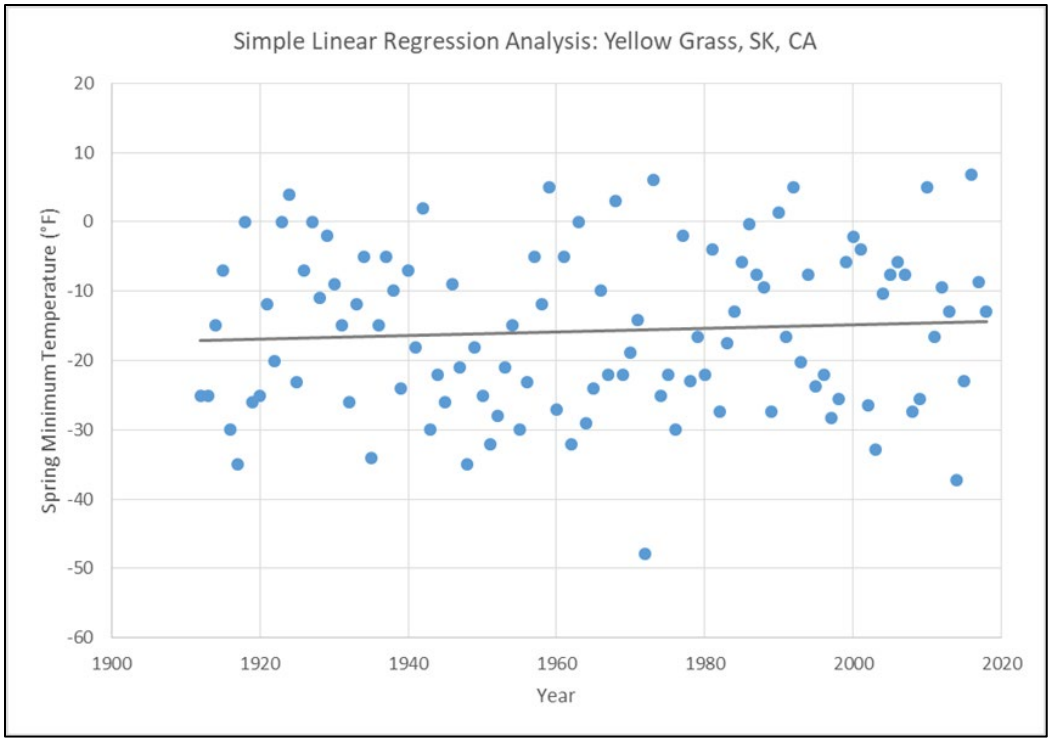

Figure 77. Trend analysis- spring, annual minimum temperatures- Yellow Grass, SK; p-value= 0.3528

In the summer, annual minimum temperature record, the Timeseries Toolbox indicates a significant monotonic trend by the t-Test (p-value= 0.002), Mann-Kendall (p-value= 8.23×10^{-4}), and Spearman Rank-Order (p-value= 7.25×10^{-4}) statistical tests. Linear regression analysis for the full period of record does not suggest a significant trend in summer minimum temperatures (p-value= 0.072), see Figure 78 for a plot of the timeseries.

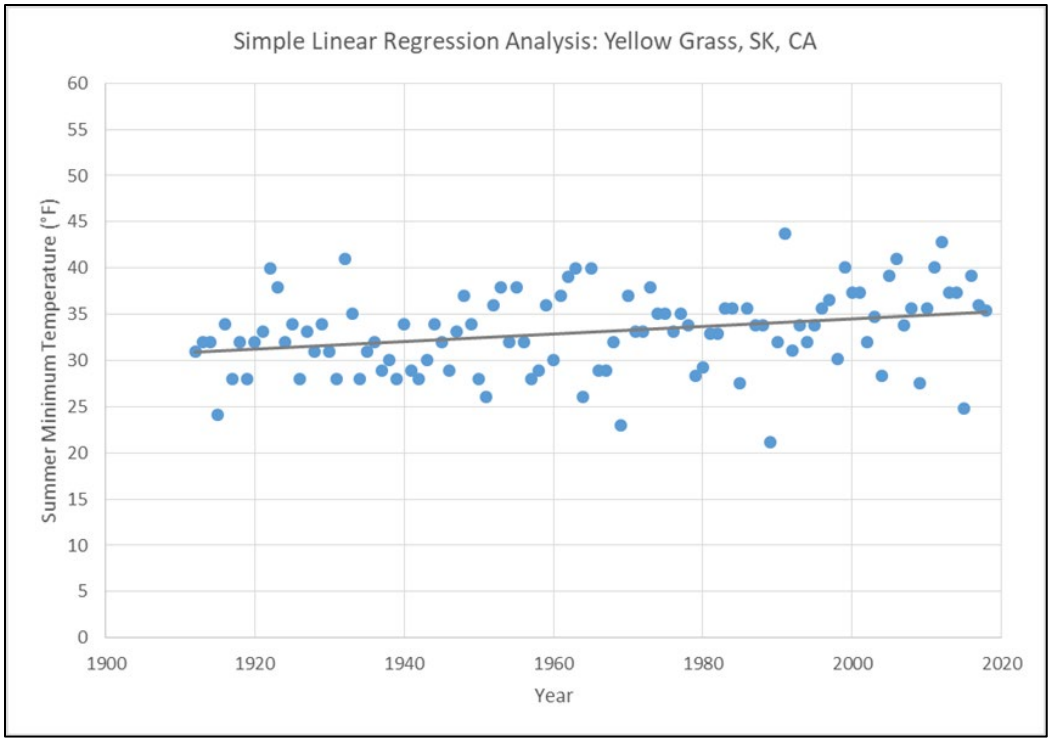

Figure 78. Trend analysis- summer, annual minimum temperatures- Yellow Grass, SK; p-value= 0.0720

In the fall, annual minimum temperature timeseries, the Timeseries Toolbox does not detect a significant trend using the t-Test (p-value=0.870), Mann-Kendall (p-value= 0.857), and Spearman Rank-Order (p-value= 0.843) statistical tests. Linear regression does not indicate a significant trend, with a p-value=0.742, see Figure 79 for a plot of the timeseries.

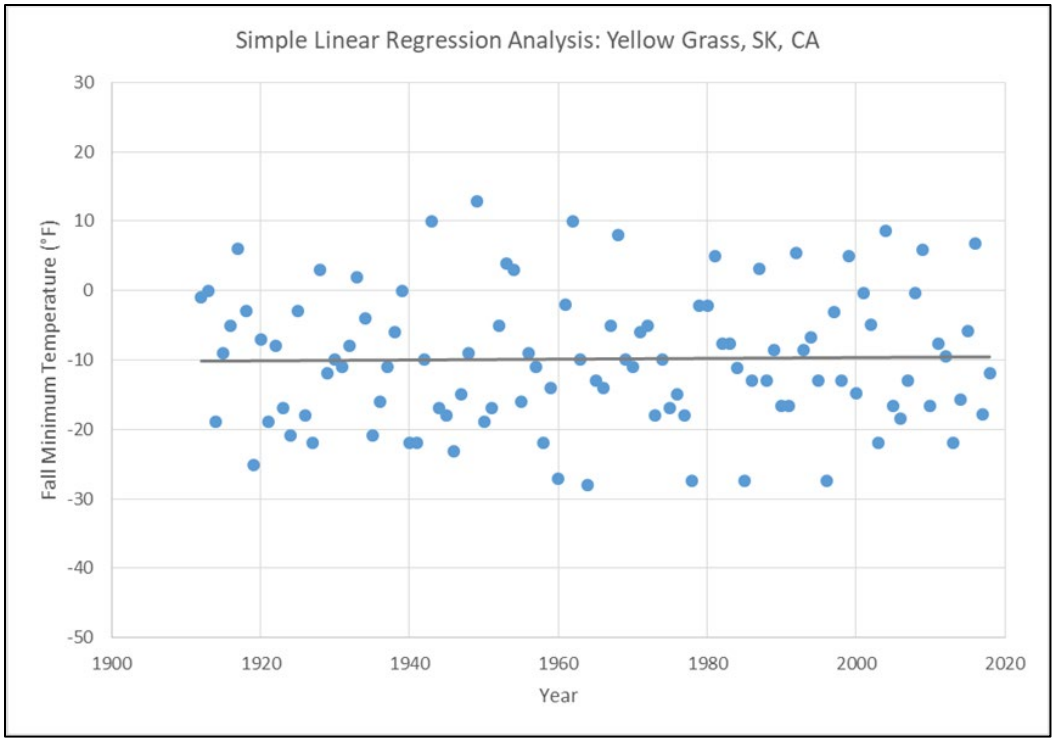

Figure 79. Trend analysis- fall, annual minimum temperatures, Yellow Grass, SK; p-value= 0.7415

In the winter, annual minimum temperatures, the Timeseries Toolbox detects statistically significant trends in the period of record (1912-2018) using the t-Test (p-value=0.040), Mann-Kendall (p-value= 0.0282), and Spearman Rank-Order (p-value= 0.023). Linear regression analysis using Microsoft Excel also indicates a significant increasing trend, with a p-value of 0.004 (see Figure 80).

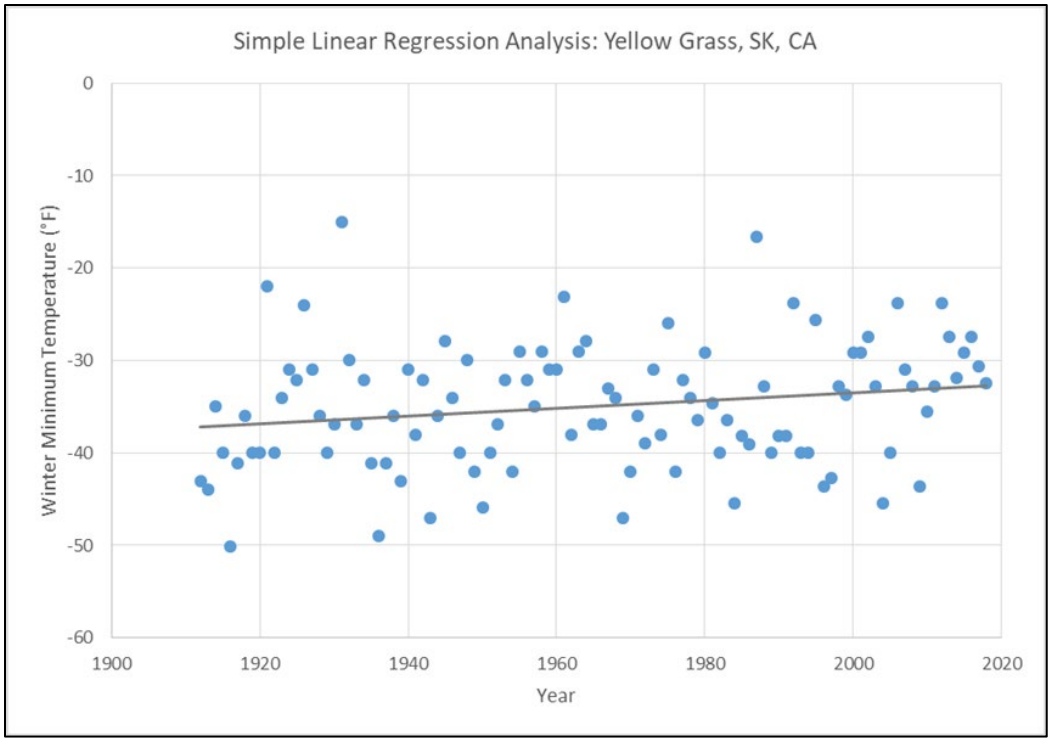

Figure 80. Trend analysis- winter, annual minimum temperatures- Yellow Grass, SK; p-value= 0.0039

5.5 Trends and Nonstationarities in Average Annual Temperatures

5.5.1 Detection of Nonstationarities in Annual Average Temperatures

5.5.1.1 Nonstationarity Analysis- Annual Average Temperatures- Minot International Airport Station

Daily average temperature data collected between 1949 and 2018 at the Minot International Airport meteorological station (Reference 6) is analyzed using the USACE Timeseries Toolbox (Reference 20). Nonstationarity analysis does not indicate any strong nonstationarities in the period of record. Several tests indicate changepoints in the late 1970s and early 1980s, but none that meet the criteria of consensus, robustness, and magnitude, see Figure 81. The Timeseries Toolbox indicates a shift in mean between 1969 and 1986 by the Smooth Lombard Wilcoxon (SLM) test.

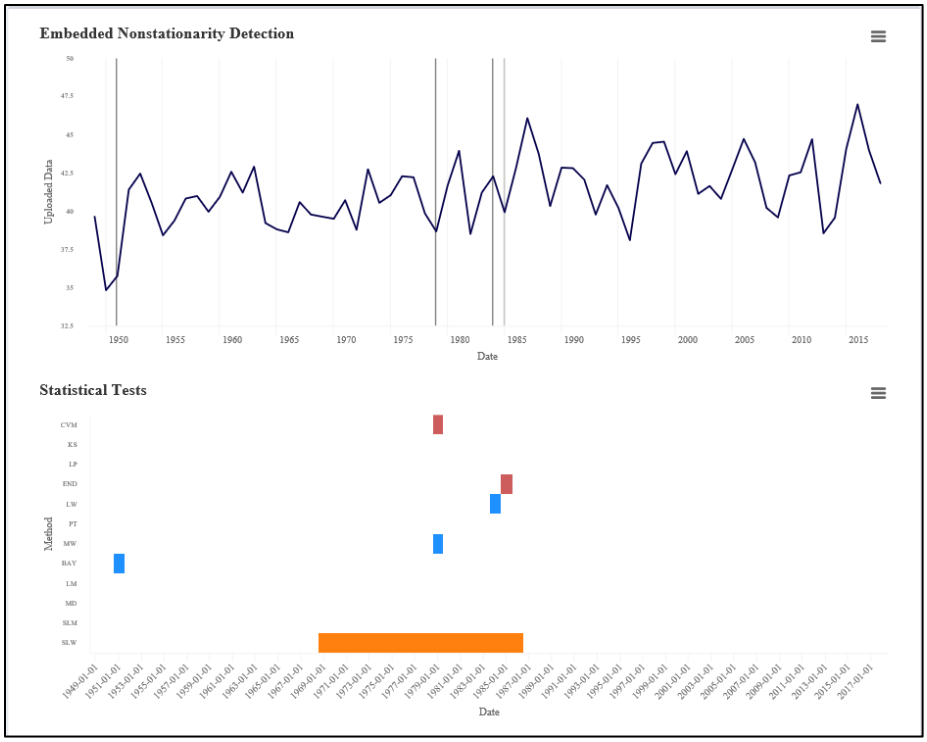

Type: Mean Distribution Variance Smooth

Note: y-axis is average annual temperature in degrees Fahrenheit

Abbreviation	Statistical Method	Abbreviation	Statistical Method
CVM	Cramer-von-Mises	BAY	Bayesian
KS	Kolmogorov-Smirnov	LM	Lombard Mood
LP	LePage	MD	Mood
END	Energy Divisive	SLM	Smooth Lombard Mood
LW	Lombard Wilcoxon	SLW	Smooth Lombard Wilcoxon
PT	Pettitt	MW	Mann-Whitney

Figure 81. Nonstationarity analysis - annual average temperature - Minot International Airport

5.5.2 Detection of Trends in Annual Average Temperatures

5.5.2.1 Trend Analysis- Annual Average Temperatures- Minot International Airport Station

In addition to testing for nonstationarities, the USACE Timeseries Toolbox (Reference 20) trend analysis function is applied using the t-Test (p-value= 3.02×10^{-5}), Mann-Kendall (p-value=1.98×10^{-4}) and Spearman Rank-Order (p-value=1.47×10^{-4}) statistical tests to evaluate the dataset for monotonic trends. Microsoft Excel is used to carry out linear regression analysis (p-value=0.009). All statistical tests identify a statistically significant, increasing trend in average, annual temperatures at Minot between 1949 and 2018. Figure 82 displays the results of the linear regression analysis.

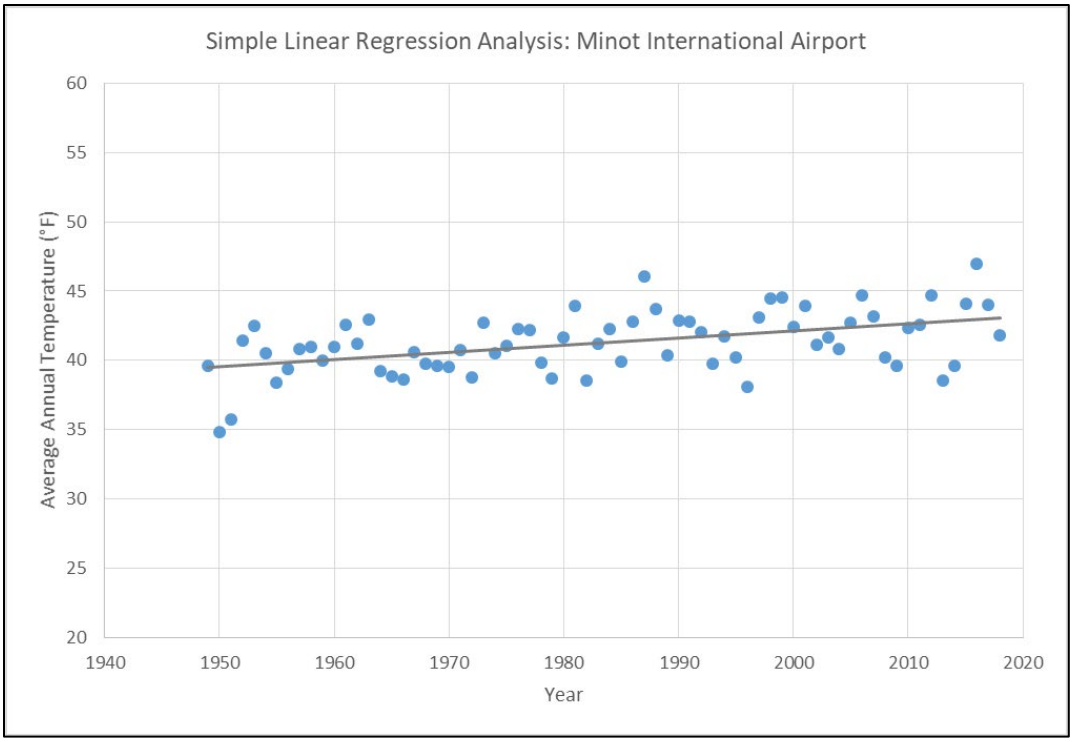

Figure 82. Trend analysis - annual average temperatures - Minot International Airport Station, ND; p-value= 0.0094.

5.6 Trends & Nonstationarities in Average Seasonal Temperatures

5.6.1 Detection of Nonstationarities in Seasonal Average Temperatures

5.6.1.1 Nonstationarity Analysis- Seasonal Average Temperatures- Minot International Airport Station

The USACE Timeseries Toolbox (Reference 20) is used to assess seasonal, average temperature records for nonstationarities and monotonic trends. No nonstationarities are detected within the average summer, fall, and winter temperature datasets.

Within the average, spring temperature dataset a nonstationarity is detected in 1975 by the following statistical tests Cramer-von-Mises (CVM; 1975), Energy Divisive Method (END; 1975), Mann Whitney (MW; 1975), Lombard Wilcoxon (LW; 1974) and LePage (LP; 1976). 1975 is considered a strong nonstationarity because it demonstrates the criteria of consensus, robustness, and a shift in the magnitude of the dataset's statistical properties. Consensus is met because multiple tests detect an abrupt change in distribution (CVM, END, and LP) circa 1975. Tests based on changes in different statistical properties (distribution and mean) detect 1975 as a nonstationarity, meeting the criteria of robustness. Additionally, the Timeseries Toolbox indicates a shift in the magnitude of mean and variance between the following subsets of data: 1949-1973 (mean= 39 degrees Fahrenheit (F); variance= 7.7) and 1977-2018 (mean=42 degrees F; variance=15). See Figure 83.

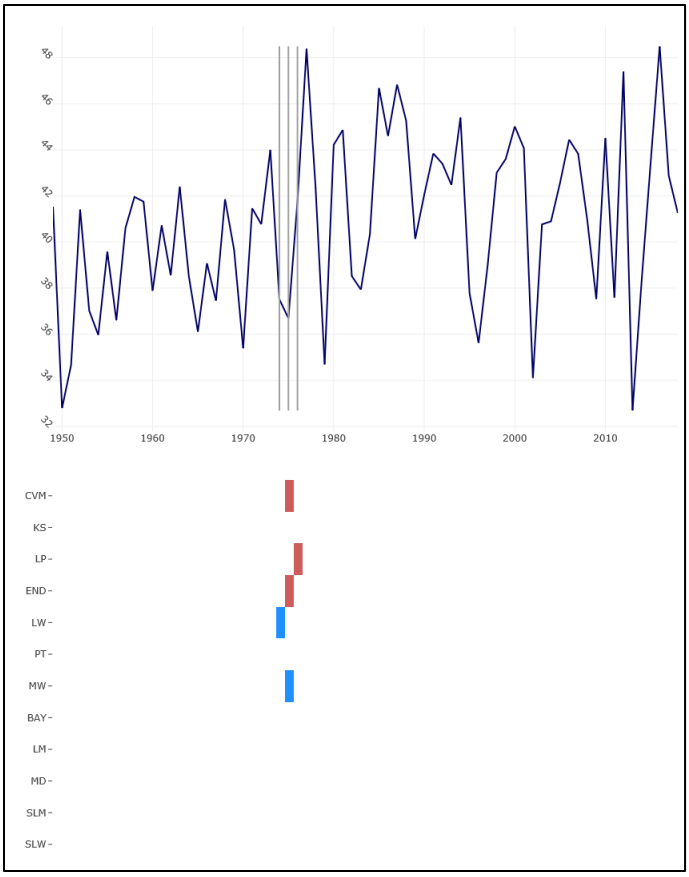

Type: Mean Distribution Variance Smooth

Note: y-axis is average annual spring temperature in degrees Fahrenheit

Abbreviation	Statistical Method	Abbreviation	Statistical Method
CVM	Cramer-von-Mises	BAY	Bayesian
KS	Kolmogorov-Smirnov	LM	Lombard Mood
LP	LePage	MD	Mood
END	Energy Divisive	SLM	Smooth Lombard Mood
LW	Lombard Wilcoxon	SLW	Smooth Lombard Wilcoxon
PT	Pettitt	MW	Mann-Whitney

Figure 83. Nonstationarity analysis- spring annual average temperatures- Minot International Airport, ND

5.6.2 Detection of Trends in Average Seasonal Temperatures

5.6.2.1 Trend Analysis- Seasonal Average Temperatures- Minot International Airport Station

Trend analysis is carried out on the seasonal annual average records using the Timeseries Toolbox (Reference 20) and Microsoft Excel linear regression. The t-Test (p-value=0.007), Mann-Kendall (p-value 0.003), and Spearman Rank-Order (p-value 0.004) statistical tests found a statistically, significant increasing trend in annual average spring temperatures. However, linear regression analysis for the full period of record calculated a p-value=0.075; this is slightly

above the threshold of statistical significance (p-value< 0.05; Figure 84). Because the p-value associated with the linear regression analysis is fairly close to the accepted threshold for significance (p-value< 0.05) and the Mann-Kendall and Spearman Rank-Order tests are well within the threshold for a significant trend, it is assumed that annual average spring temperatures are increasing. When linear regression analysis is generated for the portions of the period of record prior to and after 1975 no statistically significant trends are identified (1949-1974 p-value=0.269; 1976-2018 p-value=0.316).

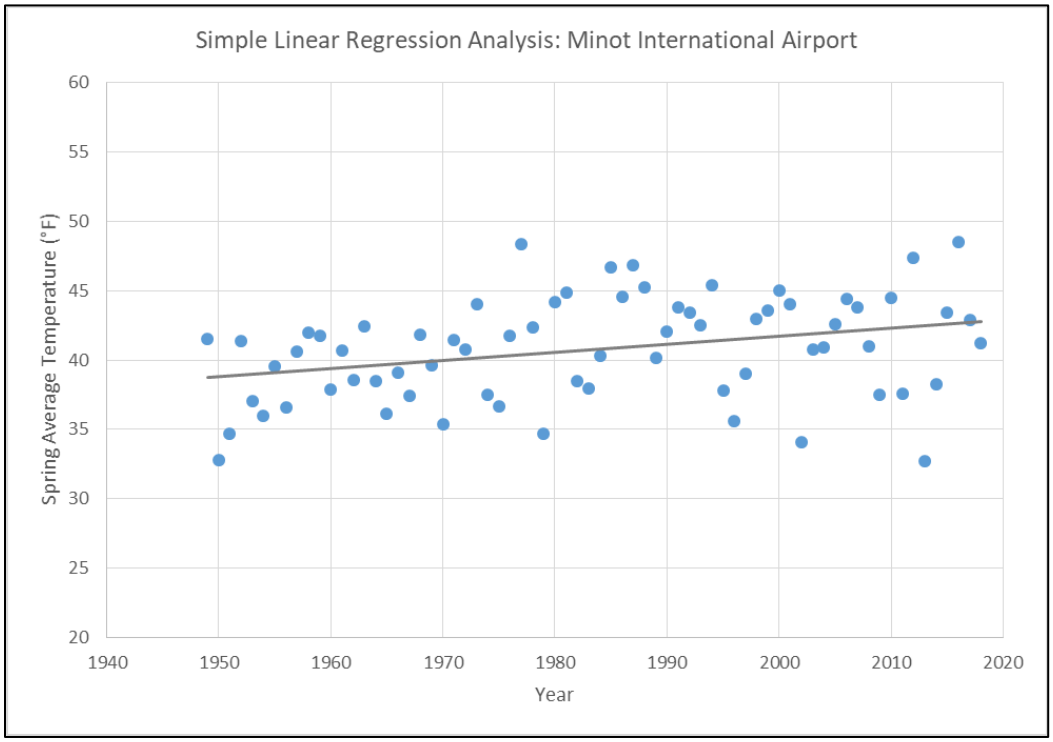

Figure 84. Trend analysis – spring, annual average temperatures - Minot International Airport Station, ND; p-value=0.075.

Trend analysis on annual average summer temperatures using the t-Test (p-value= 0.043), Mann-Kendall (p-value= 0.011), and Spearman Rank-Order (p-value=0.013) indicate a statistically significant increasing trend over the period of record 1949-2018. Linear regression analysis does not indicate a trend in annual average summer temperatures (p-value= 0.542), see Figure 85.

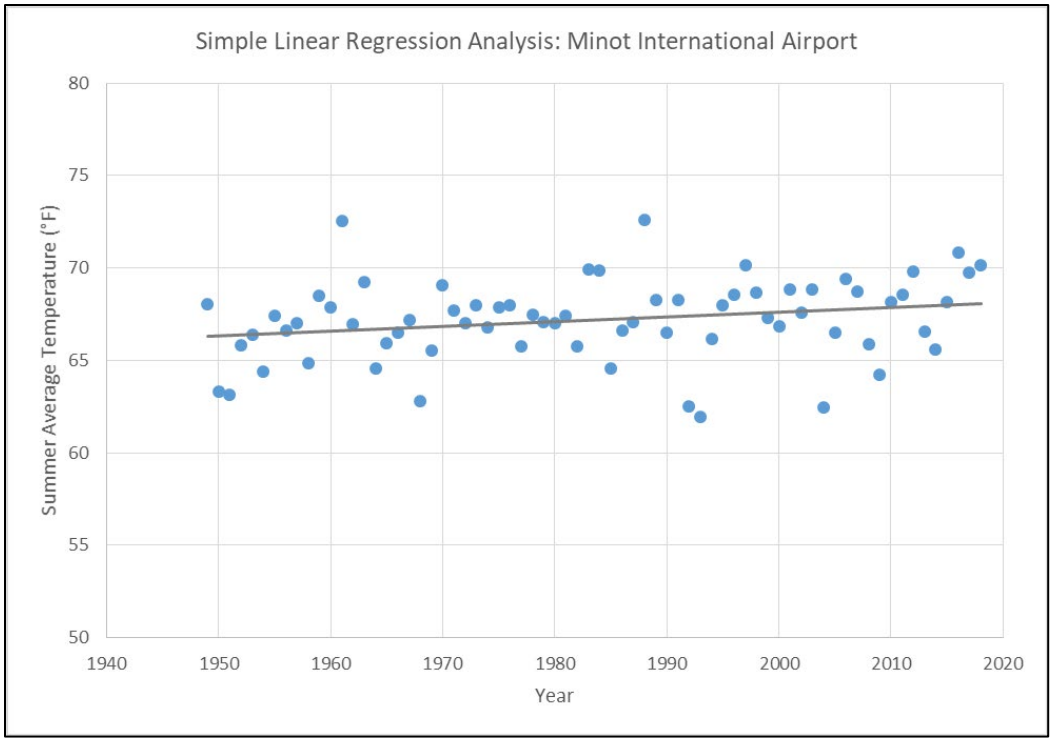

Figure 85. Trend analysis – summer, annual average temperatures - Minot International Airport Station, ND; p-value= 0.5422.

Trend analysis applied to the fall annual average temperature data does not indicate a statistically significant trend by the t-Test (p-value= 0.128), Mann-Kendall (p-value= 0.121), Spearman Rank-Order (p-value= 0.139), and linear regression (p-value= 0.880) for the period of record (1949-2018), see Figure 86.

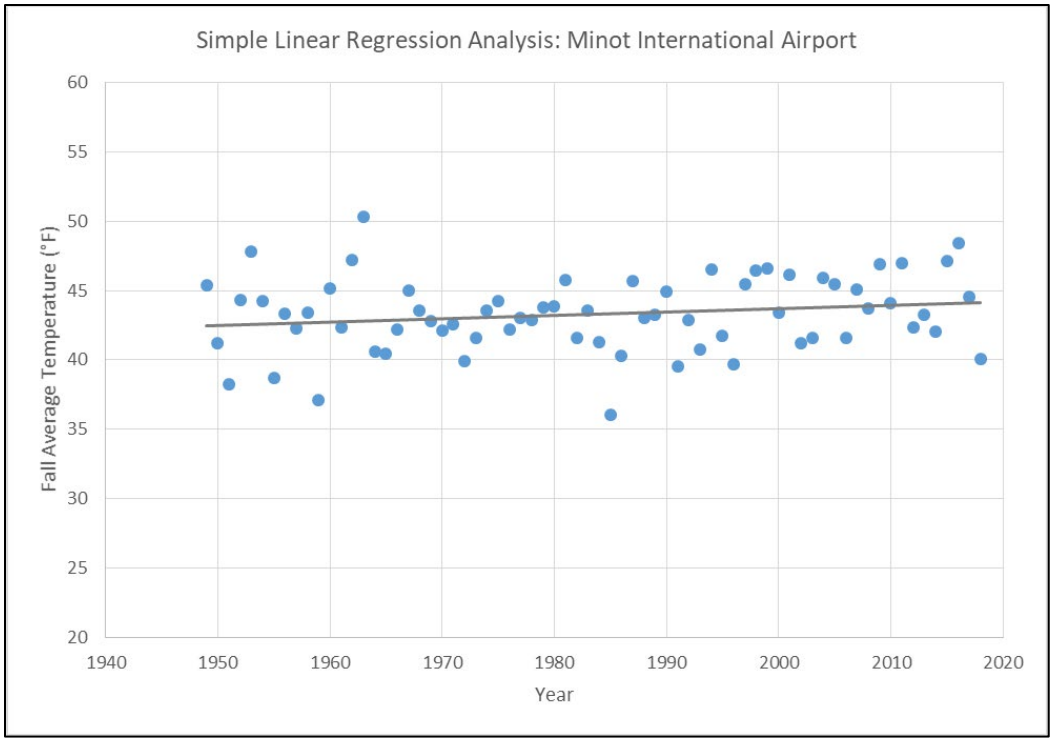

Figure 86. Trend analysis – fall, annual average temperatures - Minot International Airport Station, ND; p-value= 0.8802.

When winter average annual temperatures are analyzed for trends using the t-Test (p-value= 0.001), Mann-Kendall (p-value= 0.007), Spearman Rank-Order (p-value= 0.007) and linear regression (p-value= 0.003) tests, a statistically significant, increasing trend is observed. A plot of the winter average temperatures is displayed in Figure 87.

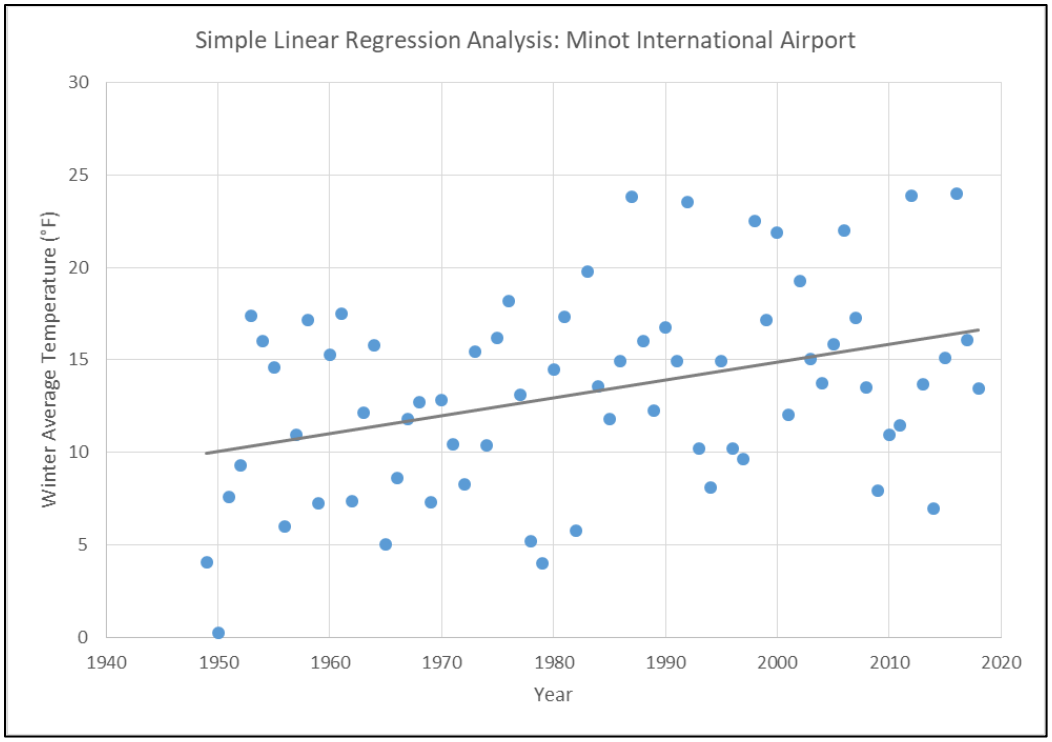

Figure 87. Trend analysis – winter, annual average temperatures - Minot International Airport Station, ND; p-value= 0.0027.

6 First Order Statistical Analysis of Historic Precipitation Records

Trends in precipitation are analyzed using the NCDEI's daily precipitation timeseries recorded at the Minot Experimental Station (Reference 10) and Environment and Climate Change Canada's (ECCC) precipitation timeseries reported by the Yellow Grass Climate Station (Reference 5).

The Minot Experimental Station reports daily accumulated precipitation between June 1905 and present. Data are analyzed from 1906 to 2018. Data from 1905 is excluded from analysis because the precipitation record only starts in June of 1905. Three months of precipitation data are missing in the summer of 1928. Precipitation data are also missing for April 1984, August 2001, November 2002, and June 2008. One to seven days of consecutive daily measurements are missing sporadically throughout the period of record. Three stations were used to fill in data gaps larger than nine consecutive days at the Minot Experimental Station: Minot International Airport (Reference 11), Foxholm, ND (Reference 8), and Velva, ND (Reference 12). All stations used to fill the data gaps are within a 25-mile radius of the Minot Experimental Station. For sequences of missing data less than nine days in duration, linear interpolation in HEC-DSSVue (Reference 2) is used to estimate missing daily precipitation. Data are analyzed from 1906-2018 in water years (beginning October 1), both annually and seasonally.

The Yellow Grass, SK station has a fairly continuous precipitation record between 1912 and 2016. There are 1,561 days of missing data in the observed record, approximately 4% missing for a full period of record. To fill-in missing data, the "nearest neighbor" approach is adopted

using the Saskatchewan, CA stations Weyburn, Francis, and Regina. The R software package "weathercan" (Reference 8) is used to download and process precipitation data. The data from the Regina stations is utilized for gap-filling more than the other stations, accounting for 2% of the period of record. The Regina station is approximately 50 miles from the Yellow Grass station. Ideally a weighted approach, such as Theisen polygons, would be implemented to gap-filling data, particularly precipitation. Given the available resources for the assessment and that the data are being considered and applied on an annual and seasonal basis, rather than daily, the nearest neighbor approach is sufficient. Precipitation measurements reported by ECCC in millimeters (mm) are converted to inches (in). Data are analyzed from 1912-2016 in water years (beginning October 1), both annually and seasonally.

6.1 Trends and Nonstationarities in Annual Average 3-Day Precipitation

HEC-DSSVue (Reference 2) is used to compute a forward moving average over a 3-day period. HEC-DSSVue computes a forward moving average using a specified number of values to average over (NAVG). For this application the NAVG is specified as three. The forward moving average function computes a moving average of the last NAVG values for the time series data. If the averaging interval contains a missing value, the forward moving average is computed from the remaining valid values in the interval. However, if there are less than two valid values in the interval, the value in the resultant data is set to missing. The calculated, average 3-day precipitation data is then multiplied by three to determine the cumulative 3-day precipitation volume as a daily timeseries.

6.1.1 Detection of Nonstationarities in Annual Average 3-Day Precipitation

6.1.1.1 Nonstationarity Analysis- Annual Average 3-Day Precipitation- Minot Experimental Station, ND

Annual, average cumulative 3-day precipitation is analyzed using the NCEI's daily precipitation timeseries (Reference 10) at the Minot Experimental Station (1905 to present). A period of record of 1906-2018 is used for analysis. The USACE Timeseries Toolbox (Reference 20) is used to detect nonstationarities and monotonic trends in the annual average 3-day volume precipitation record collected between 1906 and 2018. A strong, nonstationarity is detected in the year 1962 (see Figure 88) by the statistical tests LePage (LP), Energy Decisive Method (END), and Lombard Wilcoxon (LW; in 1961).

The 1962 nonstationarity meets the criteria of consensus and robustness to define a strong nonstationarity. The criteria of consensus is fulfilled because multiple tests targeted at detecting shifts in the distribution (LP & END) of the dataset are indicating a nonstationarity in 1962. The nonstationarity is considered robust because tests targeted at detecting change points in multiple types of statistical properties are indicating a nonstationarity (overall distribution and mean). Additionally, the results presented by the Timeseries Toolbox indicate a slight shift in the magnitude of mean and standard deviation (std. dev.) between the subsets of data collected prior to and after the identified nonstationarity: 1906-1960 (mean= 0.13 in.; std.

dev. = 0.028), 1963-1966 (mean=0.14 in.; std. dev. = 0.042), and 1968-2018 (mean=0.16 in.; std. dev. = 0.034).

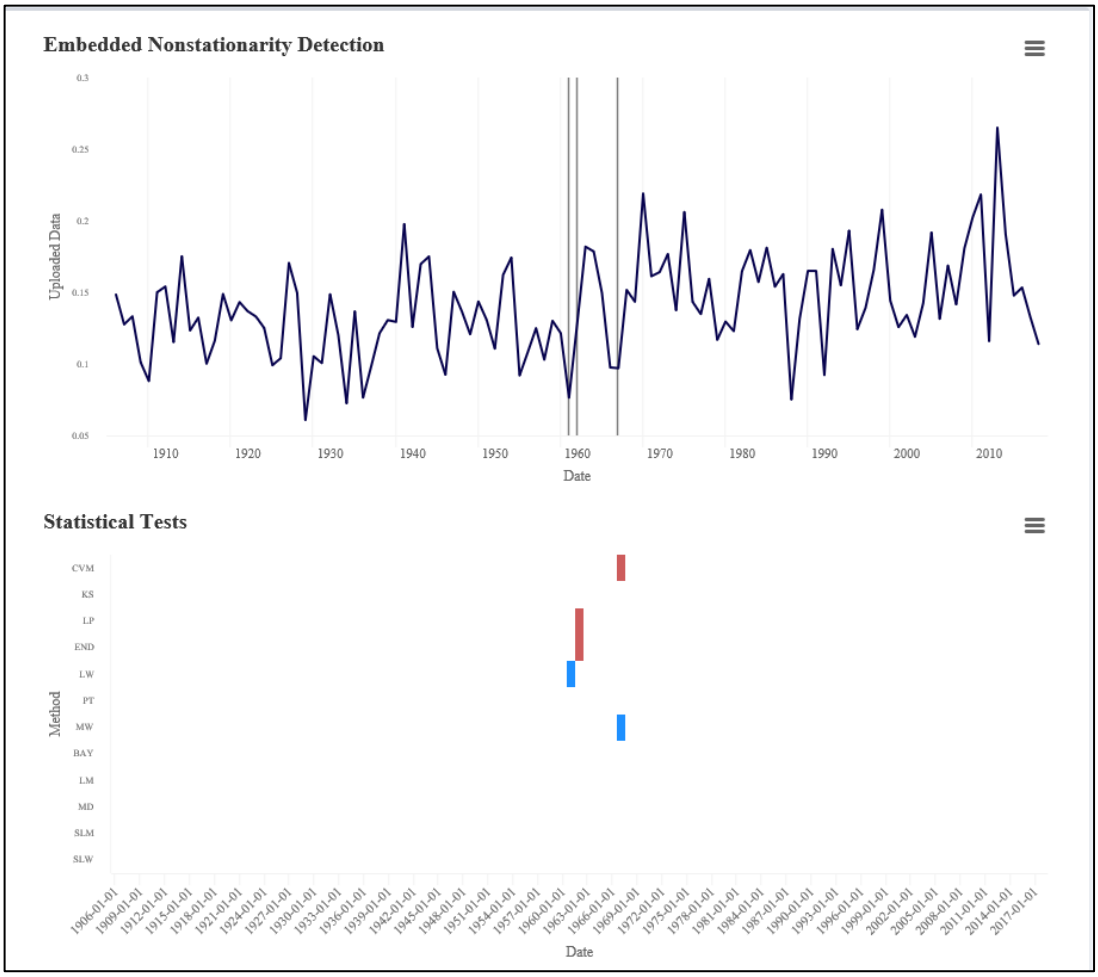

Type: Mean Distribution Variance Smooth

Note: y-axis is annual average cumulative 3-day precipitation in inches

Abbreviation	Statistical Method	Abbreviation	Statistical Method
CVM	Cramer-von-Mises	BAY	Bayesian
KS	Kolmogorov-Smirnov	LM	Lombard Mood
LP	LePage	MD	Mood
END	Energy Divisive	SLM	Smooth Lombard Mood
LW	Lombard Wilcoxon	SLW	Smooth Lombard Wilcoxon
PT	Pettitt	MW	Mann-Whitney

Figure 88. Nonstationarity Analysis - annual average cumulative 3-day precipitation – Minot Experimental Station, ND

6.1.1.2 Nonstationarity Analysis- Annual Average 3-Day Precipitation- Yellow Grass Station, SK

The Yellow Grass, SK, Canada annual average, 3-day cumulative precipitation timeseries (period of record 1912-2018) is analyzed for nonstationarities using the USACE Timeseries Toolbox. The daily 3-day cumulative precipitation timeseries at Yellow Grass, SK is calculated using the same methodology as the Minot Experimental Station annual average 3-Day precipitation timeseries. No nonstationarities are detected in the annual average, 3-day cumulative precipitation period of record.

6.1.2 Detection of Trends in Annual Average 3- Day Cumulative Precipitation Volume

6.1.2.1 Trend Analysis- Annual Average 3-Day Precipitation- Minot Experimental Station, ND

Trend analysis performed using the t-test (p-value= 4.17×10^{-5}), Mann-Kendall (p-value=2.20×10^{-4}), Spearman Rank-Order (p-value= 1.25×10^{-4}), and linear regression (p-value= 6.69×10^{-4}) tests indicate a statistically significant, increasing trend. Figure 89 shows the linear trend analysis for the annual average, cumulative 3-day precipitation record at Minot, ND.

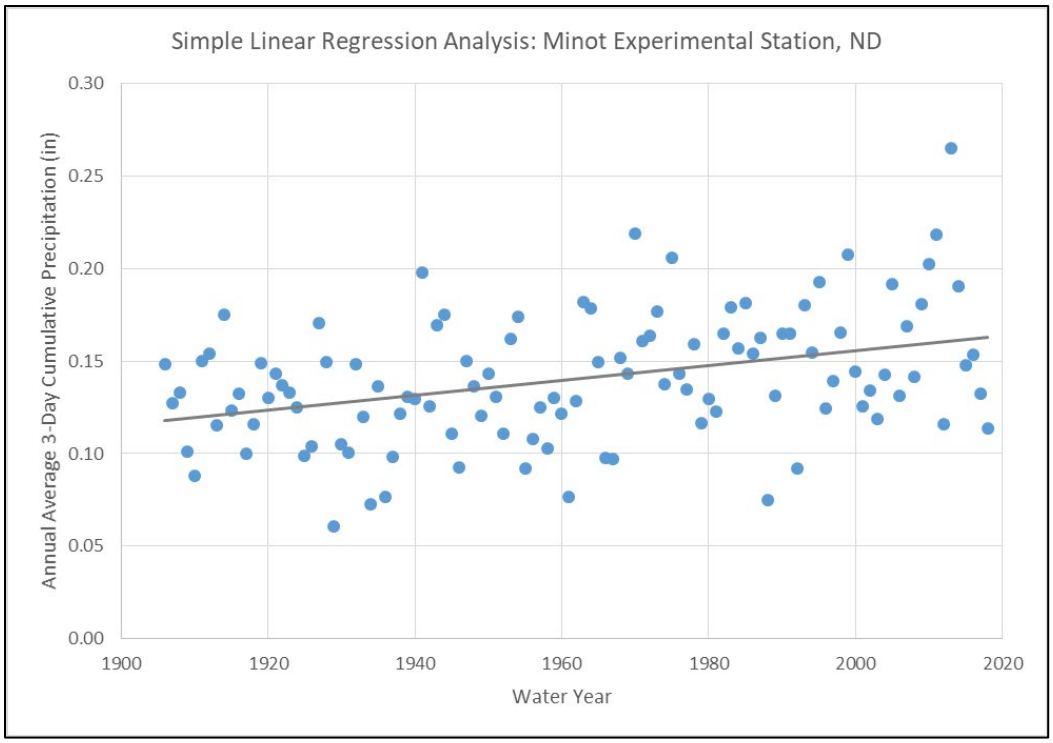

Figure 89. Trend analysis - annual average 3-day cumulative precipitation volume - Minot Experimental Station, ND; p-value= 6.69×10^{-4}.

In addition to performing trend analysis using the entire period of record, subsets of data prior to and after the detected 1962 nonstationarity are assessed for trends. Both portions of the period of record collected prior to and after 1962 indicate no statistically significant, linear trends in the data (p-value=0.505 and p-value=0.649, respectively).

6.1.2.2 Trend Analysis- Annual Average 3-Day Precipitation- Yellow Grass Station, SK

The Timeseries Toolbox is used to identify monotonic trends in the annual average 3-day cumulative precipitation record for Yellow Grass Station. The USACE generally accepted threshold of a p-value < 0.05 is the basis in determining statistical significance. A statistically significant increasing trend is identified by the t-test (p-value= 0.008), Mann-Kendall (p-value= 0.015), and Spearman Rank-Order (p-value= 0.015) tests over the entire period of record 1912-2018. Linear regression analysis using Microsoft Excel also indicates an increasing trend, with a p-value= 0.048. See Figure 90 for a plot of the annual average 3-Day precipitation at Yellow Grass, SK.

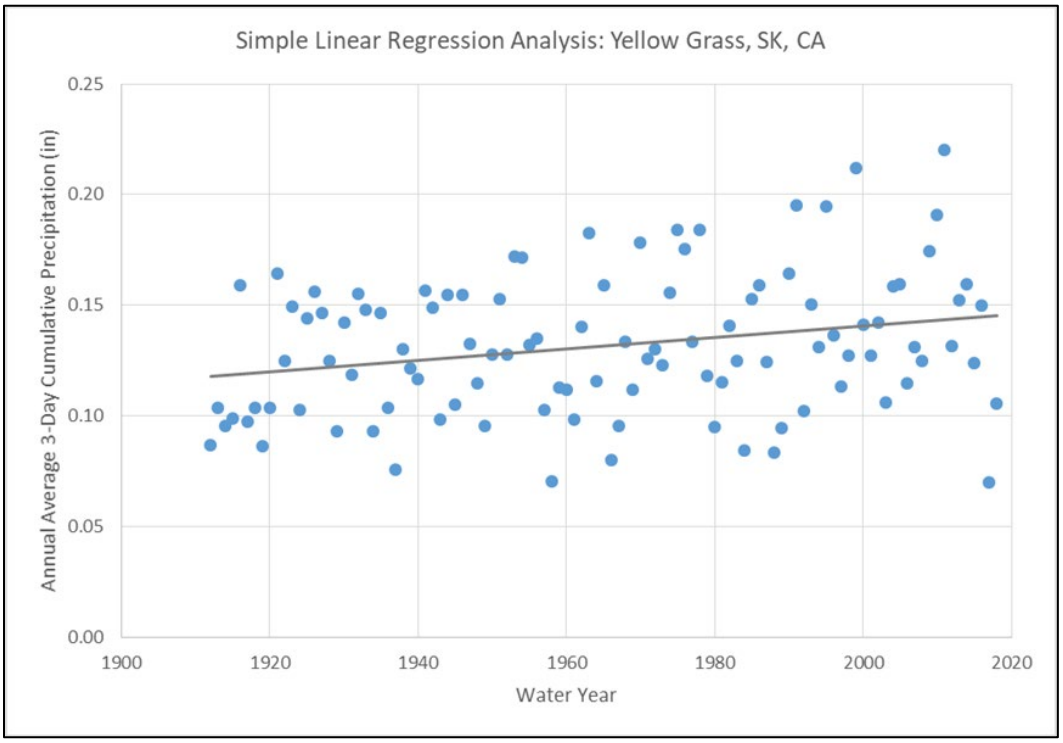

Figure 90. Trend analysis- annual, average 3-day cumulative precipitation volume- Yellow Grass, SK; p-value= 0.0476

6.2 Trends and Nonstationarities in Annual Maximum 3-Day Precipitation

6.2.1 Detection of Nonstationarities in Annual Maximum 3-Day Precipitation

6.2.1.1 Nonstationarity Analysis- Annual Maximum 3-Day Precipitation- Minot Experimental Station, ND

The Minot Experimental Station daily precipitation timeseries is used to calculate the annual maximum 3-day precipitation record (water years 1906-2018 using HEC-DSSVue (Reference 2)). The USACE Timeseries Toolbox (Reference 20) is used to assess the annual maximum 3-day cumulative precipitation record for nonstationarities and monotonic trends. Strong nonstationarities are not identified within the dataset between 1906 and 2018.

6.2.1.2 Nonstationarity Analysis- Annual Maximum 3-Day Precipitation- Yellow Grass Station, SK

The annual, maximum 3-day cumulative precipitation timeseries at Yellow Grass is analyzed for nonstationarities using the Timeseries Toolbox. This timeseries is developed using the same methodology as is applied to define the annual maximum 3-Day precipitation timeseries for the Minot Experimental Station. No nonstationarities are detected over the period of record with the Timeseries Toolbox.

6.2.2 Detection of Trends in Annual Maximum 3-Day Precipitation

6.2.2.1 Trend Analysis- Annual Maximum 3-Day Precipitation- Minot Experimental Station, ND

Trend analysis for the annual maximum 3-day precipitation record (1906-2018) does not indicate a statistically significant trend. Statistical tests used are the t-Test (p-value= 0.389), Mann-Kendall (p-value= 0.232), Spearman Rank-Order (p-value= 0.199), and simple linear regression (p-value= 0.693) tests. Figure 91 displays the results of the annual maximum 3-day cumulative precipitation data trend analysis.

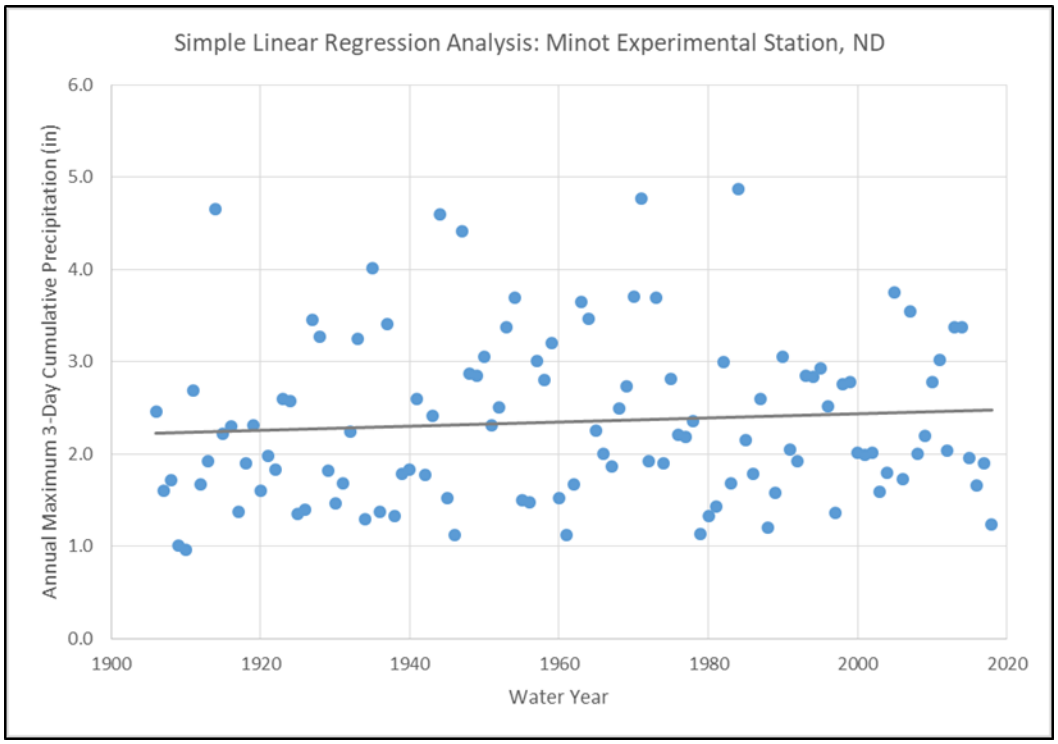

Figure 91. Trend analysis - annual maximum 3-day precipitation - Minot Experimental Station, ND; p-value= 0.693.

6.2.2.2 Trend Analysis- Annual Maximum 3-Day Precipitation- Yellow Grass Station, SK

When the annual maximum 3-day timeseries recorded on Yellow Grass Creek was analyzed, the Timeseries Toolbox did not detect any monotonic trends in the timeseries. Statistical tests applied include the t-Test (p-value= 0.761), Mann-Kendall (p-value= 0.959), and Spearman Rank-Order (p-value= 0.917) statistical tests. Linear regression analysis with Microsoft Excel also does not indicate a significant trend, with a p-value of 0.885. See Figure 92 for a plot of the annual maximum 3-day precipitation at Yellow Grass, SK.

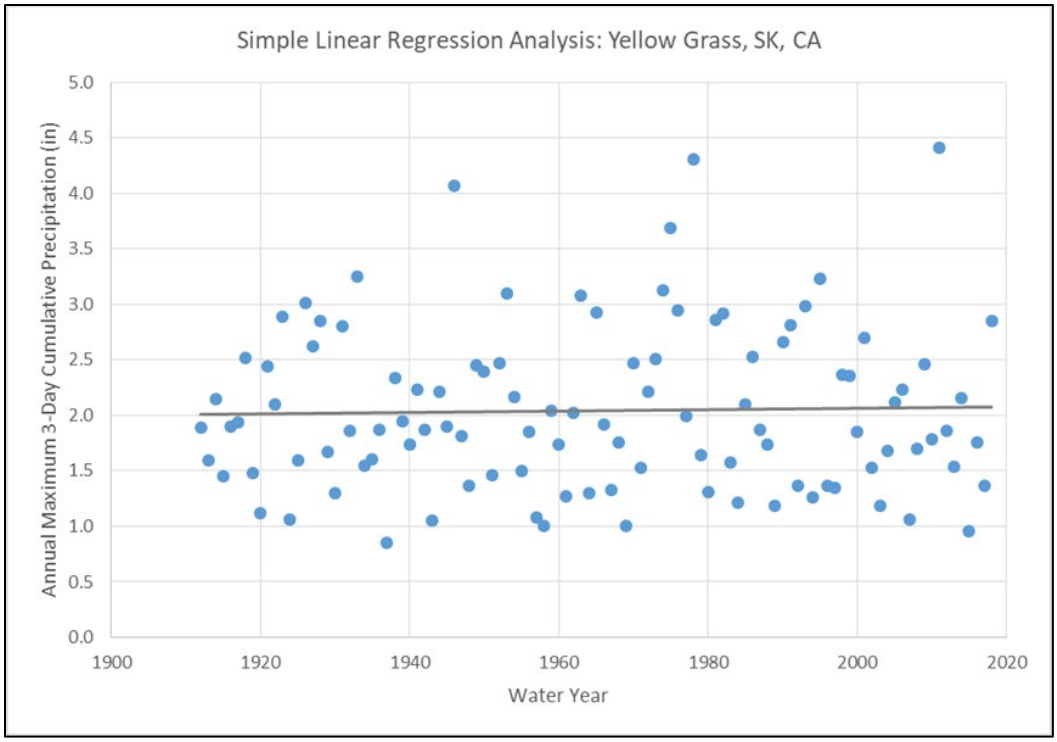

Figure 92. Trend Analysis- annual, maximum 3-day cumulative precipitation- Yellow Grass, SK; p-value= 0.8851

6.3 Trends and Nonstationarities in Annual Cumulative Precipitation

6.3.1 Detection of Nonstationarities in Annual Cumulative Precipitation

6.3.1.1 Nonstationarity Analysis- Annual Cumulative Precipitation- Minot Experimental Station, ND

Using HEC-DSSVue (Reference 2), an annual cumulative precipitation dataset is calculated from the average daily precipitation timeseries developed as is stated in Section 6 for water years 1906-2018. Annual cumulative precipitation is defined as the sum of all observed precipitation (in inches) for each water year.

A nonstationarity is detected in 1962 by the LePage (LP), Energy Divisive (END), and Lombard Wilcoxon (LW; 1961) tests. 1962 is a strong nonstationarity because it meets the criteria of consensus, robustness, and magnitude. Consensus is met because multiple tests (LP and END) indicate a shift in the dataset's overall statistical distribution. The 1962 nonstationarity is considered robust because tests targeted at detecting shifts in different statistical properties (distribution and mean) detect it as a nonstationarity. Additionally, a shift in the magnitude of the mean and variance is indicated by the USACE Timeseries Toolbox (Reference 20) between the subsets of data collected in 1906-1960 (mean=15 in.; variance=12), 1963-1966 (mean=17 in.; variance=26), and 1968-2018 (mean=19 in.; variance= 19). Figure 93 shows the output from the Timeseries Toolbox nonstationarity detection analysis.

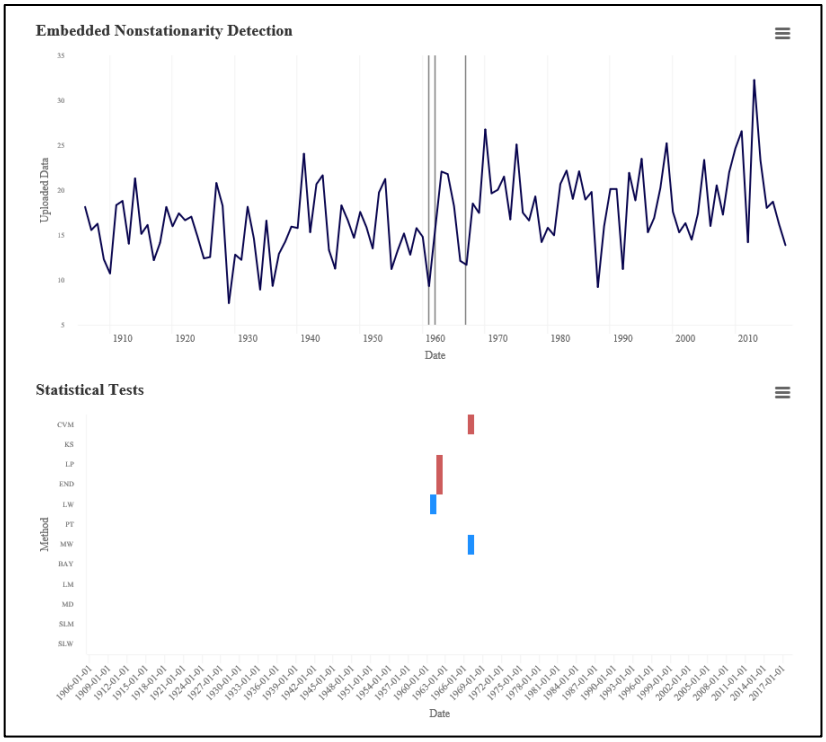

Note: y-axis is annual cumulative precipitation in inches

Abbreviation	Statistical Method	Abbreviation	Statistical Method
CVM	Cramer-von-Mises	BAY	Bayesian
KS	Kolmogorov-Smirnov	LM	Lombard Mood
LP	LePage	MD	Mood
END	Energy Divisive	SLM	Smooth Lombard Mood
LW	Lombard Wilcoxon	SLW	Smooth Lombard Wilcoxon
PT	Pettitt	MW	Mann-Whitney

Figure 93. Nonstationarity analysis - annual cumulative precipitation – Minot Experimental Station, ND

6.3.1.2 Nonstationarity Analysis- Annual Cumulative Precipitation- Yellow Grass Station, SK

The USACE Timeseries Toolbox is used to assess nonstationarities in the annual cumulative precipitation timeseries at Yellow Grass (period of record: 1912-2018). The annual cumulative precipitation is derived from the daily, cumulative precipitation data using HEC-DSSVue. Annual cumulative precipitation is computed by water year. The Timeseries Toolbox did not detect nonstationarities in the timeseries.

6.3.2 Detection of Trends in Annual Cumulative Precipitation

6.3.2.1 Trend Analysis- Annual Cumulative Precipitation- Minot Experimental Station, ND

The t-Test (p-value= 4.47×10^{-5}), Mann-Kendall (p-value=2.02×10^{-4}), Spearman Rank-Order (p-value= 1.13×10^{-4}), and linear regression (p-value=7.13×10^{-4}) tests are applied to assess trends in the cumulative, annual, precipitation record collected at Minot. All tests indicate a statistically significant, increasing trend (see Figure 94). In addition to analyzing the full period of record

from 1906 to 2018, portions of the period of record prior to and after the 1962 nonstationarity are assessed for trends. No trends are found within the data collected prior to 1962 (1906-1961; p-value= 0.497) or in the data collected post-1962 (1963-2018; p-value= 0.663).

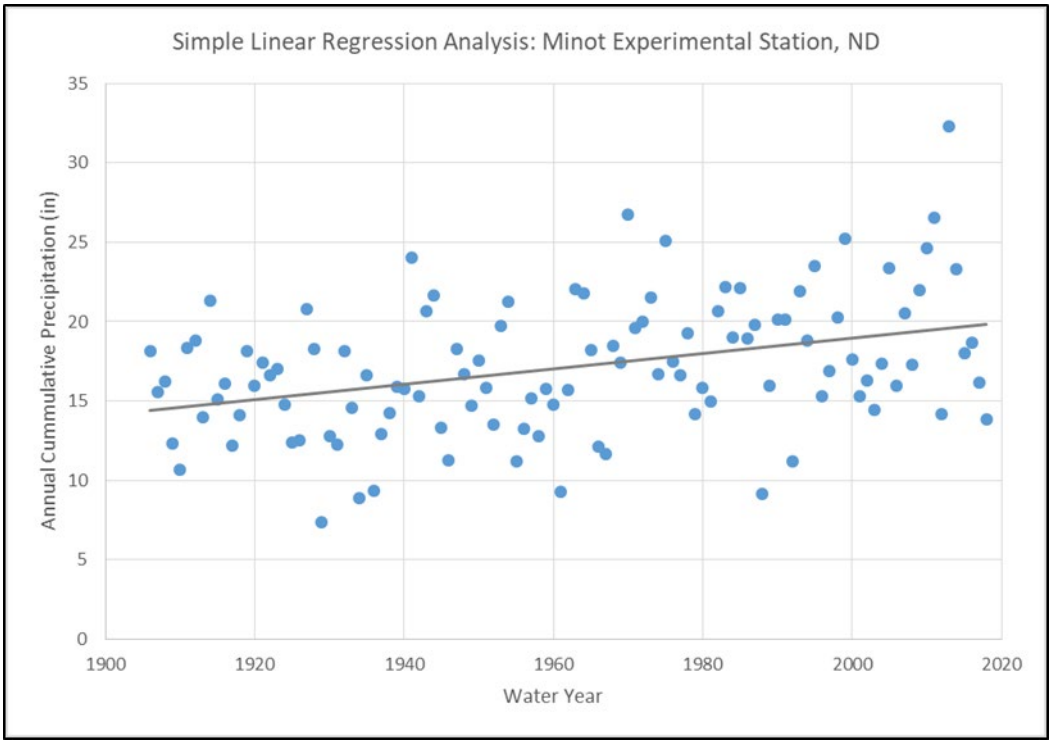

Figure 94. Trend analysis - annual cumulative precipitation - Minot Experimental Station, ND; p-value= $7.13x10^{-4}$.

6.3.2.2 Trend Analysis- Annual Cumulative Precipitation- Yellow Grass Station, SK

The Timeseries Toolbox is used to detect trends in the annual cumulative precipitation dataset collected at the Yellow Grass station. A statistically significant, increasing trend is indicated by the t-Test (p-value= 0.008), Mann-Kendall (p-value= 0.012), and Spearman Rank-Order (p-value= 0.014) statistical tests. Linear regression analysis with Microsoft Excel also suggests a significant increasing trend, with a calculated p-value of 0.048. See Figure 95 for a plot of the annual cumulative precipitation at Yellow Grass.

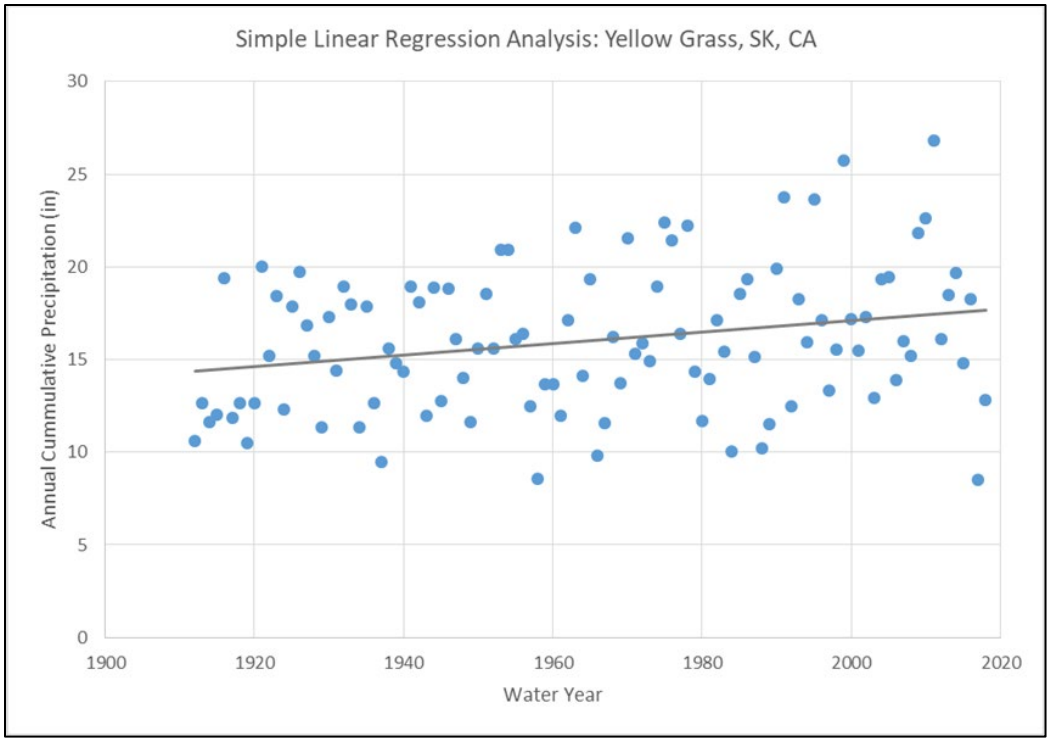

Figure 95. Trend analysis- annual cumulative precipitation- Yellow Grass, SK; p-value= 0.0483

7 Conclusion

Analysis is performed on observed streamflow, temperature, and precipitation data in the Souris River Basin. Timeseries datasets are analyzed to identify nonstationarities and trends in these relevant hydrometeorological variables. Nonstationarities and trends detected may be indicative of the impacts of human driven climate change in the Souris River Basin. However, it is difficult to conclusively attribute detected trends and nonstationarities to human driven climate due to other compounding factors like natural climate trends and changes in watershed characteristics (streamflow only). As indicated in Appendix B and Section 2.2 of the main report, studies which have integrated tree-ring based paleo-hydroclimatology as part of an evaluation of climate trends in the region encompassing the Souris basin have conclude that the climate within the region that encompasses the Souris River Basin fluctuates cyclically between dry and wet climate states within any given 100 year subset of the observed hydrometeorological record. The record length of observed hydrometeorological data are also a factor in assessing trends at a climatic scale.

There is little evidence of nonstationarity or trends in the annual peak flows recorded at the pristine, tributary gages analyzed. Based on the observed records at each of the tributary sites no nonstationarities are detected. For the Wintering River at Karlsruhe a nonstationarity is detected in 1941 when the record is back extended to 1930, but there is still no significant trend in the dataset. A nonstationarity is detected circa 1941 within the unregulated, peak streamflow record (1930 to 2017) at Minot, ND. When the unregulated record at Minot is

truncated to 1942 to 2017 no nonstationarities are detected. This indicates that post-1941, the peak streamflow record is relatively homogenous. In general, there is not a lot of evidence indicating that annual peak flows are decreasing or increasing in the Souris River Basin post-1941. Similar to the pristine, tributary gages analyzed in North Dakota, the Antler River near Melita, MB gage had no evidence of nonstationarity or trends in the annual peak flow for the period of record (1943 – 2017).

Seasonal annual peak streamflows collected along the Wintering River and approximated for the Souris River at Minot (unregulated) indicate little evidence of changing conditions in annual, peak spring flows. There is evidence indicating that peak flows are changing in both summer and fall. At both locations an increasing trend is observed in fall flows and a nonstationarity is observed in the forties. Both locations exhibit a statistically significant increasing trend within their peak, summer streamflow records. Within the peak, summer streamflow record, the Wintering River record indicates a nonstationarity in 1992, while the unregulated record approximated for the Souris River at Minot indicates a nonstationarity in 1942. The seasonal annual peak streamflows collected along Antler River near Melita, MB indicate no evidence of changing conditions in the annual, peak spring flows. There is some evidence indicating that summer and fall peak flows are changing. A nonstationarity for fall peak flows is observe in 2008. However neither season exhibits a statistically significant trend for peak flow.

Both the annual, average streamflow record recorded along the Wintering River and the approximation of annual, average unregulated flows generated for Minot exhibit strong evidence of an increasing trend and nonstationarities in 1941. If the average, annual streamflow records are broken down seasonally, similar increasing trends are observed on the Souris River at Minot and along the Wintering River in spring, summer and fall. Nonstationarities in summer and fall average, annual streamflows are detected in the early forties at both locations. Overall, there appears to be some consistent evidence of nonstationarity and increasing trends in average streamflows. These trends persist when the daily record is assessed seasonally versus annually. The Antler River near Melita gage indicated some evidence of nonstationarity for annual, average streamflow for the period of record (1943-2017). The seasonal annual average streamflows indicated no evidence of change in spring, and some evidence of change in summer and fall. A nonstationarity was observed in 2008 for the fall annual, average streamflow. No statistically significant trends were observed for average streamflow. A summary of trends detected within the unregulated record for the Souris River at Minot and the Wintering River at Karlsruhe is displayed in Table 1.

Table 1. Summary of First Order Statistical Analysis - Streamflow

	Long Creek near Noonan, ND		Des Lacs River at Foxholm, ND	
	Period of Analysis: 1960-2014		Period of Analysis:1946-2014	
Variable	Trend	Nonstationarity	Trend	Nonstationarity
Peak Annual Streamflow	None	None	None	None

	Souris River- Minot (Unregulated)				Wintering River (Unregulated)		
	Period of Analysis: 1930-2017						
Variable	Trend	Nonstationarity			Trend	Nonstationarity	
Peak Annual Streamflow	Increasing	1941			None	1941[1]	
Average Annual Streamflow	Increasing	1941			Increasing	1941	1987
Spring Peak Streamflow	Increasing	None			None	None	
Spring Average Streamflow	Increasing	1945			Increasing	1968	1987
Summer Peak Streamflow	Increasing	1942			Increasing	1992	
Summer Average Streamflow	Increasing	1942			Increasing	1941	1992
Fall Peak Streamflow	Increasing	1941	1945	1990	Increasing	1940	
Fall Average Streamflow	Increasing	1940	1990		Increasing	1940	1992

	Antler River near Melita, MB	
	Period of Analysis: 1943-2017	
Variable	Trend	Nonstationarity
Peak Annual Streamflow	None	None
Average Annual Streamflow	None	None
Spring Peak Streamflow	None	None
Spring Average Streamflow	None	None
Summer Peak Streamflow	None	None
Summer Average Streamflow	None	None
Fall Peak Streamflow	None	2008
Fall Average Streamflow	None	2008

[1]When the record back-extended to 1930 is analyzed through 2017 using the Timeseries Toolbox a strong nonstationarity is detected in 1941, however there is still no statistically significant trend observed within the dataset. There is no nonstationarity in the observed record: 1937-2014.

For the Minot Experimental Station, annual maximum temperature extremes exhibit a decreasing trend annually, as well as for the summer and winter seasons. A nonstationarity is detected in 1942 within both the annual maximum temperature record and the summer annual maximum temperature record. This is intuitive because the maximum annual temperature in the Souris River Basin generally occurs over the summer months. In general there does not appear to be much evidence of a statistically significant change in maximum temperature at Yellow Grass, SK.

Annual minimum temperature extremes at the Minot Experimental Station exhibit a nonstationarity in 1939. As would be anticipated based on the basin's climate, the nonstationarity is also identified within the winter minimum temperature record. Minimum temperatures appear to be increasing at Minot. Analysis at Yellow Grass, SK does not indicate nonstationarities within the minimum temperature timeseries. A consistent increasing trend is present in the annual minimum temperature data, as well as the summer and winter months at Yellow Grass.

Average annual temperatures at the Minot International Airport Station exhibit increasing trends annually and throughout all seasons, except fall. Only the spring annual average temperature record exhibits a nonstationarity (1975). Trends in temperature can be attributed to either human-driven climate change and/or natural climate trends. There is not a lot of evidence of changing temperature at Yellow Grass. A summary of temperature trends and nonstationarities identified is displayed in Table 2.

Table 2. Summary of First Order Statistical Analysis - Temperature

Summary: First Order Statistical Analysis Temperature Trends				
Variable	**Maximum Temperature Assessment**			
	Minot Experimental Station, ND		**Yellow Grass Station, SK**	
	1906-2018		1912-1918	
	Trend	Nonstationarity	Trend	Nonstationarity
Maximum Annual Temperature	Decreasing	1942	None	None
Maximum Fall Temperature	None	None	Increasing	None
Maximum Spring Temperature	None	1994	None	None
Maximum Summer Temperature	Decreasing	1942	None	None
Maximum Winter Temperature	Decreasing	None	None	1986
Variable	**Minimum Temperature Assessment**			
	Minot Experimental Station, ND		**Yellow Grass Station, SK**	
	1906-2018		1912-2018	
	Trend	Nonstationarity	Trend	Nonstationarity
Minimum Annual Temperature	Increasing	1939	Increasing	None
Minimum Fall Temperature	None	None	None	None
Minimum Spring Temperature	Increasing	None	None	None
Minimum Summer Temperature	Increasing	1929 2004	Increasing	None
Minimum Winter Temperature	Increasing	1939	Increasing	None

Summary: First Order Statistical Analysis Temperature Trends (Table 2 continued)		
Variable	**Average Temperature Assessment**	
	Minot International Airport Station, ND	
	1949-2018	
	Trend	Nonstationarity
Average Annual Temperature	Increasing	None
Average Fall Temperature	None	None
Average Spring Temperature	Increasing	1975
Average Summer Temperature	Increasing	None
Average Winter Temperature	Increasing	None

Trends in precipitation can be attributed to either human-driven climate change and/or natural climate trends in the prairie pothole region. An increasing trend and evidence of the same change point year (1962) are found within both the annual average 3-day precipitation record and annual cumulative precipitation record at Minot. The Yellow Grass records also exhibit increases in annual average 3-day precipitation and annual cumulative precipitation. No trends or nonstationarities are present when maximum 3-day precipitation volume is assessed at either the Minot Experimental Station or the Yellow Grass Station. A summary of precipitation trends detected within precipitation records is displayed in Table 3.

Table 3. Summary of First Order Statistical Analysis – Precipitation

Summary: First Order Statistical Analysis Precipitation Trends				
Variable	**Minot Experimental Station, ND**		**Yellow Grass Station, SK**	
	1906-2018		1912-2018	
	Trend	Nonstationarity	Trend	Nonstationarity
Annual 3-Day Average Precipitation	Increasing	1962	Increasing	None
Annual 3-Day Maximum Precipitation	None	None	None	None
Annual Cumulative Precipitation	Increasing	1962	Increasing	None

At Minot there is evidence of changing temperature circa 1940. This is consistent with the nonstationarities in the Minot and Wintering River streamflow records detected at the same point in time. The directionally of detected trends in streamflow, precipitation and minimum/average annual temperature is the same (increasing). However, the changepoint detected in precipitation occurs considerably later in the period of record (1962). Meteorological data collected at Yellow Grass Station in Saskatchewan and streamflow data collected on the Des Lacs River and Long Creek (upstream of Minot) yield less evidence of nonstationary hydrometeorological conditions. This makes it difficult to definitively attribute detected changes in hydrometeorological conditions in the Souris River Basin to a change in precipitation and/or temperature. Continued monitoring and data collection in the Souris River Basin will be beneficial for future nonstationarity and trend analysis.

8 References

1. Canada and U.S.A (1989). “Agreement between the Government of Canada and the United States for Water Supply and Flood Control in the Souris River Basin.”
2. Department of Defense, U.S. Army Corps of Engineers, Hydrologic Engineering Center (2016). “HEC-DSSVue Data Storage System Visual Utility Engine, Version 2.6,” Davis, CA.
3. Department of Defense, U.S. Army Corps of Engineers, Hydrologic Engineering Center (2018). “HEC-ResSim, Reservoir System Simulation, Version 3.3”, Davis, CA.

4. Friedman, D., J. Schechter, B. Baker, C. Mueller, G. Villarini, and K. D. White. (2016) US Army Corps of Engineers Nonstationarity Detection. US Army Corps of Engineers: Washington, D.C.
5. Government of Canada. (2019). Historical Data - Climate - Environment and Climate Change Canada. https://climate.weather.gc.ca/historical_data/search_historic_data_e.html
6. Iowa Environmental Mesonet" *Iowa State University*, North Dakota ASOS, https://mesonet.agron.iastate.edu/request/download.phtml. 10/11/2019.
7. Kolars, K.A., Vecchia, A.V., and Ryberg, K.R. (2016) Stochastic model for simulating Souris River Basin precipitation, evapotranspiration, and natural streamflow: U.S. Geological Survey Scientific Investigations Report 2015–5185, 55 p. [Also available at http://dx.doi.org/10.3133/sir20155185.]
8. LaZerte, Stefanie E and Sam Albers (2018). weathercan: Download and format weather data from Environment and Climate Change Canada. The Journal of Open Source Software 3(22):571. doi:10.21105/joss.00571.
9. Menne, Matthew J., Imke Durre, Bryant Korzeniewski, Shelley McNeal, Kristy Thomas, Xungang Yin, Steven Anthony, Ron Ray, Russell S. Vose, Byron E. Gleason, and Tamara G. Houston (2012): Global Historical Climatology Network - Daily (GHCN-Daily), Version 3. Foxholm 7 N, ND US. NOAA National Climatic Data Center. doi: 10.7289/V5D21VHZ 06/08/2020
10. Menne, Matthew J., Imke Durre, Bryant Korzeniewski, Shelley McNeal, Kristy Thomas, Xungang Yin, Steven Anthony, Ron Ray, Russell S. Vose, Byron E.Gleason, and Tamara G. Houston (2012): Global Historical Climatology Network - Daily (GHCN-Daily), Version 3. Minot Experimental Station, ND US. NOAA National Climatic Data Center. doi:10.7289/V5D21VHZ 09/24/2019.
11. Menne, Matthew J., Imke Durre, Bryant Korzeniewski, Shelley McNeal, Kristy Thomas, Xungang Yin, Steven Anthony, Ron Ray, Russell S. Vose, Byron E.Gleason, and Tamara G. Houston (2012): Global Historical Climatology Network - Daily (GHCN-Daily), Version 3. Minot International Airport, ND US. NOAA National Climatic Data Center. doi: 10.7289/V5D21VHZ 06/08/2020
12. Menne, Matthew J., Imke Durre, Bryant Korzeniewski, Shelley McNeal, Kristy Thomas, Xungang Yin, Steven Anthony, Ron Ray, Russell S. Vose, Byron E.Gleason, and Tamara G. Houston (2012): Global Historical Climatology Network - Daily (GHCN-Daily), Version 3. Velva, ND US. NOAA National Climatic Data Center. doi: 10.7289/V5D21VHZ 06/08/2020
13. USACE (2013) Regional and Reconstructed Hydrology of the Souris River. USACE, St. Paul District, MN.
14. USACE (2018) Engineering and Construction Bulletin 2018-14: Guidance for Incorporating Climate Change Impacts to Inland Hydrology in Civil Works Studies, Designs, and Projects.

15. USACE (2019) HH1: 2019 Regional Reconstructed Hydrology. USACE, St. Paul District, MN.
16. USACE (2019) Souris River Plan of Study HEC-ResSim Alternative Assessment. USACE, St. Paul District, MN.
17. USACE (2019) Souris River Plan of Study HEC-ResSim Model Phase 2. USACE, St. Paul District, MN.
18. USACE (2020). *Climate Hydrology Assessment Tool.* U.S. Army Corps of Engineers Climate Preparedness and Resilience Team. http://corpsmapu.usace.army.mil/cm_apex/f?p=313:10:0::NO
19. USACE (2020). *Nonstationarity Detection Tool.* U.S. Army Corps of Engineers Climate Preparedness and Resilience Team. http://corpsmapu.usace.army.mil/cm_apex/f?p=257:10:0::NO
20. USACE (2020). *Timeseries Toolbox.* U.S. Army Corps of Engineers Climate Preparedness and Resilience Team. http://34.205.128.255:8080/tst_app/